2-Periodic Compensation of DC-DC Boost Converter in Photovoltaic Cell Applications

A Thesis

Submitted in partial fulfilment of the requirement for the Degree of

Master in Control System Engineering

(Electrical Engineering Department)

By

Siddhartha Chakraborty

Registration No.: 163520 of 2022-2023

Examination Roll No.: M4CTL24002B

Under the Guidance of

Dr. Sayantan Chakraborty

Department of Electrical Engineering

Jadavpur University, Kolkata-700032, India.

November, 2024

FACULTY OF ENGINEERING AND TECHNOLOGY
JADAVPUR UNIVERSITY

CERTIFICATE

This is to certify that the dissertation entitled **"2-Periodic Compensation of DC-DC Boost Converter in Photovoltaic Cell Applications"** has been carried out by SIDDHARTHA CHAKRABORTY (University Registration No.: 163520 of 2022-2023) under my guidance and supervision and be accepted as partial fulfilment of the requirement for the Degree of Master in Control System Engineering. The research results presented in the thesis have not been included in any other paper submitted for the award of any degree to any other University or Institute.

_____

Dr. Sayantan Chakraborty
Thesis Supervisor

Dept. of Electrical Engineering
Jadavpur University

_____

Prof. Biswanath Roy
Head of the Department
Dept. of Electrical Engineering
Jadavpur University

_____

Prof. Rajib Bandyopadhyay
Dean
Faculty of Engineering and Technology

Jadavpur University

FACULTY OF ENGINEERING AND TECHNOLOGY
JADAVPUR UNIVERSITY

CERTIFICATE OF APPROVAL*

The forgoing thesis is hereby approved as a creditable study of an engineering subject and presented in a manner satisfactory to warrant acceptance as prerequisite to the degree for which it has been submitted. It is understood that by this approval the undersigned do not necessarily endorse or approve any statement made, opinion expressed or conclusion drawn there in but approve the thesis only for which it is submitted.

Committee on final examination for the evaluation of the thesis.

_____

Signature of the Examiner

_____

Signature of the Supervisor

*Only in the case the thesis is approved.

FACULTY OF ENGINEERING AND TECHNOLOGY
JADAVPUR UNIVERSITY

DECLARATION OF ORIGINALITY AND COMPLIANCE OF ACADEMIC THESIS

I hereby declare that this thesis entitled **"2-Periodic Compensation of DC-DC Boost Converter in Photovoltaic Cell Applications"** contains literature survey and original research work by the undersigned candidate, as part of his Degree of Master in Control System Engineering. All information here have been obtained and presented in accordance with academic rules and ethical conduct. It is hereby declared that, as required by these rules and conduct, all materials and results that are not original to this work have been properly cited and referenced.

Candidate Name: **Siddhartha Chakraborty**

Examination Roll. No.: M4CTL24002B

Thesis Title: **2-Periodic Compensation of DC-DC Boost Converter in Photovoltaic Cell Applications**

Date: _____

Place: Signature of the candidate

Acknowledgement

I would like to express my earnest gratitude and sincere thanks to my thesis supervisor Dr. Sayantan Chakraborty, Department of Electrical Engineering, Jadavpur University, for giving me the opportunity to work under him and inspiring me to explore the field of Control System Engineering. I am indebted to him for his patient guidance, critical and constructive views and untiring support that shaped my work.

I am also grateful to Prof. Smita Sadhu (Ghosh), Prof. Ranjit Kumar Barai, and Prof. Madhubanti Maitra, Department of Electrical Engineering, for all the guidance and knowledge that they have imparted during the tenure of the course.

I would also like to thank my friend and co-worker Rajdeep Dutta for his active support and constant encouragement throughout my thesis work.

Lastly, I am thankful to my parents, for their continuous support, encouragement and unending faith in my abilities.

Date:

Siddhartha Chakraborty

Department of Electrical Engineering

Examination Roll. No.: M4CTL24003

Jadavpur University

Abstract

This thesis explores the development and implementation of a 2-periodic compensation technique for DC-DC boost converters in photovoltaic (PV) cell applications. Boost converters, essential for managing the low and variable DC voltage output of PV cells, often face challenges in respect of poor stability margins due to non-minimum phase zeros. A double-loop Proportional-Integral (PI) controller configuration is one of the commonly used methods to address these challenges but remains limited in its achievable gain margin and design simplicity. This work proposes a novel compensation scheme involving a 2-periodic controller in place of the outer-loop PI controller thus enhancing gain margin and reducing design complexity. The proposed system is studied through mathematical modelling, small-signal analysis, and simulations in MATLAB/Simulink, demonstrating improved stability and efficiency. Applications for this enhanced control system include renewable energy systems, emphasizing its potential to optimize the integration of PV cells with energy storage or grid systems.

Key words: Boost converter, photovoltaic cell, NMPZ, 2-periodic controller.

List of Figures

List of Tables

List of abbreviations

NMP	:	Non-Minimum-Phase
NMPZ	:	Non-Minimum-Phase Zeros
CL	:	Closed Loop
RL	:	Root Locus
Eqn.	:	Equation
LTI	:	Linear Time Invariant
LDTI	:	Linear Discrete Time Invariant
PWM	:	Pulse Width Modulation
DOF	:	Degrees-of-Freedom
DC	:	Direct Current
AC	:	Alternating Current
MPPT	:	Maximum Power Point Tracking
SISO	:	Single Input Single Output
GM	:	Gain Margin

TABLE OF CONTENTS

Chapter 1

Introduction and Literature Review

1.1 Introduction:

Solar energy is a renewable, clean energy source generated by capturing sunlight and converting it into usable electricity or heat. This energy is harnessed through technologies like photovoltaic (PV) panels, which convert sunlight directly into electricity, and solar thermal systems, which use the sun's heat for applications like water heating and electricity generation. Solar energy offers numerous environmental benefits, including reducing greenhouse gas emissions and dependency on fossil fuels, and has become a key component in the global shift toward sustainable energy solutions. With advancements in technology and decreasing costs, solar energy is increasingly accessible for residential, commercial, and large-scale power applications worldwide. DC-DC boost converters play a crucial role in solar energy systems by efficiently managing and transforming the voltage produced by solar panels. Solar panels generate direct current (DC) at a relatively low and variable voltage, which can fluctuate depending on factors like sunlight intensity, temperature, and shading. DC-DC boost converters enhance the efficiency and reliability of solar energy systems by transforming fluctuating solar panel output into a stable and optimized power source, making them an indispensable component of modern solar applications. This chapter mainly focusses on energy conversion components of solar PV cells and DC-DC boost converters which are the main components of this thesis.

1.1.1 Solar Energy Conversion Systems

Solar energy conversion systems are made up of several key components that work together to capture, convert, store, and distribute solar power. Here's an overview of the main components:

1. **Solar Panels (Photovoltaic Modules)**: These are the primary components that capture sunlight and convert it into direct current (DC) electricity through the photovoltaic effect [1]. Solar panels consist of numerous solar cells made from semiconductor materials like silicon.
2. **Inverter:** Solar panels produce DC electricity, but most household and commercial devices operate on alternating current (AC). The inverter converts DC into AC electricity, making it compatible with standard electrical systems [2]. Inverters can also manage power flow and sometimes include advanced monitoring and control features**.**
3. **Battery Storage:** Batteries store excess energy generated during sunny periods for later use, such as during nighttime or cloudy days [1]. Lithium-ion and lead-acid batteries are common in solar energy storage, enabling energy independence and reliability [2].
4. **Charge Controller:** This component regulates the voltage and current going from the solar panels to the battery, preventing overcharging or discharging, which can damage the battery and shorten its lifespan. Many charge controllers also include maximum power point tracking (MPPT) to maximize energy harvested from the panels [4].
5. **DC-DC Converters**: These are sometimes used to manage and adjust the voltage levels within the system [2]. For example, a DC-DC boost converter can increase the voltage from the panels to meet the requirements of the battery or inverter, enhancing efficiency [4].
6. **Mounting and Racking Systems**: Solar panels need to be securely mounted to a surface, like a roof or ground installation. Mounting and racking systems position the panels for maximum sun exposure and ensure they withstand weather conditions.
7. **Monitoring and Control System**: Modern solar energy systems often include monitoring tools to track performance and efficiency [4]. These systems can provide real-time data on energy production, consumption, and storage, allowing users to optimize their energy usage [4].

These components create a fully functional solar energy system capable of capturing sunlight, converting it into electricity, storing or using that power, and maintaining safety and efficiency throughout the process.

1.1.2 DC-DC Boost Converters

A DC-DC boost converter is an electronic device that steps up (boosts) a lower input DC voltage to a higher output DC voltage. It operates based on the principle of energy storage in inductors and capacitors, using switching elements like transistors to control the energy transfer. The main components of a boost converter include:

- **Inductor**: Stores energy when the switch is on and releases it when the switch is off.
- **Capacitor**: Smoothens the output voltage.
- **Diode**: Prevents the capacitor from discharging back into the circuit.
- **Switch (usually a MOSFET)**: Controls the charging and discharging of the inductor.

1.1.3 Role of Boost Converters in Solar Energy Applications

Boost converters are essential in solar energy applications because they adjust and stabilize the voltage generated by solar panels, which typically produce variable, lower DC voltages. Here's a look at their primary roles:

1. **Voltage Regulation:** Solar panels output a DC voltage that varies with sunlight intensity and other environmental factors. Boost converters step up this fluctuating voltage to meet the requirements of the energy storage system or the load, ensuring stable operation of the system [5].
2. **Maximum Power Point Tracking (MPPT):** Many boost converters are equipped with MPPT capabilities, which optimize the voltage and current output of solar panels to operate at their maximum power point [5]. By continuously adjusting to changing sunlight conditions, MPPT-enabled boost converters maximize energy harvested from the panels, enhancing overall system efficiency [5].
3. **Compatibility with Batteries and Inverters**: For energy storage or AC power output, the boost converter can raise the solar panel's voltage to match the input requirements of the battery or inverter, ensuring efficient charging and minimizing energy loss [6].

4. **Improved Efficiency in Solar Power Conversion**: By stepping up the low input voltages, boost converters help make efficient use of solar energy even under low-light or cloudy conditions, allowing the system to continue operating closer to the optimal power levels [2].
5. **Reduction of Energy Losses**: Directly connecting low-voltage solar panels to batteries or inverters can lead to high current levels and greater losses [g]. Boost converters reduce current levels by raising the voltage, helping to minimize power losses and extend the system's lifespan.

1.2 Solar energy and Photovoltaic Cell:

Solar energy is a renewable resource that harnesses sunlight using technologies like solar panels to produce electricity or heat. It's a clean, sustainable power source that reduces reliance on fossil fuels and helps lower greenhouse gas emissions. Photovoltaic cells, commonly found in solar panels, convert sunlight directly into electricity through the photovoltaic effect, making them a key technology in renewable energy production.

1.2.1 Solar Energy

Solar energy is the energy obtained from the Sun's radiation, which can be converted into electricity or heat. It is a renewable and sustainable energy source that plays a crucial role in reducing greenhouse gas emissions and reliance on fossil fuels. Solar energy can be harnessed through photovoltaic cells (solar panels) that convert sunlight directly into electricity or through solar thermal systems that capture heat for various applications. As a clean energy solution, solar power is increasingly being adopted worldwide, offering significant environmental and economic benefits while contributing to the fight against climate change.

Despite its many benefits, solar energy faces several challenges that hinder its widespread adoption. One major issue is its intermittent nature; solar power generation depends on sunlight, which varies by time of day, weather, and location, making it less reliable without energy storage solutions. Additionally, the high initial cost of installing solar panels and associated infrastructure can be a barrier for many individuals and businesses, though prices have been decreasing over time. Solar energy also requires large areas of land for installation, which may not always be available in densely populated regions. Moreover, the production and disposal of solar panels involve environmental concerns, such as the use of rare materials and waste management. Despite these challenges, ongoing advancements in technology, storage

solutions, and policy support continue to improve the viability of solar energy as a mainstream power source.

1.2.2 Photovoltaic Cell

A photovoltaic cell, commonly known as a solar cell, is a semiconductor device that converts light energy directly into electrical energy through the photovoltaic effect. These cells are the building blocks of solar panels, widely used in renewable energy systems [1].

To describe the working principle of Photovoltaic Cell we can say that the cell absorbs photons from sunlight, which excites electrons in the semiconductor material [8]. This energy creates electron-hole pairs, and an electric field within the cell drives the electrons towards the front surface [8]. The movement of these electrons generates a flow of electricity when connected to an external circuit.

The key components of Photovoltaic cell mainly include semiconductor material, p-n junction, anti-reflective Coating, conductive contacts.

Advantages [11]

- Renewable and sustainable energy source.
- Reduces dependence on fossil fuels.
- Low operating and maintenance costs.
- Environmentally friendly with no greenhouse gas emissions during operation.

Disadvantages [10]

- High initial cost of installation.
- Efficiency depends on sunlight availability.
- Requires large areas for significant power generation.

Applications [9]

- Residential and commercial power generation.
- Portable devices like calculators and chargers.
- Spacecraft and satellites.
- Solar farms and off-grid power systems.

Photovoltaic cells play a critical role in the transition towards clean energy, contributing to a more sustainable and eco-friendly future.

1.3 Boost Converter:

A boost converter, also known as a step-up converter, is a type of DC-DC converter that increases (or "boosts") the input voltage to a higher output voltage. DC-DC boost converters are integral to the efficient operation of wind energy systems. It plays a key role in voltage stabilization, MPPT, grid compatibility, and energy storage integration [12]. By optimizing the voltage levels and ensuring that wind turbines operate at their maximum efficiency, boost converters contribute to the overall effectiveness and reliability of wind energy systems.

1.3.1 Operating Principle

The basic operation of a boost converter is relatively straightforward. It consists of four main components: an inductor, a switch (usually a transistor), a diode, and a capacitor. The operation can be divided into two primary modes:

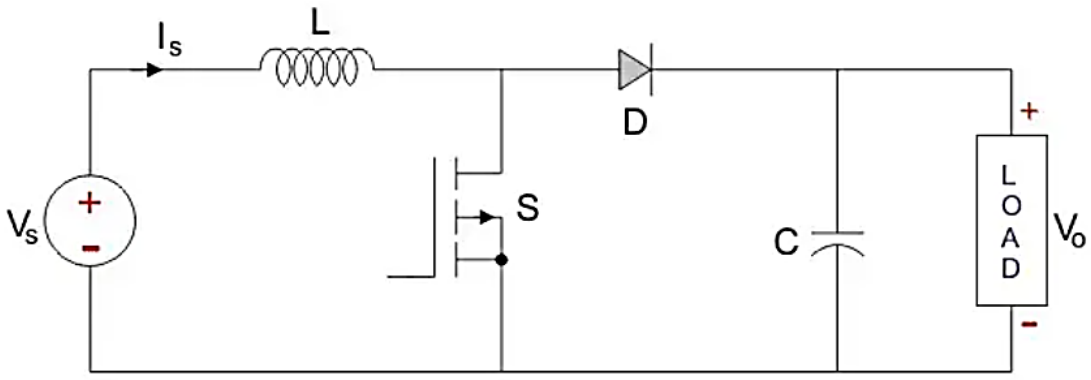

Fig.1.1: A Boost Converter [13]

1. **<u>Switch ON Mode</u>:**

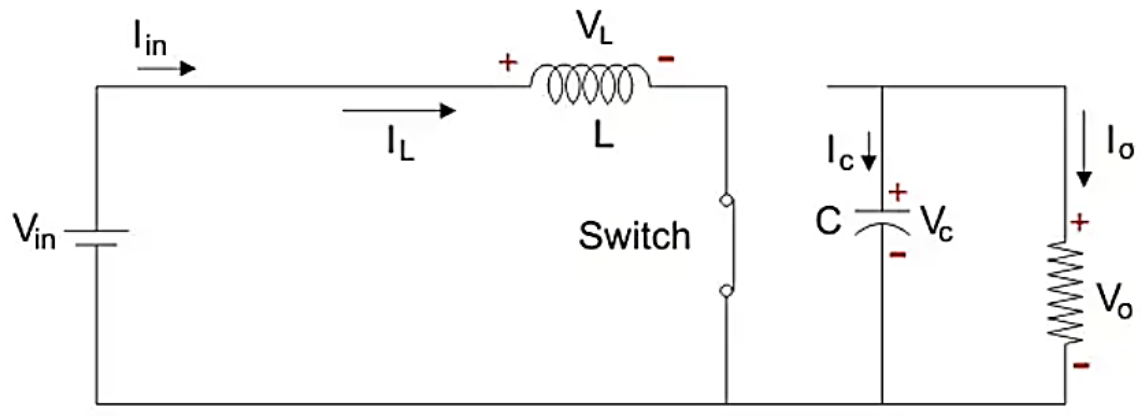

Fig.1.2: Switch ON and Diode OFF [13]

When the switch is closed (turned on), the input voltage is applied across the inductor. This causes the inductor to store energy in the form of a magnetic field. During this time, the diode is reverse-biased, preventing current from flowing to the output [14].

Let us say the switch is on for a time T_{ON} and is off for a time T_{OFF}. We define the time period, T, as $T = T_{ON} + T_{OFF}$.

Let us now define another term, the duty cycle, $D = \frac{T_{ON}}{T}$

Using KVL in the inductor loop:

$$V_{in} = V_L = L\frac{di_L}{dt} \dots\dots\dots (1.1)$$

$$=> \frac{di_L}{dt} = \frac{\Delta i_L}{\Delta t} = \frac{\Delta i_L}{DT} = \frac{V_{in}}{L} \dots\dots\dots (1.2)$$

Since the switch is closed for a time $T_{ON} = DT$ we can say that $\Delta t = DT$.

$$\therefore (\Delta i_L)_{closed} = \left(\frac{V_{in}}{L}\right) DT \dots\dots\dots (1.3)$$

While performing the analysis of the Boost converter, we have to keep in mind that the inductor current is continuous and this is made possible by selecting an appropriate value of L. The inductor current in steady state rises from a value with a positive slope to a maximum value during the ON state and then drops back down to the initial value with a negative slope [13]. Therefore, the net change of the inductor current over anyone complete cycle is zero.

2. <u>Switch OFF Mode</u>:

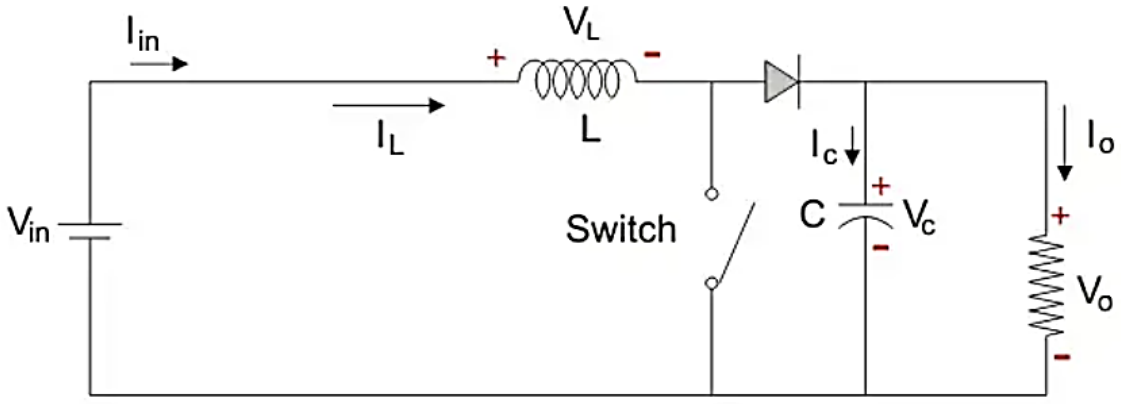

Fig.1.3: Switch OFF and Diode ON [13]

Since, the switch is open for a time $T_{OFF} = T - T_{ON} = T - DT = (1 - D)T$

We can say that $\Delta t = (1 - D)T$

In this mode using KVL we get:

$$(\Delta i_L)_{open} = \left(\frac{V_o - V_{in}}{L}\right)(1 - D)T \quad \ldots\ldots\ldots (1.4)$$

It is already established that the net change of the inductor current over any one complete cycle is zero.

$$\therefore (\Delta i_L)_{closed} + (\Delta i_L)_{open} = 0 \quad \ldots\ldots\ldots (1.5)$$

$$=> \frac{V_o}{V_{in}} = \frac{1}{1 - D} \quad \ldots\ldots\ldots (1.6)$$

The duty cycle (D) varies between 0 and 1.

1.3.2 Application of Boost Converter

Boost converters are used in a wide range of applications:

- **Battery-Powered Devices:** To step up the voltage from a battery to a higher level required by the device circuitry.
- **Renewable Energy Systems:** In photovoltaic (solar) systems, boost converters are used to step up the low voltage output from solar panels to a higher voltage for grid-tie inverters or battery charging [12].
- **Power Supply Systems:** In systems where the input voltage may drop below the required operating level, a boost converter can maintain a stable output voltage [15,16].

1.3.3 Challenges and Design Considerations

Designing a boost converter involves several challenges, including managing the non-minimum phase behaviour, selecting appropriate components, and ensuring stability under varying load conditions.

- **Non-Minimum Phase Behaviour:** The boost converter exhibits a right-half-plane zero in its transfer function, which can complicate control design. Advanced control strategies are often employed to manage this issue.
- **Component Selection:** The inductor size, switch rating, and diode selection must be carefully chosen to handle the desired power levels while minimizing losses.

- **Stability and Transient Response:** Ensuring a fast transient response and maintaining stability under load changes are crucial, particularly in dynamic applications like power supplies for portable electronics [17,18,19].

The boost converter is a versatile and widely used power conversion device that plays a critical role in many modern electronic systems. Its ability to efficiently step up voltage levels makes it indispensable in applications ranging from consumer electronics to renewable energy systems. Ongoing advancements in control techniques and component technologies continue to enhance the performance and efficiency of boost converters, enabling their use in increasingly demanding applications.

1.3.4 Control Strategies implemented for DC-DC boost Converters

Implementing a control strategy in a DC-DC boost converter is crucial to ensure optimal performance, efficiency, and stability of the system. The control strategy primarily focuses on regulating the output voltage, maintaining a constant output despite variations in the input voltage or load, and maximizing the efficiency of the conversion process. Below is an overview of the key aspects of implementing a control strategy in a DC-DC boost converter:

1.3.5 The Control Objectives

The main objectives of a control strategy in a DC-DC boost converter are:

- **Output Voltage Regulation**: Maintain a stable output voltage regardless of changes in input voltage or load conditions.
- **Efficiency Optimization**: Minimize energy losses during conversion.
- **Dynamic Response**: Quickly respond to changes in input or load to minimize transients.
- **Protection**: Prevent over-voltage, over-current, and other fault conditions [20].

Different control strategies offer various advantages depending on the specific application and performance requirements. Below are some of the key control strategies commonly used in DC-DC boost converters:

Voltage-mode control is a widely used control strategy where the output voltage is regulated by comparing it to a reference voltage. The error between the reference and the actual output

voltage is processed by a compensator, usually a Proportional-Integral-Derivative (PID) controller, which adjusts the duty cycle of the switch to maintain the desired output voltage[21].

- **Advantages**:
    - Simple to implement.
    - Well-suited for applications with relatively stable input voltage and load conditions.
- **Disadvantages**:
    - May have slower dynamic response compared to current-mode control.
    - Less effective in handling large variations in input voltage.

Current-mode control adds an inner current loop to the voltage loop. This strategy regulates the inductor current directly, in addition to the output voltage. The inner loop controls the inductor current by adjusting the duty cycle based on the error between the measured current and a reference current. The outer voltage loop adjusts the reference current to maintain the desired output voltage.

- **Advantages**:
    - Improved dynamic response and stability.
    - Inherent over-current protection.
    - Better performance under varying input voltage and load conditions.
- **Disadvantages**:
    - More complex to implement due to the need for current sensing.
    - Potential for subharmonic oscillation in continuous conduction mode (CCM), requiring slope compensation.

Hysteretic control, also known as bang-bang control, directly regulates the output voltage by turning the switch on or off based on whether the output voltage is above or below certain thresholds [20]. This approach is known for its simplicity and fast dynamic response.

- **Advantages**:
    - Extremely simple to implement.
    - Fast response to changes in load or input voltage.
- **Disadvantages**:
    - Results in variable switching frequency, which can complicate filter design and EMI management.

- Less precise control compared to other strategies.

Sliding mode control is a non-linear control method that forces the system to operate on a predefined sliding surface, regardless of disturbances or parameter variations. It is robust and capable of handling large variations in input and load.

- **Advantages**:
  - Robust to parameter variations and external disturbances.
  - Good dynamic performance and fast response.
- **Disadvantages**:
  - Complex to design and implement.
  - Potential for chattering (rapid switching), which can cause wear on components and generate EMI.

Average current mode control is a variation of current-mode control where the control loop regulates the average value of the inductor current, rather than its peak value. This method provides smoother operation and can be more stable than peak current-mode control [21].

- **Advantages**:
  - Smooth and stable operation.
  - Good performance in both continuous and discontinuous conduction modes.
- **Disadvantages**:
  - Requires more complex control circuitry and accurate current sensing.

Digital control involves using a microcontroller or digital signal processor (DSP) to implement the control strategy. It allows for more sophisticated algorithms, such as adaptive control, predictive control, or even machine learning-based control.

- **Advantages**:
  - Flexibility to implement complex control algorithms.
  - Easier to integrate with digital systems and communication protocols.
  - Ability to implement adaptive control that adjusts parameters in real-time.
- **Disadvantages**:
  - Requires analog-to-digital conversion, which introduces sampling delay and potential quantization errors.

- Higher cost and complexity compared to analog control.

Proportional-Integral-Derivative (PID) control is a classic control strategy that combines three terms: proportional, integral, and derivative. The proportional term responds to the current error, the integral term accounts for past errors, and the derivative term predicts future errors. This combination provides a balance of speed, stability, and accuracy [21].

- **Advantages**:
  - Widely used and well-understood.
  - Good balance between response speed and stability.
- **Disadvantages**:
  - Requires tuning of three parameters (P, I, D), which can be complex in some systems.
  - May not perform well in highly non-linear systems without additional adjustments.

Fuzzy logic control is a non-linear control method that mimics human decision-making. It uses a set of fuzzy rules to handle imprecise inputs and provides smooth control actions. This method is particularly useful in systems with a high degree of uncertainty or non-linearity.

- **Advantages**:
  - Handles non-linearities and uncertainties well.
  - No need for precise mathematical modelling.
- **Disadvantages**:
  - Requires expert knowledge to define fuzzy rules.
  - Computationally intensive, particularly for real-time applications.

Predictive control anticipates future system behaviour based on a model of the converter and adjusts the control inputs to optimize performance. This method is effective in systems where the dynamics are well understood and can be predicted accurately.

- **Advantages**:
  - Optimizes control actions based on future predictions.
  - Can improve efficiency and response time.
- **Disadvantages**:
  - Requires a precise model of the system.

- Computationally demanding, especially for real-time applications.

Implementing a control strategy in a DC-DC boost converter is a critical step in achieving reliable and efficient performance. Choosing the right control strategy for a DC-DC boost converter depends on the specific requirements of the application, including the desired performance, complexity, and cost constraints. Voltage-mode and current-mode controls are the most commonly used, offering a good balance between simplicity and performance. For applications requiring fast response or robustness to disturbances, advanced techniques like sliding mode, digital control, or predictive control may be more appropriate [21]. Proper design, implementation, and tuning of these control strategies are essential to achieving optimal performance in DC-DC boost converters. Advanced strategies, such as digital control and sliding mode control, offer additional robustness and flexibility, making them suitable for modern, high-performance applications.

1.4 Motivation

Due to the complex structure of boost converters which contain NMPZ in the current conduction mode, due to which they suffer from poor stability margins when controlled by using LTI controllers. To reduce these complexities double-loop PI control configuration is implemented with current transfer function in the inner-loop and the output voltage transfer-function as the outer-loop, still due to LTI nature of PI controller GM is less so to overcome this problem the outer-loop PI is proposed to be replaced by 2-periodic controller to improve GM and reduce complexities from design perspective so that it can be seamlessly used with Photovoltaic cell and other solar cell applications.

1.5 Thesis Organization

Chapter 1 explores the aspects solar energy, Photovoltaic cell and their application. The operating principle of boost converter is discussed here. Finally, it discusses the motivation behind this thesis.

Chapter 2 describes the working principle, equivalent circuits and I-V characteristics of photovoltaic cell and external structures and components of solar panel. Then a MATLAB simulation is provided showing the PV array on MATLAB SIMULINK and the working of boost converters taking output of PV array block as input is discussed.

Chapter 3 includes simulation of a boost converter using PWM. Then the small signal model of a boost converter is discussed. A key aspect of this thesis – two-loop PI compensation of boost converter is analysed.

Chapter 4 revisits a 1-DOF 2-periodic controller configuration and synthesis of controller parameters. Further, the conditions for ripple-free steady state response are presented. Finally, numerical examples are discussed to establish the conditions.

Chapter 5 shows use of generalised 2-periodic controller for a boost converter in the outer-loop in a two-loop configuration with photovoltaic cell output as the reference source of input energy.

Chapter 2

Photovoltaic Cell: Mathematical Modelling and MATLAB Simulation

2.1 Photovoltaic Cell:

A solar photovoltaic (PV) cell is a semiconductor device that converts sunlight directly into electricity through the photovoltaic effect. When photons from sunlight strike the cell, they excite electrons in the semiconductor material, typically silicon, creating electron-hole pairs. These charge carriers are then separated by an internal electric field, generating a direct current (DC) of electricity. PV cells are widely used in solar panels for power generation, either in standalone systems or as part of a grid-connected system. Their performance is influenced by factors like cell material, incident light intensity, temperature, irradiance and cell efficiency.

2.1.1 Working Principle:

The operation of a solar photovoltaic (PV) cell is fundamentally grounded in the photovoltaic effect, a process that directly converts sunlight into electrical energy. When photons from sunlight hit the PV cell's surface, they impart energy to electrons in the semiconductor—commonly silicon—causing the material to absorb this energy. This absorption boosts the

electrons to a higher energy state, resulting in the formation of electron-hole pairs within the semiconductor structure. The cell's internal electric field, generally located at a p-n junction, facilitates the separation of these charge carriers by directing electrons toward the n-type layer and holes toward the p-type layer. This movement of charges creates a direct current (DC) flow when an external circuit is connected.

The effectiveness of energy conversion in a PV cell relies on factors such as the semiconductor material quality, cell architecture, and environmental influences, including irradiance and temperature.

- **Semiconductor material quality:** The quality of semiconductor material in a PV cell significantly impacts its energy conversion efficiency by influencing the recombination rate of electron-hole pairs and the cell's ability to absorb sunlight. High-quality materials with fewer defects reduce recombination losses, allowing more charge carriers to contribute to the electric current, thereby enhancing overall efficiency [24].
- **Cell architecture**: The architecture of a PV cell affects energy conversion efficiency by optimizing light absorption, carrier collection, and reducing resistance losses. Advanced cell structures, such as multi-junction cells or surface texturing, enhance light trapping and minimize recombination, allowing more efficient use of the incident sunlight to generate electricity.
- **Irradiance**: Irradiance, or the intensity of sunlight incident on a PV cell, directly affects its power output and efficiency. Higher irradiance levels increase the generation of electron-hole pairs, resulting in greater electrical current and enhanced energy conversion. Conversely, low irradiance reduces power generation and may lower overall cell efficiency[25].
- **Temperature**: Temperature has a notable impact on PV cell efficiency, as higher temperatures increase the semiconductor material's intrinsic carrier concentration, which leads to higher recombination rates and lower open-circuit voltage. This effect reduces the overall energy conversion efficiency of the cell. Cooler temperatures generally improve performance by minimizing these losses [25].

2.1.2 Equivalent circuit and characteristics:

The equivalent circuit of an ideal solar photovoltaic cell models its behaviour using an ideal current source in parallel with a diode where current source is the photon generated current, I_{ph}, which is generated as a result of receiving solar radiation or photon particles. So, it is clear that I_{ph} is directly proportional to irradiance (which is powering the solar cell).

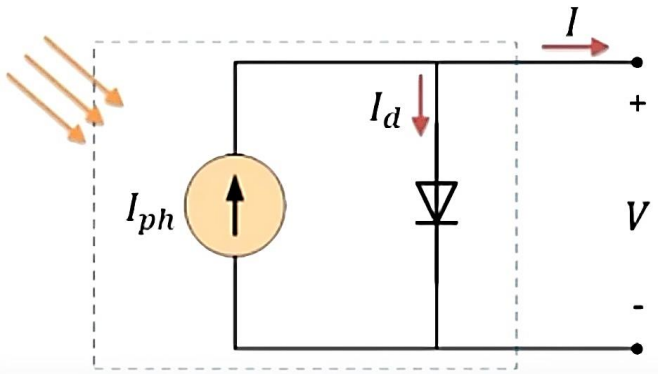

Fig.2.1: Equivalent circuit of an Ideal solar cell [27]

From, Fig.2.1, we can say that the current flowing out of the ideal solar cell (I) is given as:

$$I = I_{ph} - I_o\left(e^{\frac{qV}{\alpha kT}} - 1\right) \quad \ldots\ldots\ldots (2.1)$$

where:

- I_{ph}- Photon current at a given irradiance
- I_o- Reverse saturation current of the diode
- q- Charge of an electron (1.602 X 10^{-19} C)
- k- Boltzman's constant
- T- Temperature in K
- α – Diode Ideality factor

Now, in practical scenario all solar cells are not ideal there will be losses, so in order to account for these losses we have to add resistances:

- Series resistance (R_s) due to the combined resistances of contacts, metal grids and p and n layers.
- Shunt resistance (R_{sh}) due to leakage current through the p-n junction.

So in the equivalent circuit of the practical solar cell we will have practical current source instead of an ideal current source as a resistance (R_{sh}) is present in parallel to that source.

From, Fig.2.2, we can say that the current flowing out of the ideal solar cell (I) is given as:

$$I = I_{ph} - I_d - I_{R_{sh}} \quad \ldots\ldots\ldots (2.2)$$

where:

- I_d – Diode current which can be represented as $I_d = I_o\left(e^{\frac{q(V+IR_S)}{\alpha kT}} - 1\right)$

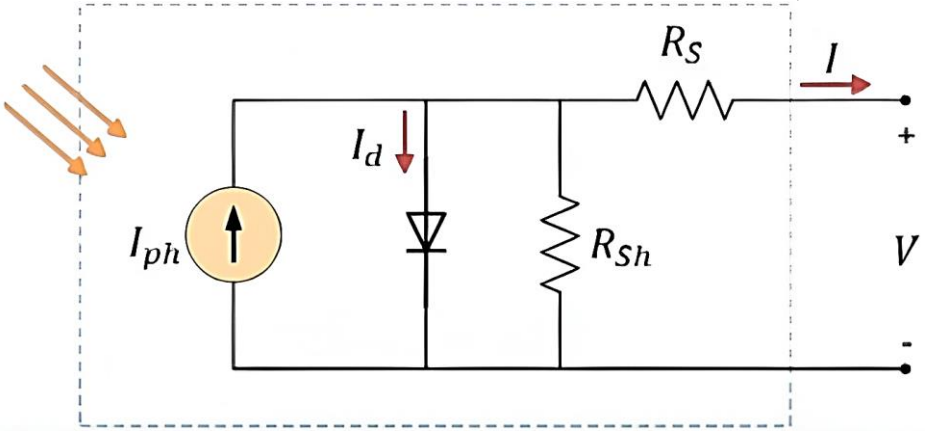

Fig.2.2: Equivalent circuit of a practical solar cell

- $I_{R_{sh}}$– Current through Shunt resistance (R_{sh}) expressed as $I_{R_{sh}} = \frac{V+IR_S}{R_{sh}}$

Hence, eq. ( ) can be rewritten as:

$$I = I_{ph} - I_o\left(e^{\frac{q(V+IR_S)}{\alpha kT}} - 1\right) - \frac{V + IR_S}{R_{sh}} \quad \ldots\ldots\ldots (2.3)$$

In summary, the equivalent circuit of a solar cell provides a simplified yet effective model to analyse its performance, accounting for the internal losses and leakage currents that affect efficiency, and enabling better design and optimization of solar energy systems.

The characteristics of a solar cell describe its performance in converting sunlight into electrical energy, typically represented by parameters like open-circuit voltage, short-circuit current, fill factor, and efficiency. These characteristics help evaluate and optimize solar cells for maximum power output under varying conditions.

- **Open-circuit voltage (V_{OC}):** Open-circuit voltage (V_{OC}) is the maximum voltage a solar cell can produce when there is no external load, directly influencing the cell's power output and efficiency. Open-circuit voltage (V_{OC}) depends on several factors:
  - V_{OC} depends on the quality of material.
  - V_{OC} is a strong function of temperature.
  - It varies slightly with irradiance.

The open-circuit voltage (V_{OC}) is expressed as:

$$V_{OC} = V_T \ln\left\{\left(\frac{I_{sc}}{I_o}\right) + 1\right\} \quad \ldots\ldots\ldots (2.4)$$

where: V_T – Voltage equivalent of temperature

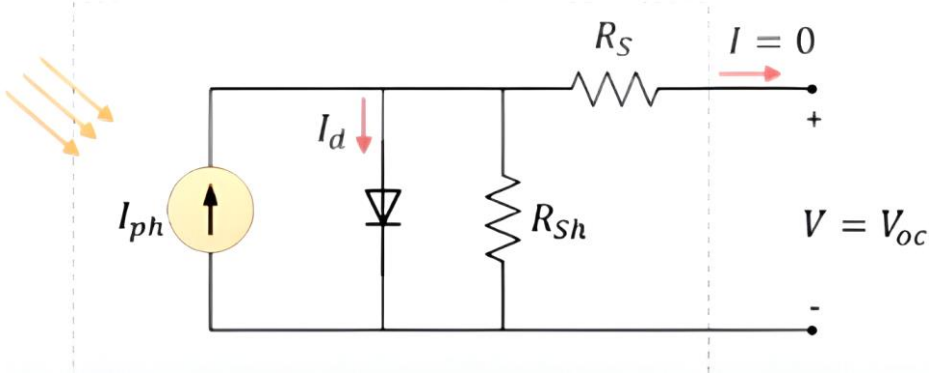

Fig.2.3: Open-circuit of a practical solar cell [27]

- **Short-circuit current (I_{sc}):** Short-circuit current (I_{sc}) is the maximum current generated by a solar cell under illumination when its output terminals are shorted, reflecting the cell's ability to convert light into electrical current. Short-circuit current depends on several factors[22]:
    - Varies linearly with solar irradiance level.
    - Area of solar cell.
    - Characteristics of the material.
    - Variation with respect to temperature can be neglected.

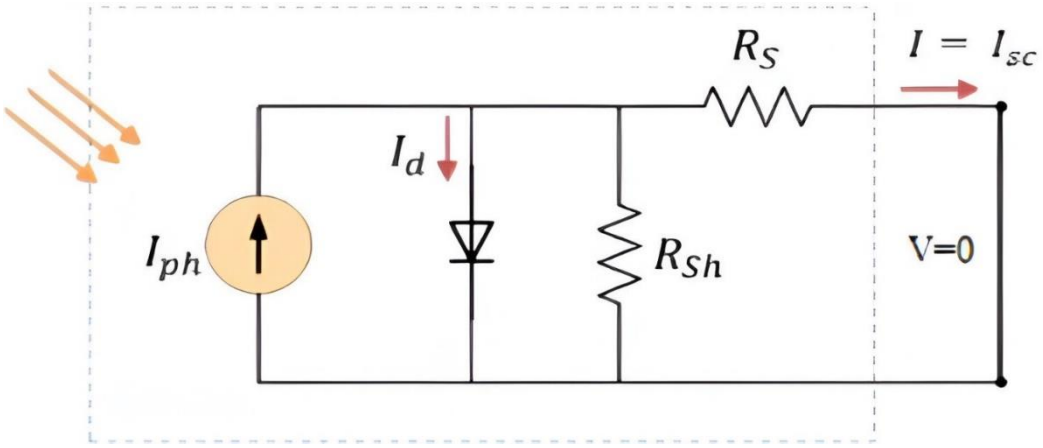

Fig.2.4: Short-circuit of a practical solar cell

- **Fill Factor (FF):** It is the ratio of the maximum power generated by solar cell to the product of open-circuit voltage and short-circuit current.

$$FF = \frac{V_{MP} I_{MP}}{V_{OC} I_{sc}}$$

It gives us an idea regarding the quality of array and closer the fill factor to 1, the more power array can provide. Typically, Fill factor ranges between 0.7 to 0.8

- **Efficiency:** Efficiency is the ratio of the electrical power output to the incident solar power, indicating how effectively a solar cell converts sunlight into usable energy.

The I-V (current-voltage) and P-V (power-voltage) characteristics of a solar cell illustrate its electrical behaviour and performance, showing how current, voltage, and power output vary with changing load conditions and illumination.

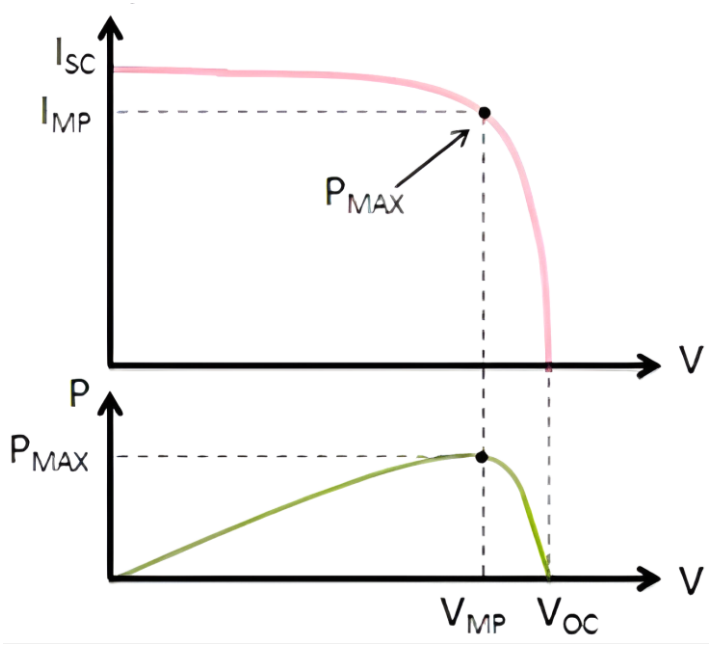

Fig.2.5: I-V and P-V characteristics of a practical solar cell [27]

The I-V (current-voltage) and P-V (power-voltage) characteristics of a solar cell are usually done at the same time as it will be easier to understand the characteristics like this. As, we can see that when Voltage is zero the current is maximum which actually refer to the short-circuit current (I_{sc}) but at the same time power is also zero as it is dependant on both voltage and current at the same time. Similarly, when voltage is maximum under open-circuit condition which is referred as open-circuit voltage (V_{OC}) where due to absence of any load current tends to zero and consecutively, power which is dependant on both voltage and current is also tending to zero here, these are the two extreme points on this curve, in between them as the load starts to increase the circuit follows it's output current equation for I-V characteristics and similarly P-V characteristics follow as it is evident here this follows a diode current like shape between

the two extremes. The most important terms in these characteristics which is usually considered from a designing point of view are P_{MAX} and V_{MP} which are:

- **Maximum Power (P_{MAX}):** The maximum power (P_{MAX}) on the I-V and P-V characteristics of a solar cell represents the optimal combination of current and voltage at which the cell produces the highest power output. It is a critical point that varies with light intensity and temperature, and tracking this point enables efficient energy harvesting by ensuring the solar cell operates at its peak efficiency. The expression of the maximum power point (P_{MAX}) in the I-V and P-V characteristics of a solar cell can be defined as:

$$P_{MAX} = V_{MP} * I_{MP} \quad \ldots\ldots\ldots (2.5)$$

where:

  - V_{MP} - voltage at the maximum power point
  - I_{MP} - current at the maximum power point

- **Voltage at maximum power point (V_{MP}):** The voltage at the maximum power point (V_{MP}) is the specific voltage at which a solar cell generates its highest power output, balancing between high current and sufficient voltage. Positioned between the open-circuit voltage and short-circuit current on the I-V curve, V_{MP} is crucial for designing and optimizing solar energy systems, as operating the cell near this voltage maximizes energy extraction. The expression of V_{MP} and I_{MP} are given as:

$$V_{MP} = V_{OC} - I_{MP} * R_S \quad \ldots\ldots\ldots (2.6)$$

$$I_{MP} = I_{sc} - \left(\frac{V_{OC} - V_{MP}}{R_{sh}}\right) \quad \ldots\ldots\ldots (2.7)$$

2.1.3 Effect of temperature and irradiance on voltage:

- **Effect of temperature on voltage**: The effect of temperature on the voltage output of a solar cell is primarily observed in the open-circuit voltage (V_{OC}), which decreases as the temperature increases. This behaviour can be explained mathematically using the following relationship [24]:

$$V_{OC} = V_{ref} - \beta\left(T - T_{ref}\right) \quad \ldots\ldots\ldots (2.8)$$

where:

  - V_{ref} – open-circuit voltage at T_{ref}(usually 25°C).

- β – temperature coefficient of V_{OC}, in volts per degree Celsius (V/°C).
- T – operating temperature in degrees Celsius
- T_{ref} – reference temperature in degrees Celsius.

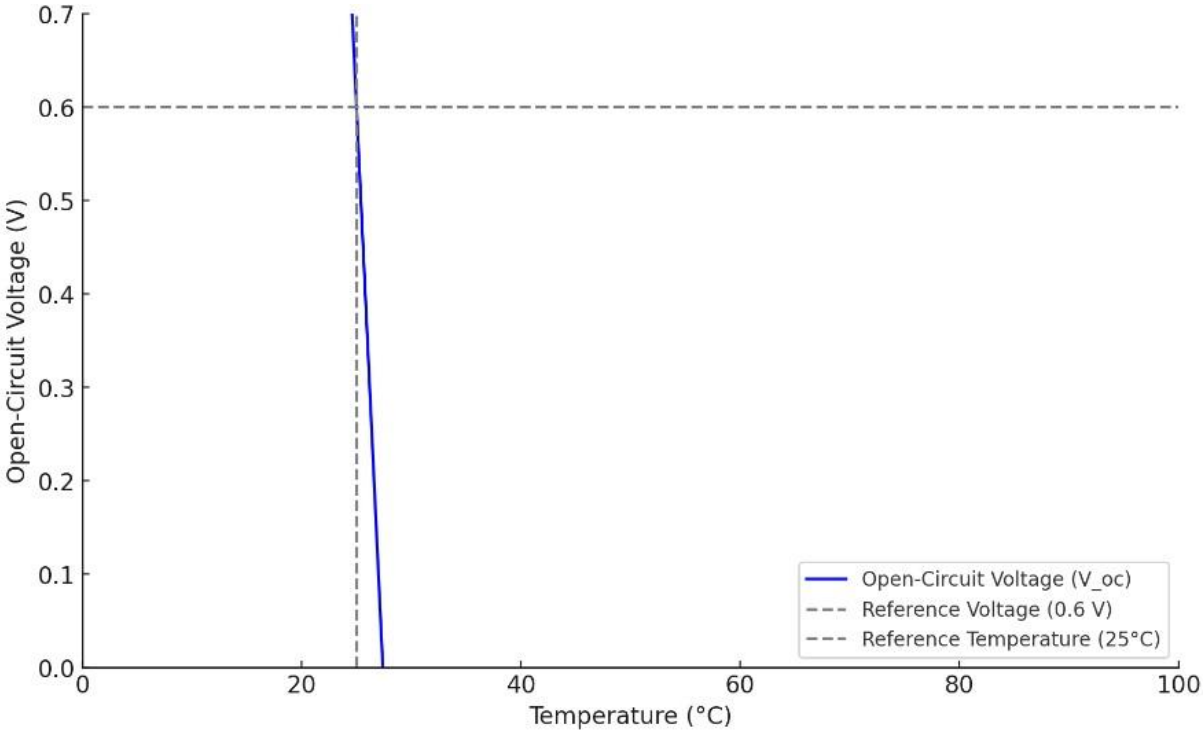

Fig.2.6: Open-circuit voltage vs Temperature graph of a practical solar cell

- **Effect of irradiance on voltage**: The irradiance (solar intensity) incident on a solar cell directly affects its output voltage. As irradiance increases, the photocurrent and the open-circuit voltage also increase. The impact of irradiance on voltage can be expressed by a mathematical expression [24]:

$$I_{ph} = G * I_{ph,ref}$$

- The photocurrent (I_{ph}) or light-generated current, is directly proportional to the irradiance (G) measured in W/m².
- $I_{ph,ref}$ - photocurrent at a reference irradiance G_{ref}(typically 1000 W/m² for standard test conditions).

The open-circuit voltage can be expressed as: $V_{OC} = V_T \ln\left\{\left(\frac{I_{ph}+I_o}{I_o}\right) + 1\right\}$, where:

- V_T – Voltage equivalent of temperature is expressed as $V_T = \frac{kT}{q}$
- I_o – saturation current, typically constant with respect to irradiance

Hence, relation between voltage and irradiance can be written as:

$$V_{OC} \approx \frac{kT}{q} \ln\left\{\frac{G * I_{ph,ref}}{I_o}\right\} \quad \ldots\ldots\ldots (2.9)$$

While both current and voltage increase with irradiance, the voltage increase is logarithmic due to its dependence on I_{ph} within the logarithmic function. Thus, under high irradiance, the output current increases substantially, while the voltage increase is more moderate, leading to a less pronounced effect on V_{OC}.

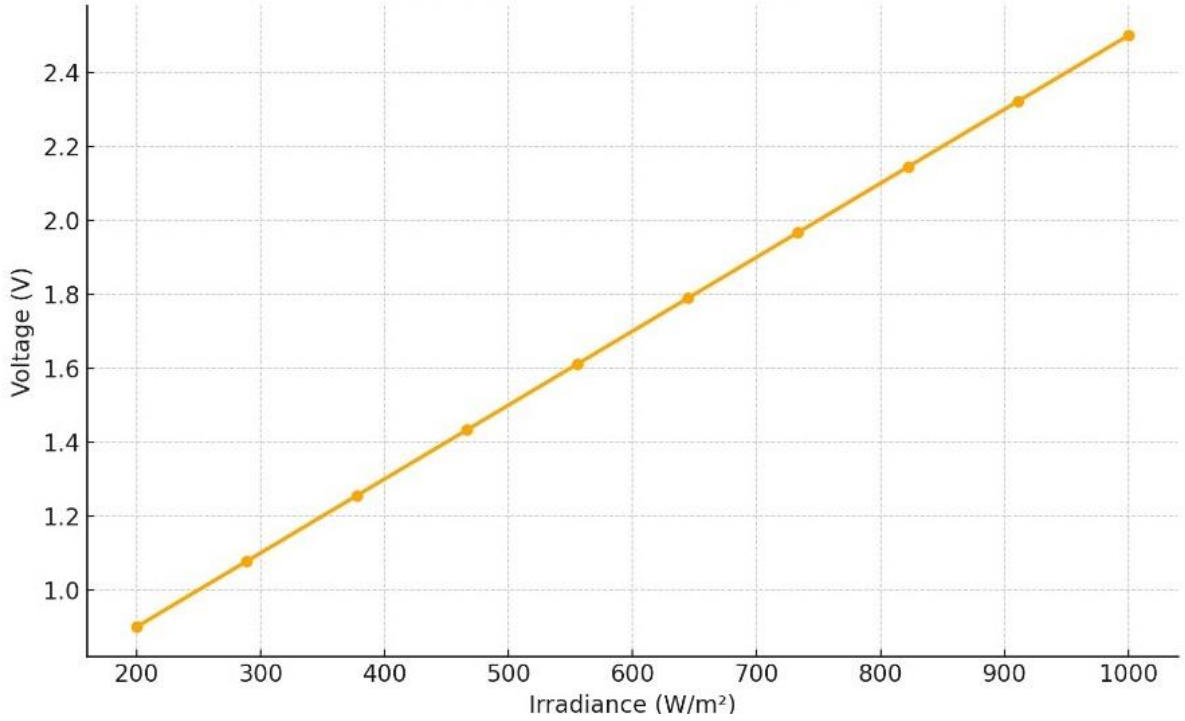

Fig.2.7: Open-circuit voltage vs Irradiance graph of a practical solar cell

2.2 External structure of a Photovoltaic Cell:

The external structure of a solar PV cell is designed to protect and safeguard the cell and maximize light absorption for efficient energy conversion. The components in the external structure includes[26]:

- Aluminium frame
- Tempered glass
- Encapsulant
- Solar cells
- Back sheet
- Junction box

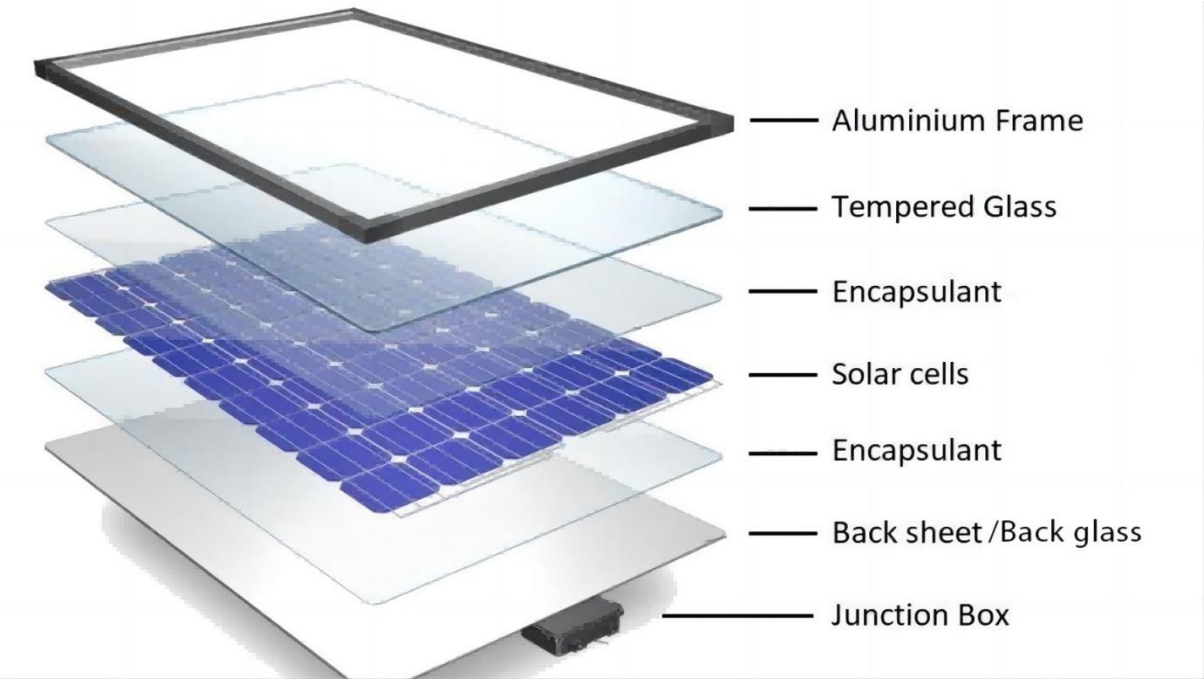

Fig.2.8: External structure and components of a solar cell [26]

Table 1: Function and description of different components of a Photovoltaic Cell

Component Name	Function	Description
Aluminium Frame	Provides structural support and stability to the panel, ensuring durability and ease of mounting.	An external layer which helps in protecting the solar cell.
Tempered Glass	Protects the solar cells from environmental factors like dust, water, and hail.	It is strong and allows maximum sunlight to pass through with minimal reflection.
Encapsulant	Protects the solar cells from moisture, dirt, and physical damage while holding the layers together.	A layer (often made of EVA - Ethylene Vinyl Acetate) that surrounds the solar cells.

Solar Cells	The core component that converts sunlight into electricity.	Made of semiconductor materials (typically silicon), these cells generate DC electricity through the photovoltaic effect.
Back sheet	Provides insulation and shields the solar cells from moisture and UV exposure.	A protective layer at the rear of the panel.
Junction Box	It serves as the point where external wires connect to the panel, allowing current to flow out.	An enclosure on the back of the panel that houses electrical connections, including bypass diodes.

2.3 Advantages and challenges of a Photovoltaic Cell:

Advantages:

- **Renewable Energy Source:** PV cells use sunlight, a limitless and sustainable energy source, reducing dependence on fossil fuels.
- **Environmentally Friendly:** They produce no emissions during operation, helping reduce greenhouse gas emissions and pollution.
- **Low Operating Costs:** Once installed, PV cells have minimal maintenance and low operating costs compared to other energy sources.
- **Scalability:** PV systems can be scaled to fit different applications, from small rooftop setups to large solar farms.
- **Energy Independence:** They allow individuals and businesses to generate their own electricity, reducing reliance on the grid.

Challenges:

- **Intermittency**: Solar energy is dependent on sunlight availability, which varies with time of day, weather, and season, affecting energy generation consistency.
- **High Initial Costs**: Although prices are decreasing, the upfront costs for PV cell production, installation, and setup can still be relatively high.

- **Efficiency Limitations**: Most PV cells have relatively low efficiency (typically between 15–22%), meaning only a portion of sunlight is converted to electricity.
- **Space Requirements**: For large-scale installations, solar panels require substantial space, which may be a constraint in densely populated areas.
- **End-of-Life Disposal**: PV cells contain materials like silicon and, in some cases, toxic heavy metals, posing challenges for disposal and recycling at the end of their lifecycle.

2.4 Simulation of a Photovoltaic Cell using PV array block and boost converter:

- **PV array:**

In MATLAB and Simulink, the PV Array block is a model of a photovoltaic cell that simulates the electrical behaviour of a solar panel system based on the characteristics of individual PV cells. This block is found in the Simulink environment, specifically in the Simscape Electrical toolbox, which is used for modelling and simulating renewable energy systems.

Key Features:

- **PV Cell Modelling**: The PV Array block models a group of PV cells connected in series and parallel configurations to form strings and arrays, allowing the simulation of large-scale PV systems.
- **Parameter Inputs**: Users can specify parameters such as cell temperature, irradiance (solar radiation), and module characteristics (e.g., short-circuit current, open-circuit voltage, and maximum power point).
- **I-V and P-V Characteristics**: The block simulates the current-voltage (I-V) and power-voltage (P-V) characteristics of the array based on real-world factors like irradiance and temperature.
- **Temperature and Irradiance Dependence**: The block allows modelling of how temperature and irradiance affect the performance of the PV array, reflecting the impact of environmental conditions.

Block parameters:

- **Module:** Any module manufactured by any manufacturer from the given drop-down arrow can be selected and according to that other specifications changes.

- **Maximum power (W):** The rated power output which can be provided by that specific module of PV cell which depends upon open-circuit voltage (V_{OC}) and short-circuit current (I_{sc}) which changes according to module.
- **Cells per module:** Specifies the number of PV cells in series per string and number of strings in parallel, allowing users to configure the array size based on their system design.
- **Temperature Coefficients**: Adjusts how temperature affects voltage and current characteristics of the array. Users can specify coefficients for V_{OC} and I_{sc} to simulate performance under varying temperatures.
- **Irradiance and Temperature Inputs**: Sets default values for irradiance (W/m²) and cell temperature (°C), simulating environmental conditions. These values can also be adjusted dynamically during simulation.
- **Breakdown Voltage**: Allows users to define the breakdown voltage at which reverse current flows, modelling the effect of reverse bias under partial shading conditions.

These parameters help accurately simulate PV array behaviour, optimizing the model's realism for different environmental conditions and configurations.

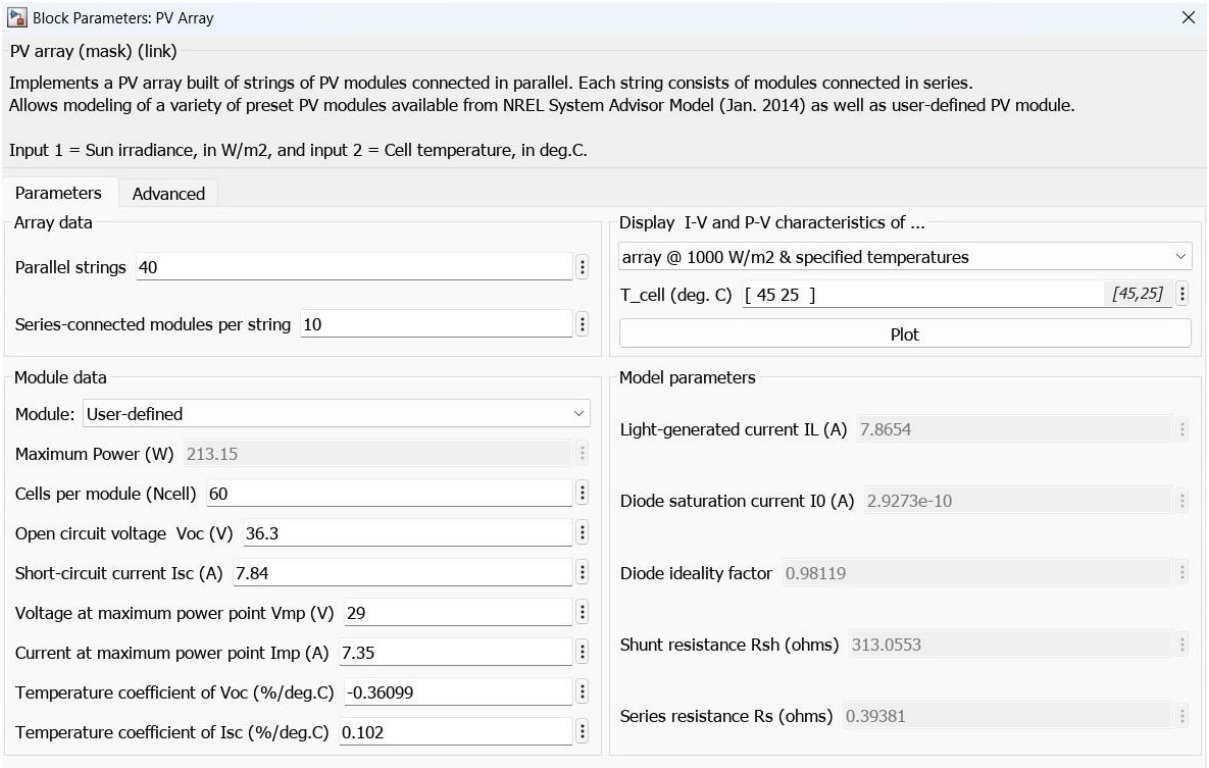

Fig.2.9: Block parameters of a PV array block in MATLAB SIMULINK

2.4.1 Simulation of PV array block:

To simulate this block, two inputs are given to the block in form of temperature and irradiance and according to the internal specifications and input it gives us output which is usually in form of voltage(V) and current(I). Measurement blocks (like voltage and current measurement) are used to monitor the output voltage and current.

The system is implemented using MATLAB Simulink with the following set of values:

1. Irradiance(W/m²): 1000
2. Temperature(°C): 25
3. Capacitance at Load end(F): 10e-4

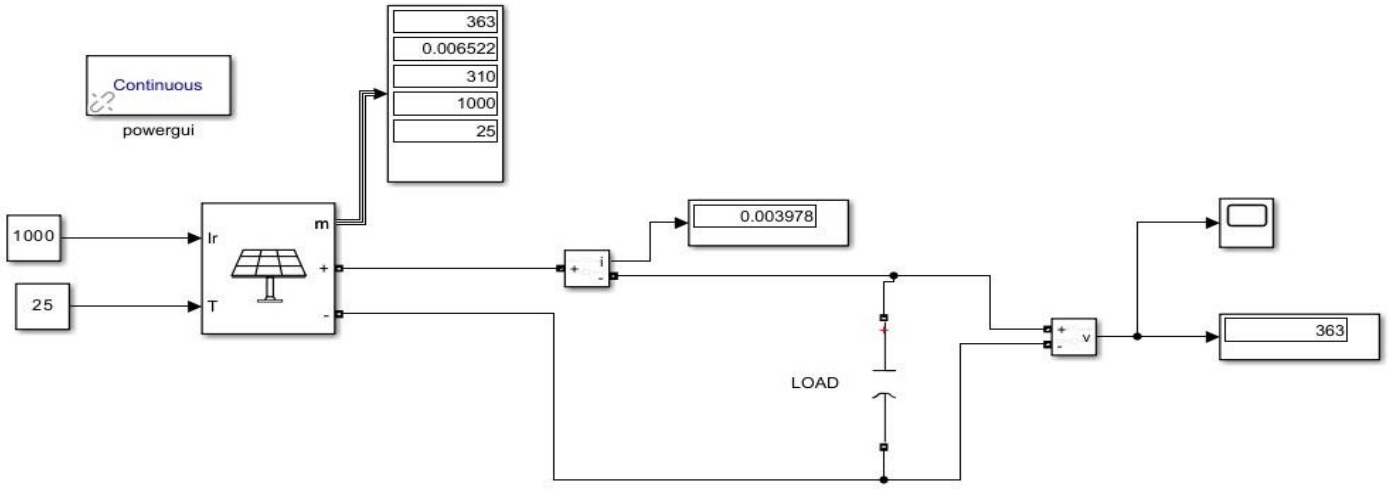

Fig.2.10: Simulation of PV array block

2.4.2 Simulation of PV array block using a boost converter:

A PV array converts input irradiance and temperature to electrical energy and output is obtained in form of DC voltage and current. This DC voltage is then fed to a boost converter, which steps up the DC voltage to a higher, more stable level suitable for grid integration or other applications.

The system is implemented using MATLAB Simulink with the following set of values:

1. Irradiance(W/m²): 1000	2. Series Capacitance(C1): 100e-3F
3. Temperature(°C): 25	4. Series Capacitance(C2): 100e-3F
5. Input Capacitance(F): 100e-6	6. Load Resistance(Ω): 50
7. Branch Resistance(Ω): 0.000001	8. Series Capacitance(C1): 100e-3F
9. Branch Inductance(H): 5e-3	10. Duty ratio(D)= 0.5

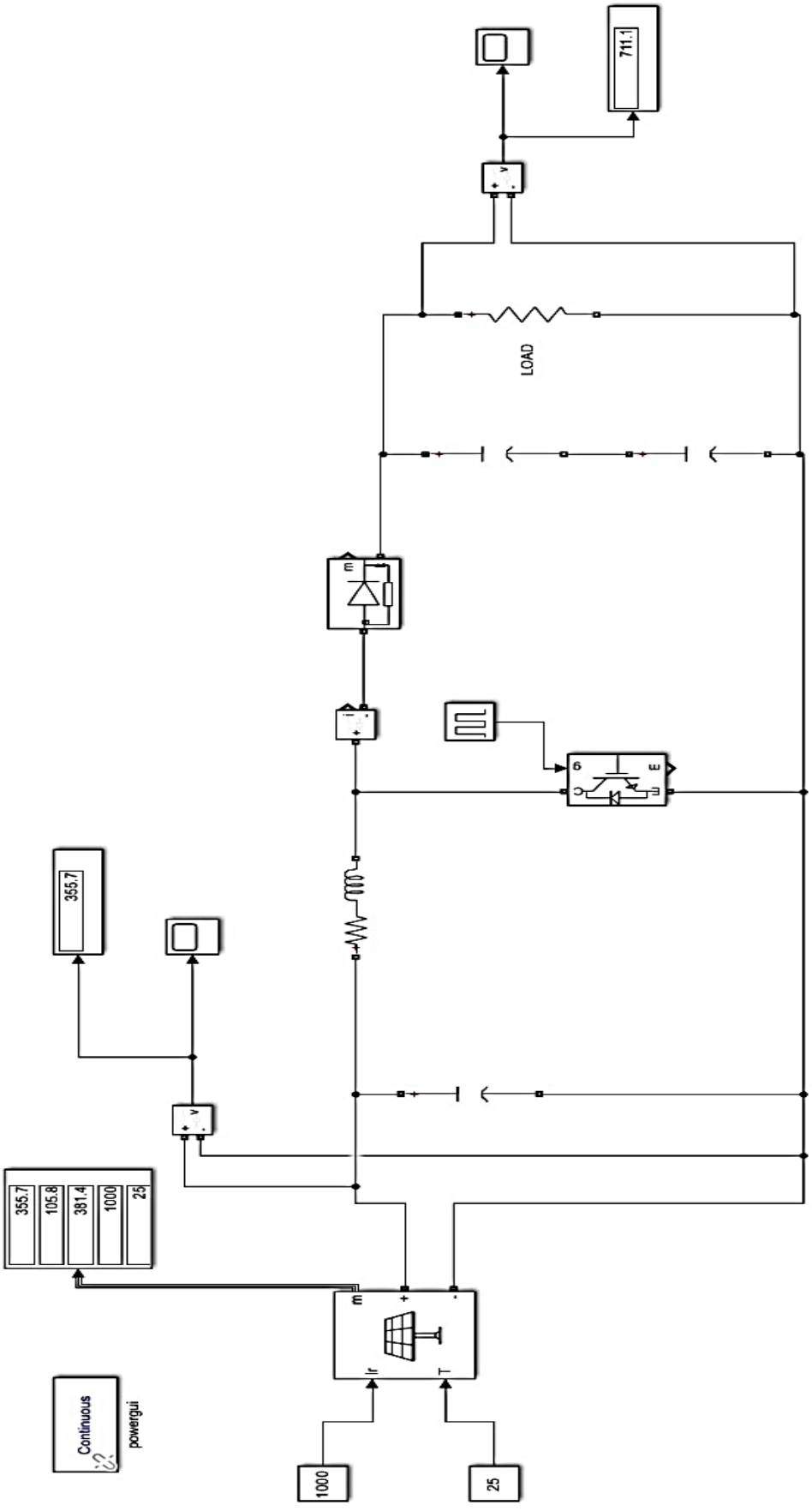

Fig.2.11: PV array block simulation using Boost Converter

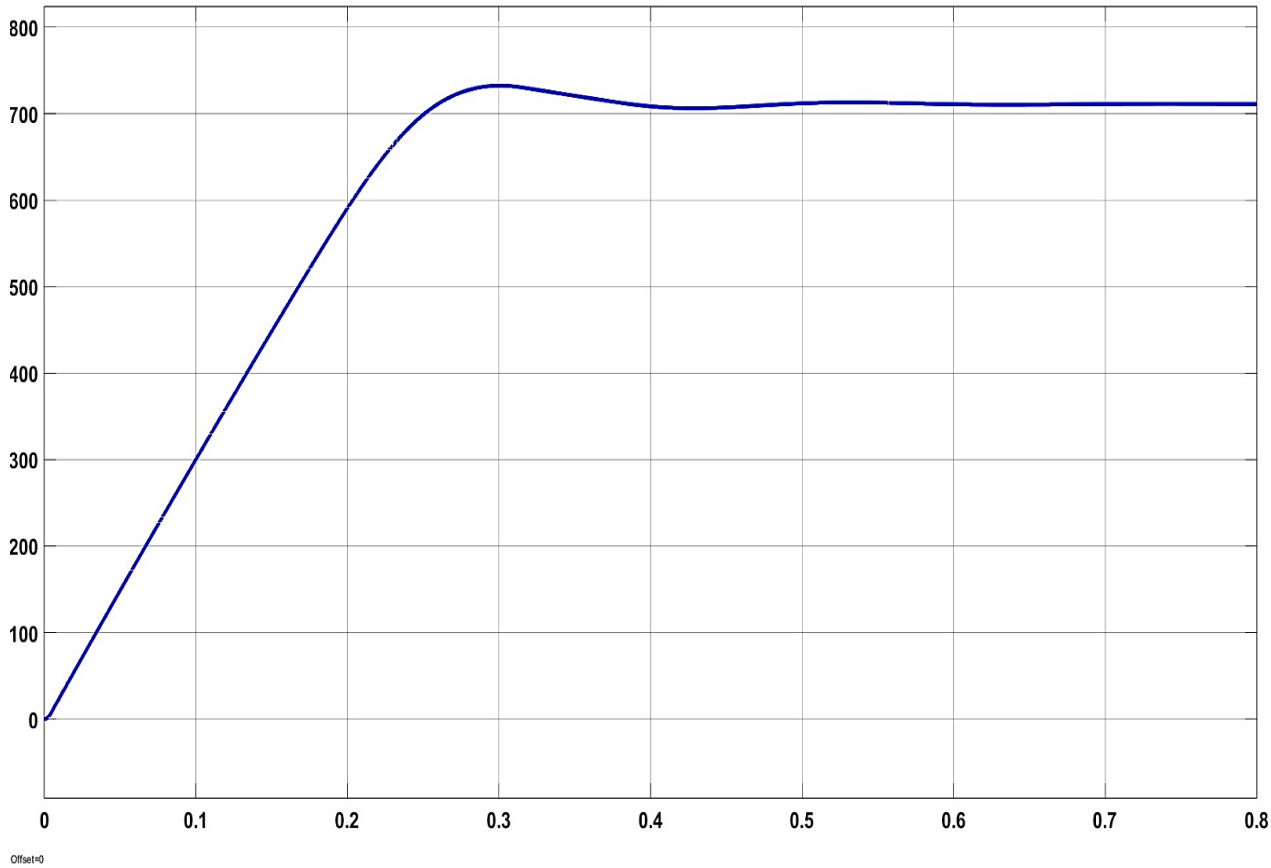

Fig.2.12: Output voltage curve of PV array block simulation using Boost Converter

Thus, for an input of 355.7V to the boost converter having a duty ratio (D) of 0.5, ideally output should have been 711.4V but here we are obtaining 711.1V so we are getting a slight offset from desired result which can be compensated by using double-loop PI controller.

Chapter 3

Small Signal AC Equivalent Model and Double-Loop PI-compensation of Boost Converter

3.1 Simulation of Boost Converter:

A brief overview and the description of DC-DC Boost converter is discussed in Section This section presents a simulation of a DC-DC Boost converter circuit using MATLAB Simulink platform.

It is already discussed how a boost converter steps up the input DC voltage to a higher output voltage by storing energy in an inductor during the "on" phase of a switch and releasing it through a diode and capacitor during the "off" phase. The output voltage V_{out} is given by the equation.

$$V_{out} = \frac{V_{in}}{1-D}$$, (as derived in eqn (1.6))

where V_{in} is the input voltage and D is the duty cycle (the fraction of time the switch is "ON"). As D increases, the output voltage increases.

In MATLAB Simulink a boost converter is implemented, using specific component values for the inductor, capacitor, and load resistance. The pulse generator provided the control signal to the switch, defining the duty cycle for the converter.

The parameters values considered for simulation are as follows:

- Input DC voltage(V_{in}) = 15V
- Inductor(L)=8mH
- Capacitor(C)=8μF
- Resistor(R)=200Ω
- Duty ratio(D)=0.5, i.e. hence, $D' = (1 - D) = 0.5$

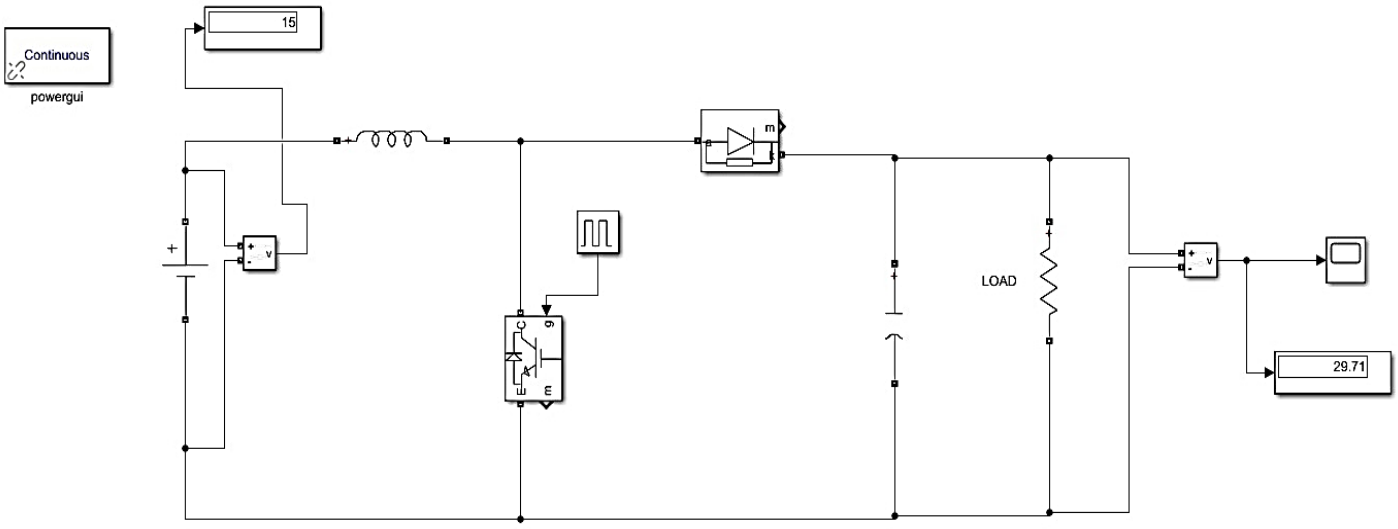

Fig.3.1: A DC-DC boost converter MATLAB Simulink model

So, here we can see that 15V DC voltage is steeped up into 29.71V due to given duty ratio of 0.5. Ideally it should had been 30V, so an offset can be seen here. The output voltage response is shown in Figure 3.1

Due to the presence of offset in output, PI compensation in boost converter is done to reduce output voltage offset by adjusting the control loop to improve stability and response. This ensures that the output voltage quickly aligns with the desired setpoint, minimizing steady-state errors and enhancing overall performance. Thus, obtaining small signal AC model of a boost converter is the primary step towards PI compensation.

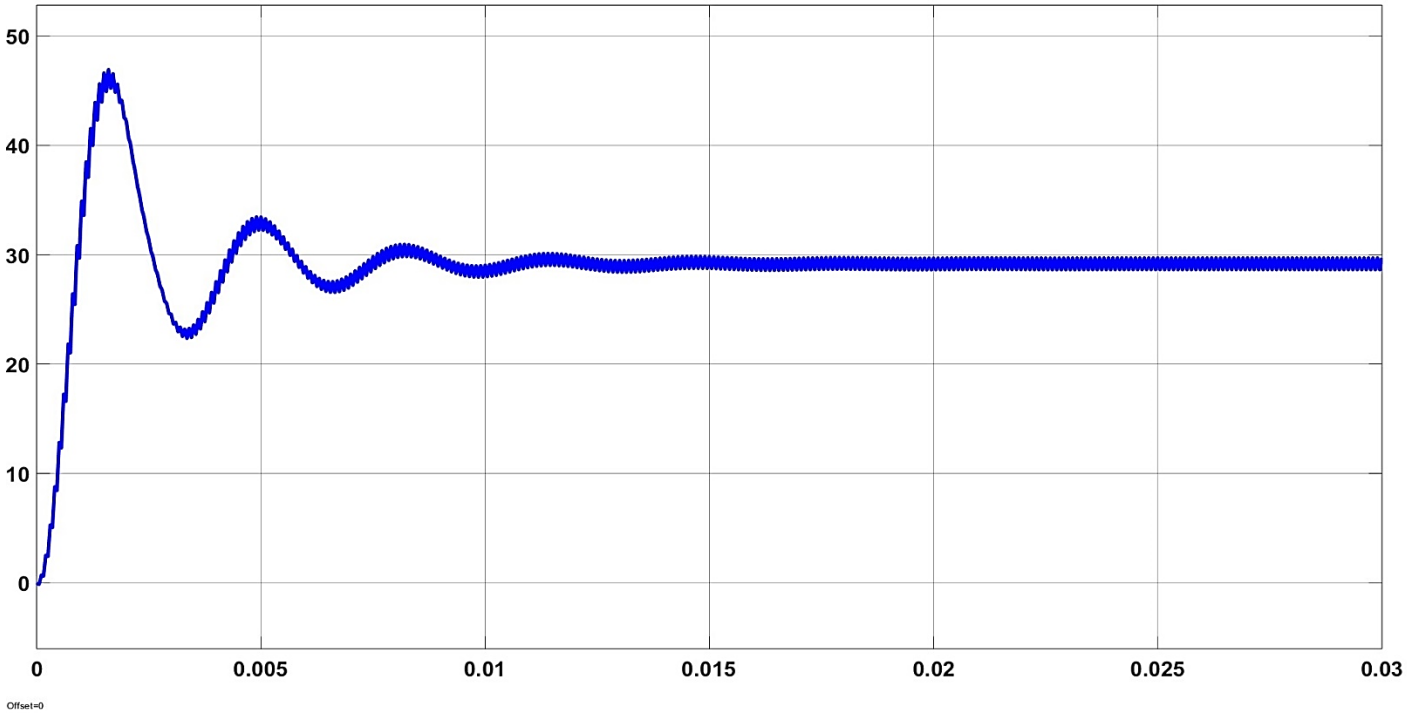

Fig.3.2: Output voltage response of Fig.8 simulation

3.2 Small signal AC model of a Boost Converter:

A boost converter circuit is considered with symbols having usual meanings:

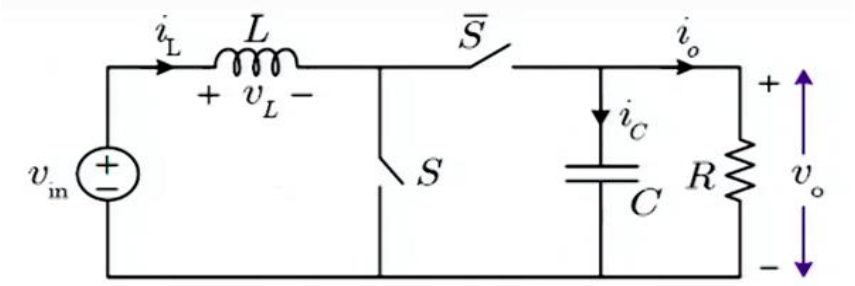

Fig.3.3: A DC-DC boost converter circuit diagram

Now, there can be two conditions with S-ON and S-OFF. Analysing both conditions:

1. <u>With S-ON and $\overline{S}$-OFF</u>:

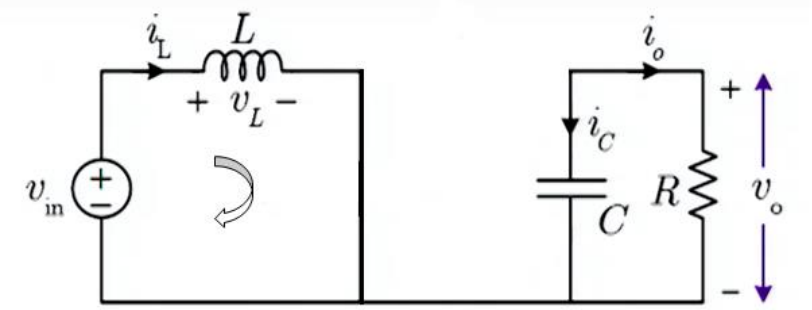

Fig.3.4: Switch-ON condition

By applying KVL in the left loop of Fig-11 we get,

$$L\frac{di_L}{dt} = v_{in} \quad \ldots\ldots\ldots (3.1)$$

Whereas, from the right loop of same Fig we get,

$$i_C = C\frac{dv_C}{dt} = -i_o = -\frac{v_o}{R} \quad \ldots\ldots\ldots (3.2)$$

By small ripple approximation we can write the above two equations as [28]:

$$v_L = L\frac{di_L}{dt} = < v_{in} >_{T_s} \quad \ldots\ldots\ldots (3.3)$$

$$and \;\; i_C = C\frac{dv_C}{dt} = -\frac{< v_o >_{T_s}}{R} \quad \ldots\ldots\ldots (3.4)$$

This < > signifies the average value of the voltage or current present inside it.

In this case the input current $i_{in} = i_L$ ..... (3.5)

2. With $\bar{S}$-ON and S-OFF :

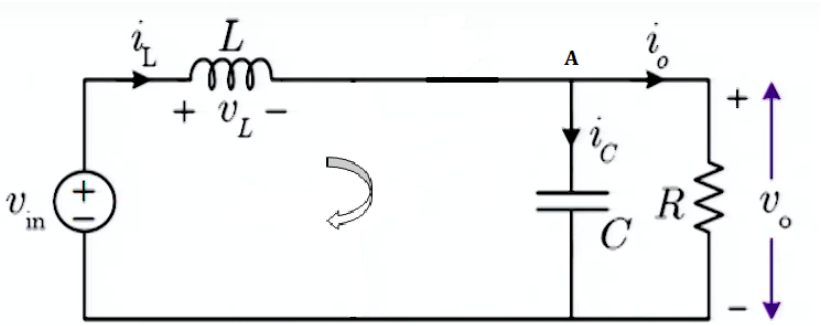

Fig.3.5: Switch-OFF condition

By KVL in the loop shown above we get:

$$L\frac{di_L}{dt} = v_{in} - v_o \quad \ldots\ldots\ldots (3.6)$$

By KCL at node A we get:

$$i_C = i_L - i_o = i_L - \frac{v_o}{R} \quad \ldots\ldots\ldots (3.7)$$

By small ripple approximation we can write the above two equations as [28]:

$$v_L = L\frac{di_L}{dt} = < v_{in} >_{T_s} - < v_o >_{T_s} \quad \ldots\ldots\ldots (3.8)$$

$$and \quad i_C = C\frac{dv_C}{dt} = < i_L >_{T_s} - \frac{< v_o >_{T_s}}{R} \quad \ldots\ldots\ldots (3.9)$$

In this case also the input current $i_{in} = i_L$ ……(3.10)

Now, by averaging the inductor voltage, capacitor current and input current from the above two cases conditions we get [28]:

- Inductor voltage: $< v_L >_{T_s} = < v_{in} >_{T_s} - (1-d) < v_o >_{T_s}$ ……(3.11)

'd' signifies the average duty cycle, (1-d) is multiplied with $< v_o >_{T_s}$ because it exists only when S-OFF

- Capacitor current: $< i_C >_{T_s} = (1-d) < i_L >_{T_s} - \frac{<v_o>_{T_s}}{R}$ ……(3.12)

(1-d) is multiplied with $< i_L >_{T_s}$ because it exists only when S-OFF

- Input current: $< i_{in} >_{T_s} = < i_L >_{T_s}$ ……(3.13)

Considering some superimposed small AC variations over DC quiescent values:

$$< v_{in} >= V_{in} + \hat{v}_{in}; < i_L >= I_L + \hat{\imath}_L; d = D + \hat{d}; < v_0 >= V_0 + \hat{v}_0; < i_{in} >= I_{in} + \hat{\imath}_{in}$$

Next, the non-linear models needs to be linearized [28].

- Perturbation of Inductor voltage equation:

$$< v_L >_{T_s} = L\frac{d < i_L >_{T_s}}{dt} = < v_{in} >_{T_s} - (1-d) < v_o >_{T_s} \quad \ldots\ldots\ldots (3.14)$$

$$=> L\frac{d(I_L + \widehat{\imath_L})}{dt} = (V_{in} + \widehat{v_{in}}) - \left(1 - \left(D + \hat{d}\right)\right)(V_o + \widehat{v_o}) \quad \ldots\ldots\ldots (3.15)$$

By solving we get:

$$L\frac{d\widehat{\imath_L}}{dt} = (V_{in} + \widehat{v_{in}}) + \hat{d}V_o - (1-D)[\,V_o + \widehat{v_o}] \quad \ldots\ldots\ldots (3.16)$$

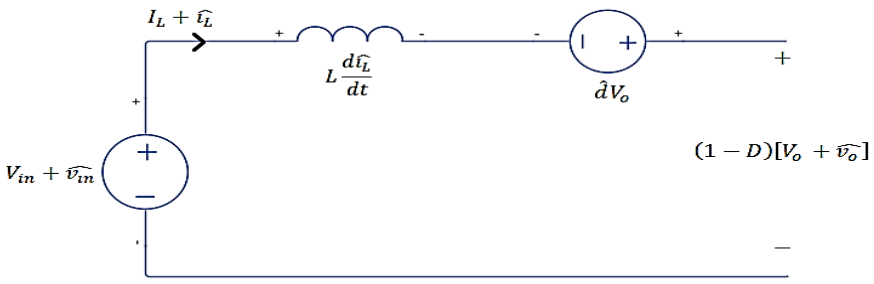

Fig.3.6: Inductor loop equation model

- Perturbation of Capacitor current equation:

$$< i_C >_{T_s} = C\frac{d < v_o >_{T_s}}{dt} = (1-d) < i_L >_{T_s} - \frac{< v_o >_{T_s}}{R} \quad \ldots\ldots\ldots (3.17)$$

$$=> C\frac{d(V_o + \widehat{v_o})}{dt} = \left(1 - (D + \widehat{d})\right)[I_L + \widehat{i_L}] - \frac{V_o + \widehat{v_o}}{R} \quad \ldots\ldots\ldots (3.18)$$

By solving we get:

$$C\frac{d\widehat{v_o}}{dt} = (1-D)[I_L + \widehat{i_L}] - \hat{d}I_L - \frac{V_o + \widehat{v_o}}{R} \quad \ldots\ldots\ldots (3.19)$$

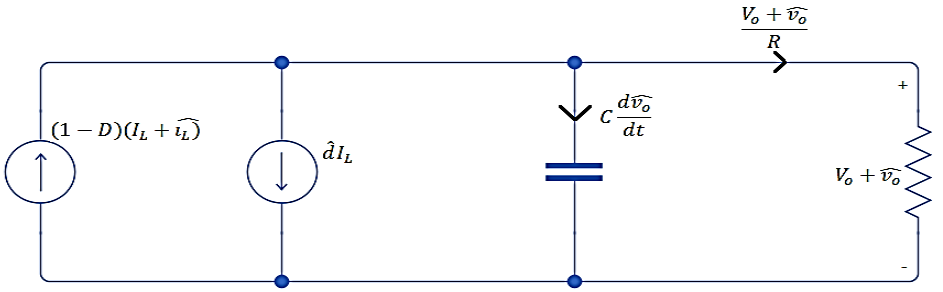

Fig.3.7: Capacitor node equation model

- Input current equation

$$< i_{in} > =< i_L >_{T_s} \quad \ldots\ldots\ldots (3.20)$$

$$=> \; I_{in} + \widehat{i_{in}} = I_L + \widehat{i_L} \quad \ldots\ldots\ldots (3.21)$$

Figures-13 and 14 and the input current equation can be now combined to form a circuit as:

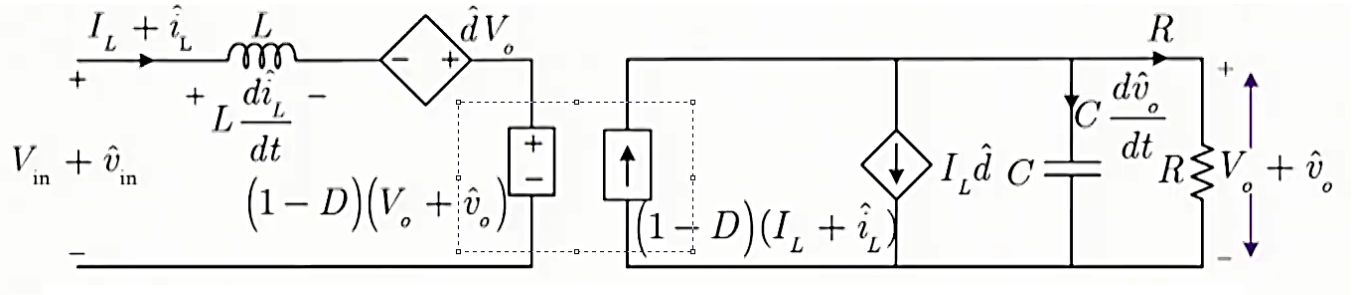

Fig.3.8 : Small signal equivalent circuit model of boost converter (without DC Transformer)

Where, the circuits can be joined by replacing the dotted portion with DC-Transformer[28]

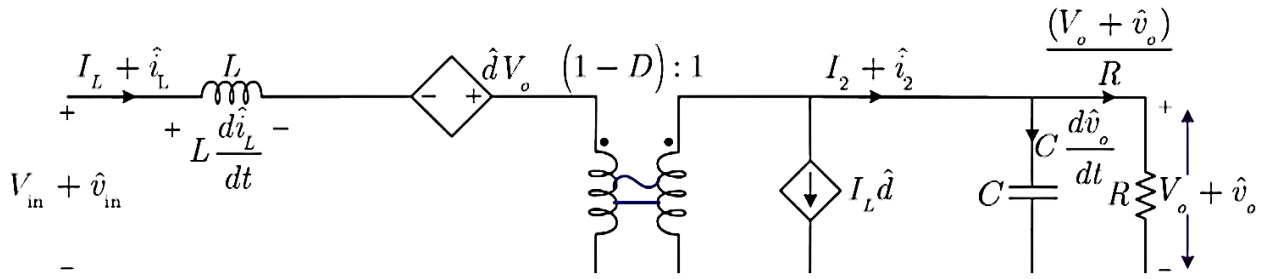

Fig.3.9: Small signal equivalent circuit model of boost converter

Thus, the AC equivalent model will be as shown in Fig. 3.10:

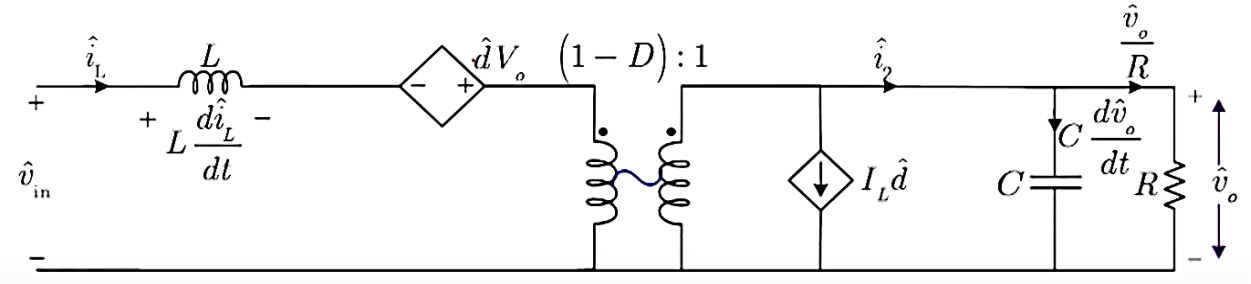

Fig.3.10: Small signal AC equivalent circuit model of boost converter

3.3 PI Compensation of Boost Converter:

Single PID control is often insufficient to ensure the dynamic response of both voltage and current outputs simultaneously in systems like DC-DC boost converters. Hence, a double-loop PI controller simplifies the design process as boost converters have a Right Half Plane Zero (RHPZ) structure, making their control complex. So, double-loop control addresses this issue by providing simultaneous control of both voltage and current outputs, especially double-loop PI control helps to maintain stability, especially in the face of disturbances and model uncertainties [29].

Below given are some steps on how to implement double-loop PI compensation on boost converter.

3.3.1 Finding the transfer function:

From the given Fig.3.10 it is clear that $\hat{\mathrm{V}}_{\mathrm{in}}$ and $\hat{\mathrm{d}}$ are two major control inputs of the boost converter.

The output voltage ($\hat{\mathrm{V}}_{\mathrm{o}}$) can be expressed as the superposition of two control inputs as given below [30]:

$$\hat{V}_o(s) = G_{\hat{V}_{in}} * \hat{V}_{in}(s) + G_{\hat{d}} * \hat{d} \qquad \ldots\ldots\ldots (3.22)$$

Now, $G_{\hat{V}_{in}}$ is obtained by keeping one of the control input ($\hat{V}_{in}$) active and at the same time another control input ($\hat{d}$) is deactivated.

Hence, the equivalent circuit after referring primary to secondary side we get:

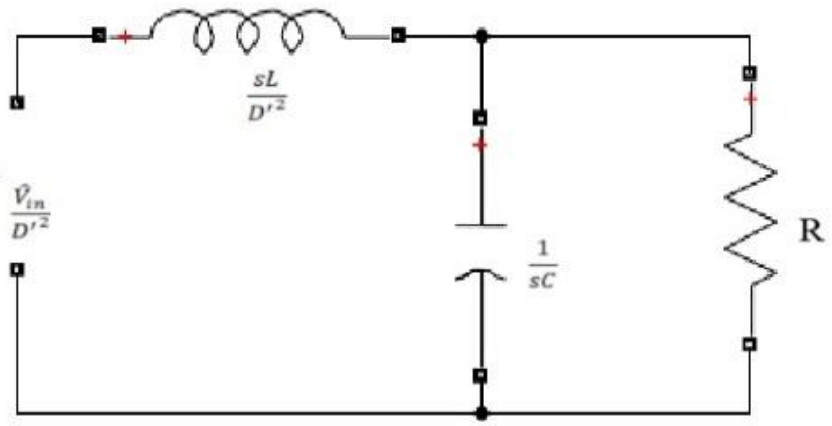

Fig.3.11: Equivalent circuit to find $G_{\hat{v}_{in}}$ after referring primary to secondary side

Voltage Division Rule is applied;

$$\frac{\frac{\hat{V}_o}{\hat{V}_{in}}}{D'} = \frac{R||\frac{1}{sC}}{sLD'^2 + (R||\frac{1}{sC})} \qquad \ldots\ldots\ldots (3.23)$$

Upon simplification, we can say;

$$G_{\hat{V}_{in}} = \frac{\hat{V}_o}{\hat{V}_{in}}\Big|\,(\hat{d}=0) = \frac{RD'}{s^2(LCR) + sL + RD'^2} \qquad \ldots\ldots\ldots (3.24)$$

Now, $G_{\hat{d}}$ is obtained by keeping one of the control input ($\hat{d}$) active and at the same time deactivating another control input ($\hat{V}_{in}$)

Hence, the equivalent circuit after referring primary to secondary side we get;

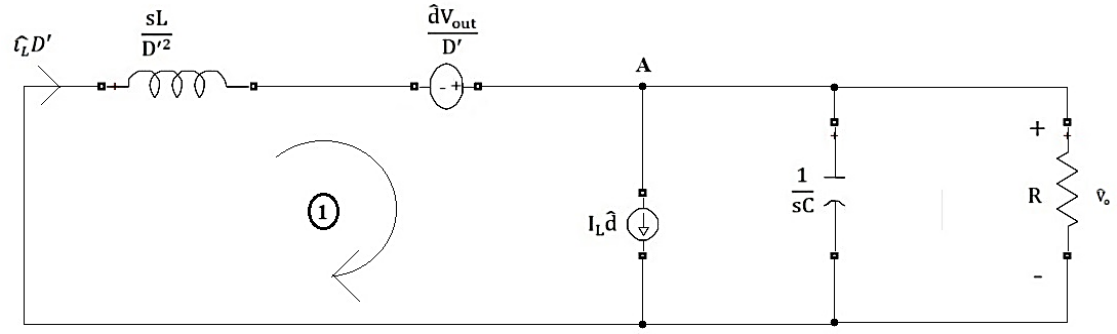

Fig.3.12: Equivalent circuit to find $G_{\hat{d}}$ after referring primary to secondary side

Applying nodal analysis at A;

$$\frac{\hat{V}_o}{R||\frac{1}{sC}} + I_L\hat{d} + \frac{\hat{V}_o - \frac{\hat{d}V_o}{D'}}{\frac{sL}{D'^2}} = 0 \qquad \ldots\ldots\ldots (3.25)$$

Upon simplification we get;

$$G_{\hat{d}} = \frac{\hat{V}_o}{\hat{d}}|(\hat{V}_{in} = 0) = \frac{RD'V_o - sRLI_L}{s^2(LCR) + sL + RD'^2} \qquad \ldots\ldots\ldots (3.26)$$

Now, during the double loop DC-DC boost converter design, the output voltage ($\hat{V}_o$) and the inductor current ($\hat{\imath}_L$) have to be measured. Therefore, the open-loop transfer functions "G_1" and "G_2" are derived respectively in the following equations.

Transfer function "G_1" between inductor current and duty ratio $\frac{\hat{\imath}_L}{\hat{d}}|(\hat{V}_{in} = 0)$ is also obtained from Fig-3.12 by keeping control input ($\hat{d}$) active and at the same time deactivating another control input ($\hat{V}_{in}$).

Applying KCL at point A;

$$-\hat{\imath}_L D' + I_L\hat{d} + \frac{\hat{V}_o}{R||\frac{1}{sC}} = 0 \qquad \ldots\ldots\ldots (3.27)$$

Upon simplification we get;

$$\hat{V}_o = \frac{\hat{\imath}_L R - I_L\hat{d}R}{sRC + 1} \qquad \ldots\ldots\ldots (3.28)$$

Applying KVL at loop 1;

$$\frac{\hat{d}V_o}{D'} - \frac{\hat{\imath}_L sL}{D'^2} - \hat{V}_o = 0 \qquad \ldots\ldots\ldots (3.29)$$

Upon simplification and by replacing $\hat{V}_o$ from eqn. (3.29) we get [29];

$$G_1 = \frac{\hat{\imath}_L}{\hat{d}}|(\hat{V}_{in} = 0) = \frac{sV_oC + 2I_LD'}{s^2LC + \frac{sL}{R} + D'^2} \qquad \ldots\ldots\ldots (3.30)$$

Similarly, transfer function between output voltage and the inductor current "G_2" is obtained from Fig-20;

$$G_2 = \frac{G_{\hat{d}}}{G_1} = \frac{\frac{\hat{V}_o}{\hat{d}}}{\frac{\hat{\imath}_L}{\hat{d}}} = \frac{\hat{V}_o}{\hat{\imath}_L}|(\hat{V}_{in} = 0) = \frac{D'V_o - sLI_L}{sV_oC + 2D'I_L} \qquad \ldots\ldots\ldots (3.31)$$

Substituting values of all defined terms in transfer functions "G_1" and "G_2" they can be expressed as

$$G_1 = \frac{\hat{\imath}_L}{\hat{d}}\left|\left(\hat{V}_{in} = 0\right) = \frac{0.0023544s + 0.3034}{s^2(6.4 * 10^{-8}) + s(0.00004) + 0.25}\right. \quad \ldots\ldots\ldots (3.32)$$

$$G_2 = \frac{\hat{V}_o}{\hat{\imath}_L}\left|\left(\hat{V}_{in} = 0\right) = \frac{14.715 - 0.0024272s}{0.00023544s + 0.3034}\right. \quad \ldots\ldots\ldots (3.33)$$

By observing the transfer function "G_2" it can be said that the outer-loop of boost converter has a Right Half Plane Zero (RHPZ) structure, hence double-loop PI control is applied to ease the complexity that occurs due to presence of a Right Half Plane Zero.

3.3.2 Double-loop Control:

Double-loop control is implemented using PI controllers for both the current (inner-loop) as well as the voltage (outer-loop). The PI parameters are calculated to ensure that the system response meets desired transient characteristics. Firstly, inner current loop is compensated with the help of PI controller "C_1" and then the outer-loop is compensated with the help of PI controller "C_2" which is attached to outer-loop.

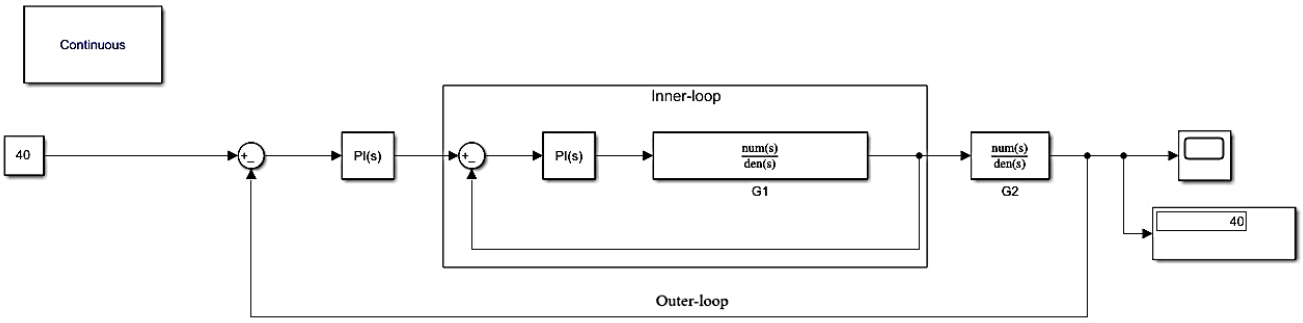

Fig-3.13: Double-loop PI structure of a boost converter in continuous time

Inner-loop transfer function "G_1" is compensated by using PI controller "C_1" such that,

$$C_1 = K_{P_1} + \frac{K_{I_1}}{s} = 0.10339 + \frac{1.0339}{s} \quad \ldots\ldots\ldots (3.34)$$

Next, the outer-loop is compensated by using the PI controller "C_2"

$$C_2 = K_{P_2} + \frac{K_{I_2}}{S} = 0.01561 + \frac{0.09395}{s} \quad \ldots\ldots\ldots (3.35)$$

Compensating both the inner-loop and outer-loop with the help of PI controllers "C_1" and "C_2" respectively, we are able to obtain a stable output which follows the reference accurately, as shown in Fig.3.14 , which can be observed through both the scope output and the display.

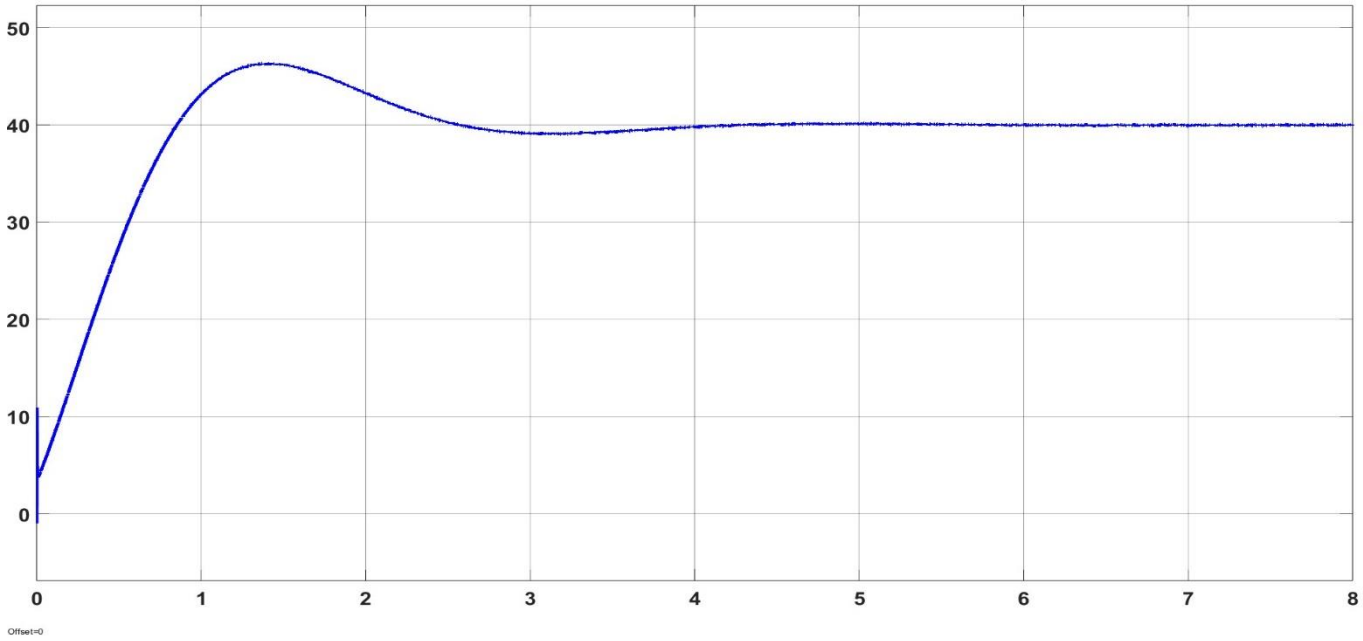

Fig-3.14 : Response of double-loop PI compensation of boost converter in continuous time

In order to, discretize the entire system a sample time of $T_s = 2.5\times10^{-6}$ seconds is chosen. The choice is made to incorporate 10 samples per 40kHz switching frequency of the converter.

After discretization, Inner-loop transfer function can be written as,

$$G_1(z) = \frac{0.091911z - 0.091911}{z^2 - 1.998z + 0.9984} \qquad \text{.....(3.36)}$$

Similarly, outer-loop transfer function can be written as,

$$G_2(z) = \frac{-10.279z + 10.433}{z - 0.9968} \qquad \text{.....(3.37)}$$

Inner-loop transfer function "G_1" is compensated by using PI controller "C_1" such that,

$$C_1 = K_{P_1} + K_{I_1}\frac{T}{z-1} = 24.962 + \frac{14.3332}{z-1} \qquad \text{... ... ... (3.38)}$$

Consequently, the outer-loop is compensated by using the PI controller "C_2"

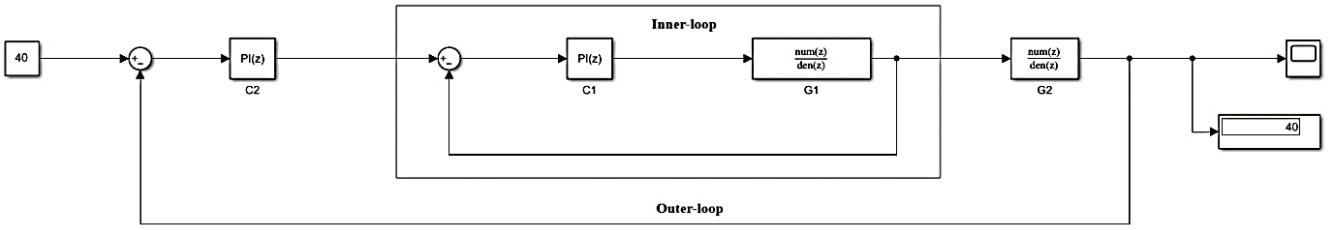

Fig.3.15: Double-loop PI structure of a boost converter in discrete time

$$C_2(z) = K_{P_2} + K_{I_2}\frac{T}{z-1} = 0.037037 + \frac{137 * 10^{-6}}{z-1} \quad \ldots\ldots\ldots (3.39)$$

Thus, the output response can be seen by the help of a scope which shows successful PI compensation after discretization of the plant,

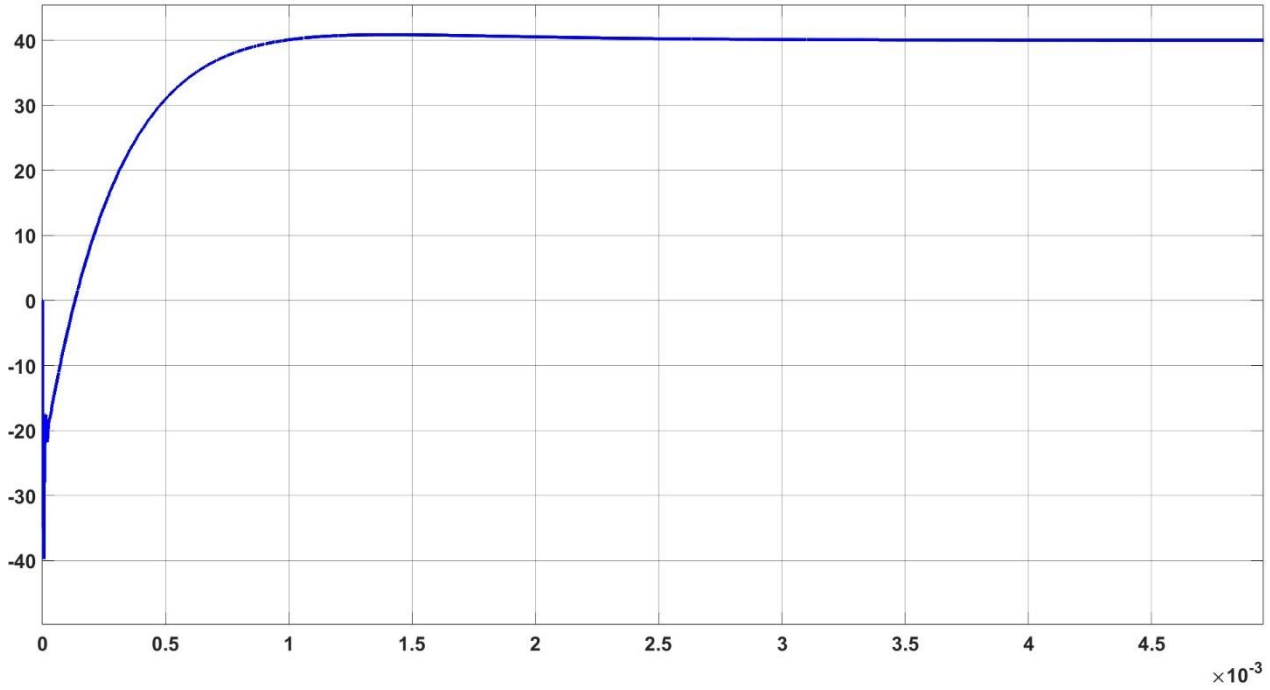

Fig.3.16(a): Response of double-loop PI compensation of boost converter in discrete time

The root locus of the OLTF of double-loop PI-compensation structure of the boost converter block is:

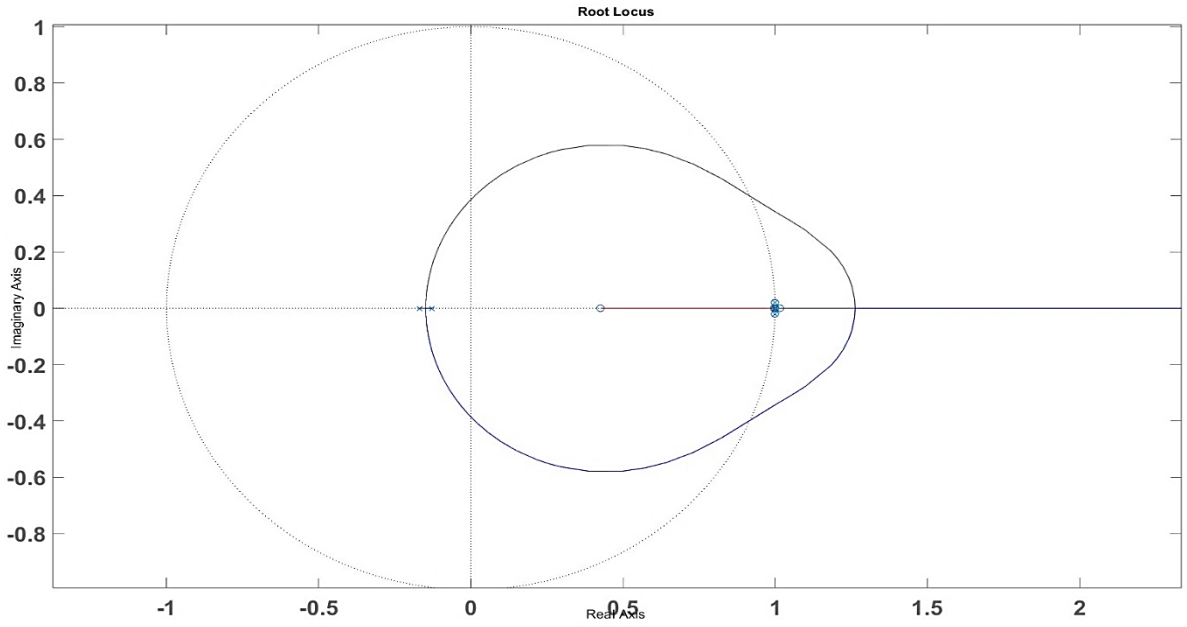

Fig.3.16(b): Root Locus of OLTF of double-loop PI-compensation structure

As can be obtained from the root locus the critical gain K_{cr}=0.0858 and loop gain(K)=0.037037,

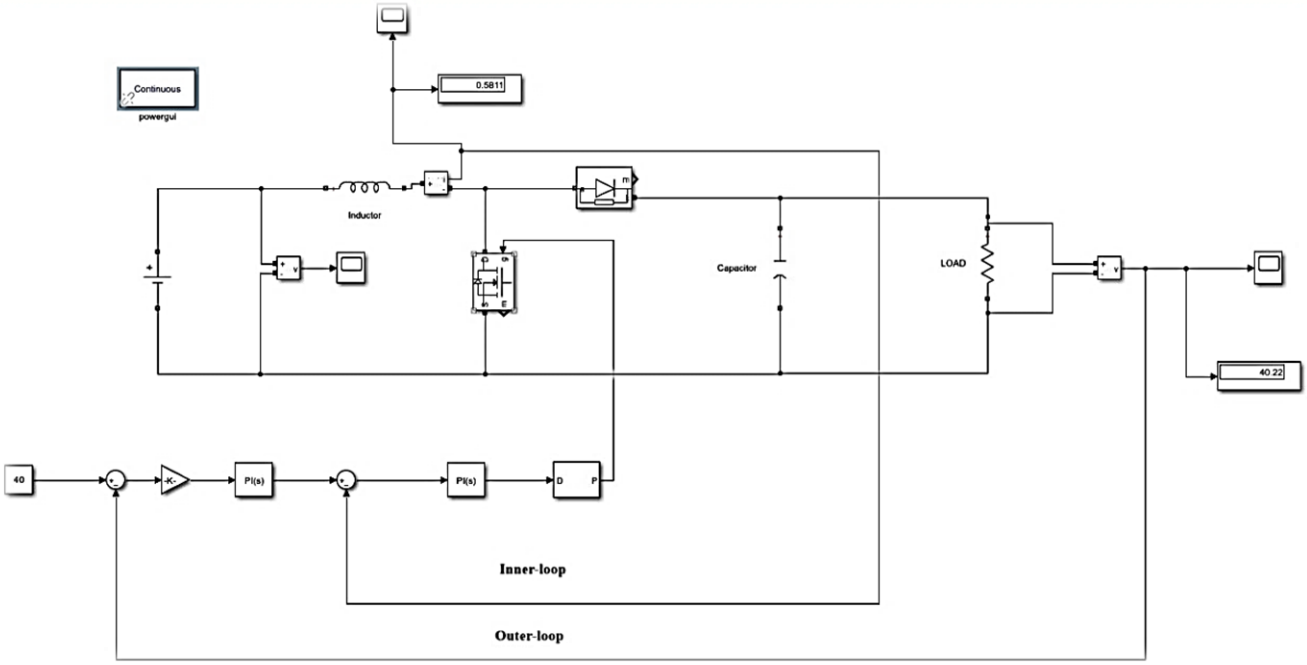

Fig.3.17: Simscape model of double-loop PI compensation of boost converter

thus GM=K_{cr}/K=2.3177 i.e. the maximum gain for stability for the double-loop PI-compensated system will be 2.3177.

Now, the double loop PI controller is implemented in Simscape model of the Boost converter by taking current and voltage measurement for inner-loop and outer-loop, respectively and keeping all the values of different components intact [29].

Keeping the PI controller gain same as we kept for continuous transfer function in both inner-loop as well as outer-loop, such as

$$C_1 = K_{P_1} + \frac{K_{I_1}}{s} = 0.10339 + \frac{1.0339}{s} \quad \ldots\ldots\ldots (3.40)$$

$$C_2 = K_{P_2} + \frac{K_{I_2}}{S} = 0.01561 + \frac{0.09395}{s} \quad \ldots\ldots\ldots (3.41)$$

The output response tries to follow the reference value as shown in Fig.3.18

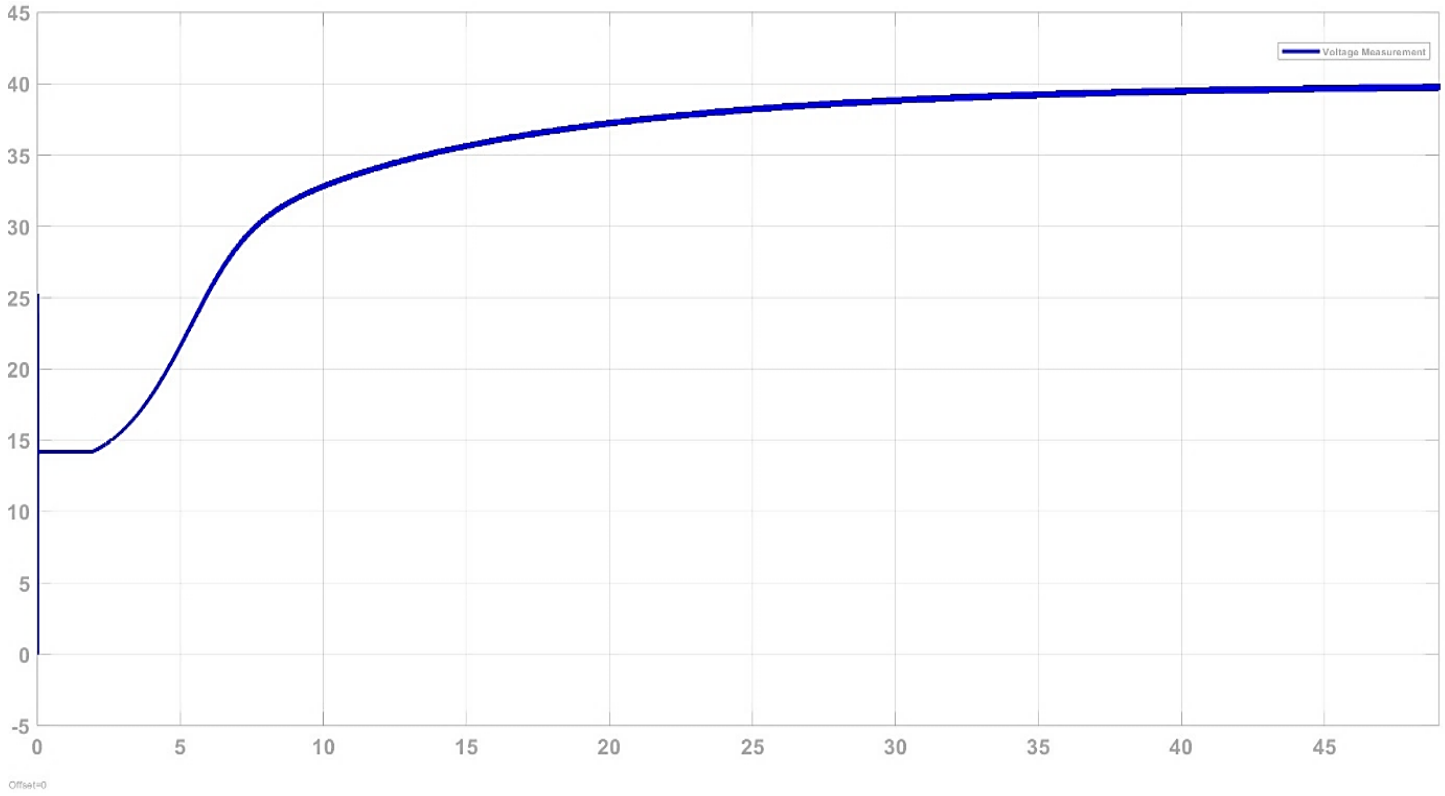

Fig.3.18: Response of Simscape model of double-loop pi compensation of boost converter

Hence, we can say from these responses it is evident that after double-loop PI compensation of boost converter the output tries to follow the reference given.

3.3.3 Limitations of Double-loop PI compensation

Despite advantages of double-loop PI compensation they do have some limitations, such as:

1. Open loop zeros cannot be placed arbitrarily.
2. Robust compensation cannot be achievable for the plant with NMP poles and zeros.
3. Arbitrary high GM cannot be achieved, due to the presence of NMP zeros.
4. Pole-zero cancellation cannot be used for safeguarding the internal stability.

Hence, in the next chapter details about 2-periodic time-varying controller is discussed that has advantages over double-loop PI compensation to stabilize the plant as well as to improve its robustness.

Chapter 4

Analysis of Discrete-time 2-periodic Controller

4.1 Introduction

From the limitations of double-loop PI controller it is evident that LTI controller faces certain limitations to compensate LDTI plant having NMP zero(s) as such zeros cannot be changed using the LDTI controllers resulting in a limited Gain Margin (GM) for compensated system. On the other hand, due to periodic changes in the parameters of periodic controllers, the system dynamics will be changed which results in relocation of the loop zeros arbitrarily [31].

In this chapter, firstly the analysis of the SISO, LDTI system using time-lifted reformulation has been described. Then a two-stage algorithm for controller synthesis for loop-zero-placement under some conditions has been represented. Finally, the conditions to eliminate the steady state ripple have been discussed [30].

4.2 Analytical techniques for discrete 2-periodic systems

The system dynamics of discrete time-varying plants is expressed using a difference equation with coefficients varying periodically with time. There are several approaches available for dealing with periodic systems. These are - Time-lifted reformulation method, Frequency-lifted reformulation method, Cyclic reformulation method and Floquet theory approach. The reformulation techniques are described as follows:

1. **Time-lifted Reformulation method**: In the time-lifted reformulation approach, periodic systems are lifted to larger LDTI forms. The main idea of this technique is to split the time axis into M parts for an M-periodic system, considering each part as an individual LTI system. An m-input n-output M-periodic system is represented by an (m×M)-input-(n×M)-output LTI system [32].
2. **Frequency-lifted Reformulation method**: In this reformulation method, the input and output signals of a M-periodic system may each be expressed by a discrete Fourier series having the fundamental and (M-1) higher harmonic components. Also a time-invariant transfer matrix is generated from the expression [30].
3. **Cyclic Reformulation method:** For an M-periodic signal, one sample is picked up per period and represented as an M×1 vector. The position of the sample in the vector is shifted as time proceeds. After completion of each consecutive period, an M×M transfer matrix is formed [30].
4. **Floquet Theory:** Floquet theory approach is a characteristic equation based approach. The characteristic equations of periodic coefficient difference equations are obtained in terms of the discrete Fourier coefficients of the periodic parameters using this theory.

The generalized design technique of 2-periodic control has been proposed in the next section**.**

4.3 2-Periodic controller

For an n-th order, SISO, LDTI plant $G(z) = k\frac{b(z)}{a(z)}$, r < n, with

$$a(z) = z^n + a_{n-1}z^{n-1} + \cdots + a_1 z + a_0 \quad \ldots\ldots\ldots (4.1)$$

$$b(z) = b_r z^r + b_{r-1}z^{r-1} + \cdots + b_1 z + b_0 \quad \ldots\ldots\ldots (4.2)$$

A m-th order M-periodic controller with maximum degrees of freedom can be expressed as,

$$y_i(N+1) = y_{i+1}(N) \quad \ldots\ldots\ldots (4.3)$$

For, i = 0,1,2, … $(m-1)$

$$y_m(N) = L(N)e(N) - \sum_{i=0}^{m-1} C_i(N)y_i(N) \quad \ldots\ldots\ldots (4.4)$$

$$u(N) = \sum_{i=0}^{m} D_i(N)y_i(N) \quad \ldots\ldots\ldots (4.5)$$

where, $e(N)$ = input of the controller,

$u(N)$ = output of the controller,

$L(N)$ = gain (nominally $L(N) = 1$),

$C_i(N)$ = feedback gains,

$D_i(N)$ = feedforward gains.

$C_i(N)$ and $D_i(N)$ can be described in the form of discrete Fourier series as [33],

$$C_i(N) = C_i(N+M) = \sum_{k=0}^{M-1} \alpha^{kN} c_{ik} \quad \ldots\ldots\ldots (4.6)$$

For, $i = 0,1,2, \ldots, (m-1)$

$$D_i(N) = D_i(N+M) = \sum_{k=0}^{M-1} \alpha^{kN} d_{ik} \quad \ldots\ldots\ldots (4.7)$$

For, $i = 0,1,2, \ldots, m$

$$\alpha = e^{\frac{j2\pi}{M}} \quad \ldots\ldots\ldots (4.8)$$

The equivalent periodic coefficient transfer function corresponding to the controller is [33],

$$C(z,N) = [Q(z,N)][P(z,N)]^{-1} \quad \ldots\ldots\ldots (4.9)$$

$$C(z,N) = [D_m(N)z^m + D_{m-1}(N)z^{m-1} + \cdots + D_1(N)z + D_0(N)][z^m + C_{m-1}(N)z^{m-1} + \cdots + C_1(N)z + C_0(N)]^{-1} \ldots\ldots\ldots (4.10)$$

Consider, following [17], the 2-periodic, m-th order controller shown in Fig.4.1, where D_i and C_i are 2-periodically time varying gains, which can be described in the form of discrete Fourier series as,

$$D_i(N) = d_{i,0} + (-1)^N d_{i,1}, \quad i = 0,1, \ldots m \quad \ldots\ldots\ldots (4.11)$$

$$C_i(N) = c_{i,0} + (-1)^N c_{i,1}, \quad i = 0,1, \ldots (m-1) \quad \ldots\ldots\ldots (4.12)$$

From eq.(4.9) and (4.10) we can write:

$$Q(z,N) = [D_m(N)z^m + D_{m-1}(N)z^{m-1} + \cdots + D_1(N)z + D_0(N)] \ldots\ldots\ldots (4.13)$$

and;

$$P(z,N) = z^m + C_{m-1}(N)z^{m-1} + \cdots + C_1(N)z + C_0(N) \ldots\ldots\ldots (4.14)$$

With

$$Q(z,N) \triangleq Q_0(z) + (-1)^N Q_1(z)$$

$$= \left[d_{m,0}z^m + \cdots + d_{0,0}\right] + (-1)^N\left[d_{m,1}z^m + \cdots + d_{0,1}\right] \ldots\ldots\ldots (4.15)$$

$$P(z,N) \triangleq P_0(z) + (-1)^N P_1(z)$$

$$= \left[z^m + c_{m-1,0}z^{m-1} + \cdots + c_{0,0}\right] + (-1)^N\left[c_{m-1,1}z^{m-1} + \cdots + c_{0,1}\right] \ldots\ldots\ldots (4.16)$$

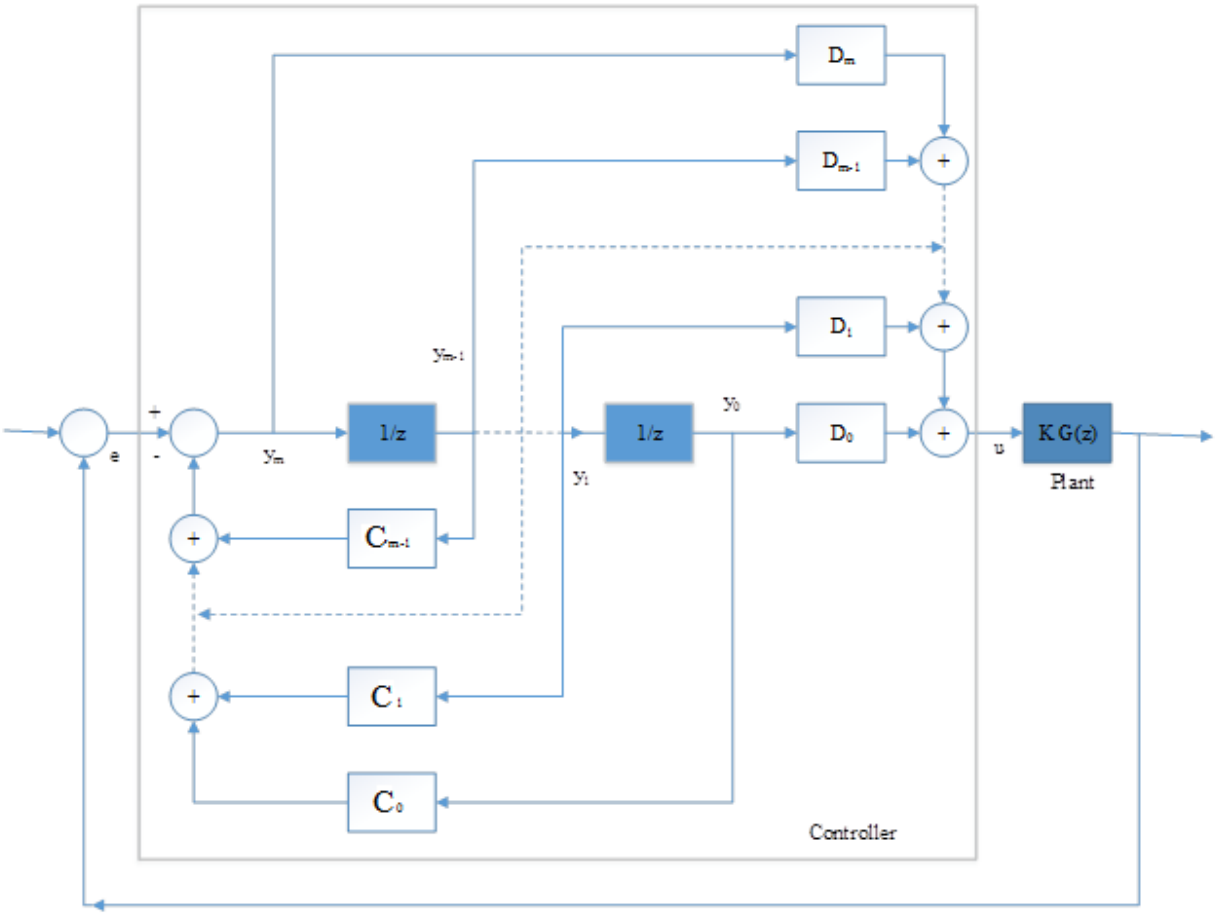

Fig.4.1:The 2-Periodic controller in 1-DOF form and the LTI plant [30]

Out of several analytical techniques reported in the literature here we will focus on Time-lifted Reformulation method in the next part.

4.3.1 Time-lifting method

Time-domain lifting technique has the advantage of representing a SISO M-periodic system to an equivalent M-input M-output LDTI system, producing a M×M transfer matrix. It is to be

noted that any LDTI system can be considered to be a 2-Periodic one and consequently it can be transformed into a MIMO time-invariant form [33].

In 2-periodic system, coefficients of all the even and odd instants are similar. So, a SISO, causal, 2-periodic map g can be lifted to a 2-input 2-output time invariant representation. As a result, it makes the lifted system expressed as even and odd LDTI systems [33].

Let us consider e(0), e(1), e(2),..... be the sequence of inputs and u(0), u(1), u(2),….. be the corresponding output sequences. Now, lifting the system to even and odd instants inputs and outputs and representing them in the transform domain as [33],

$$E_e(z^2) = \sum_{i=0}^{\infty} z^{-2i} e(2i) \quad \ldots\ldots\ldots (4.17)$$

$$z^{-1}E_o(z^2) = \sum_{i=0}^{\infty} z^{-2i-1} e(2i+1) \quad \ldots\ldots\ldots (4.18)$$

$$U_e(z^2) = \sum_{i=0}^{\infty} z^{-2i} u(2i) \quad \ldots\ldots\ldots (4.19)$$

$$z^{-1}U_o(z^2) = \sum_{i=0}^{\infty} z^{-2i-1} u(2i+1) \quad \ldots\ldots\ldots (4.20)$$

The even and odd instant input and output sequences can be written as,

$$E(z) = E_e(z^2) + z^{-1}E_o(z^2) \quad \ldots\ldots\ldots (4.21)$$

$$U(z) = U_e(z^2) + z^{-1}U_o(z^2) \quad \ldots\ldots\ldots (4.22)$$

where,

$E(z)$ = The z-transform of complete input sequence,

$E_e(z^2)$ = The z-transform of even instant of the input sequence

$z^{-1}E_0(z^2)$= The z-transform of even instant of the input sequence,

$U(z)$ = The z-transform of complete output sequence,

$U_e(z^2)$ = The z-transform of even instant of the output sequence,

$z^{-1}U_0(z^2)$ = The z-transform of even instant of the output sequence.

Now, the even and odd instant outputs can be linked to the even and odd instant inputs as,

$$\begin{bmatrix} U_e(z^2) \\ z^{-1}U_o(z^2) \end{bmatrix} = \tilde{G}(z^2) \begin{bmatrix} E_e(z^2) \\ z^{-1}E_o(z^2) \end{bmatrix} \quad \ldots\ldots\ldots (4.23)$$

with,

$$\tilde{G}(z^2) = \begin{bmatrix} G_{11}(z^2) & z^{-1}G_{12}(z^2) \\ z^{-1}G_{21}(z^2) & G_{22}(z^2) \end{bmatrix} \quad \ldots\ldots\ldots (4.24)$$

Where each G_{ij} (for i, j = 1,2) is a LDTI, proper transfer function in z^2.

$\tilde{G}(z^2)$ is the lifted LDTI transfer matrix that satisfies the causality condition that $\tilde{G}(\infty)$ is lower triangular, which is the necessary and sufficient condition for the transfer function to be realizable as SISO 2-periodic system.

4.3.2 Closed Loop Characteristic Equation

Let, for any polynomial $f(z)$, $f^{+}=f(z)$ and $f^{-}=f(-z)$.

Time domain lifting theory is applied to the controller and the plant. The transfer matrix of the polynomial $Q(z)$ becomes

$$\bar{Q}(z^2) = \begin{bmatrix} Q_{11}(z^2) & z^{-1}Q_{12}(z^2) \\ zQ_{21}(z^2) & Q_{22}(z^2) \end{bmatrix} \ldots\ldots\ldots (4.25)$$

Where,

$$Q_{11} = Q_0^+ + Q_0^- + Q_1^+ + Q_1^- \quad \ldots\ldots\ldots (4.26)$$

$$Q_{12} = Q_0^+ - Q_0^- + Q_1^+ - Q_1^- \quad \ldots\ldots\ldots (4.27)$$

$$Q_{21} = Q_0^+ - Q_0^- - Q_1^+ + Q_1^- \quad \ldots\ldots\ldots (4.28)$$

$$Q_{22} = Q_0^+ + Q_0^- - Q_1^+ - Q_1^- \quad \ldots\ldots\ldots (4.29)$$

The lifted transfer matrix of the polynomial P(z) becomes,

$$\bar{P}(z^2) = \frac{1}{2}\begin{bmatrix} P_{11}(z^2) & z^{-1}P_{12}(z^2) \\ zP_{21}(z^2) & P_{22}(z^2) \end{bmatrix} \quad \ldots\ldots\ldots (4.30)$$

Where,

$$P_{11} = P_0^+ + P_0^- + P_1^+ + P_1^- \quad \ldots\ldots\ldots (4.31)$$

$$P_{12} = P_0^+ - P_0^- + P_1^+ - P_1^- \quad \ldots\ldots\ldots (4.32)$$

$$P_{21} = P_0^+ - P_0^- - P_1^+ + P_1^- \quad \ldots\ldots\ldots (4.33)$$

$$P_{22} = P_0^+ + P_0^- - P_1^+ - P_1^- \quad \ldots\ldots\ldots (4.34)$$

As we know, controller transfer function is $C(z,N)= [Q(z)][P(z)]^{-1}$

So, from (4.25) and (4.30),

$$\bar{C}(z^2) = \frac{1}{\Delta_c}\begin{bmatrix} C_{11}(z^2) & z^{-1}C_{12}(z^2) \\ zC_{21}(z^2) & C_{22}(z^2) \end{bmatrix} \quad \ldots\ldots\ldots (4.35)$$

Where,

$$\Delta_c = 4(P_0^+P_0^- - P_1^+P_1^-) \quad \ldots\ldots\ldots (4.36)$$

$$C_{11} = Q_0^+P_0^- + Q_0^-P_0^+ - Q_0^+P_1^- - Q_0^-P_1^+ + Q_1^+P_0^- + Q_1^-P_0^+ - Q_1^+P_1^- - Q_1^-P_1^+ \quad \ldots\ldots\ldots (4.37)$$

$$C_{12} = Q_0^+P_0^- - Q_0^-P_0^+ + Q_0^+P_1^- - Q_0^-P_1^+ + Q_1^+P_0^- - Q_1^-P_0^+ + Q_1^+P_1^- - Q_1^-P_1^+ \quad \ldots\ldots\ldots (4.38)$$

$$C_{21} = Q_0^+P_0^- - Q_0^-P_0^+ - Q_0^+P_1^- + Q_0^-P_1^+ - Q_1^+P_0^- + Q_1^-P_0^+ + Q_1^+P_1^- - Q_1^-P_1^+ \quad \ldots\ldots\ldots (4.39)$$

$$C_{22} = Q_0^+P_0^- + Q_0^-P_0^+ + Q_0^+P_1^- + Q_0^-P_1^+ - Q_1^+P_0^- - Q_1^-P_0^+ - Q_1^+P_1^- - Q_1^-P_1^+ \quad \ldots\ldots\ldots (4.40)$$

Now, the lifted transfer matrix of the plant is,

$$\bar{G}(z^2) = \frac{1}{\Delta_G}\begin{bmatrix} G_{11}(z^2) & z^{-1}G_{12}(z^2) \\ zG_{21}(z^2) & G_{22}(z^2) \end{bmatrix} \quad \ldots\ldots\ldots (4.41)$$

Where,

$$\Delta_G = \frac{1}{2a^+a^-}$$

$$G_{11} = b^+a^- + b^-a^+ = G_{22}$$

$$G_{12} = b^+a^- - b^-a^+ = G_{21}$$

The closed loop characteristic equation of the overall system (including the 2-periodic controller as well as the plant) is given by,

$$\Delta = \det[I + K\bar{G}\bar{C}] = \begin{bmatrix} \Delta_{11} & z^{-1}\Delta_{12} \\ z\Delta_{21} & \Delta_{22} \end{bmatrix} = 0 \quad \ldots\ldots\ldots (4.42)$$

With,

$$\Delta_{cl} = 2a^{+}a^{-}\Delta_{c} \quad \ldots\ldots\ldots (4.43)$$

$$\Delta_{11} = 1 + \frac{K}{2\Delta_{cl}}(G_{11}C_{11} + G_{12}C_{21}) \quad \ldots\ldots\ldots (4.44)$$

$$\Delta_{12} = 1 + \frac{K}{2\Delta_{cl}}(G_{11}C_{12} + G_{12}C_{22}) \quad \ldots (4.45)$$

$$\Delta_{21} = 1 + \frac{K}{2\Delta_{cl}}(G_{21}C_{11} + G_{22}C_{21}) \quad \ldots\ldots\ldots (4.46)$$

$$\Delta_{22} = 1 + \frac{K}{2\Delta_{cl}}(G_{21}C_{12} + G_{22}C_{22}) \quad \ldots\ldots\ldots (4.47)$$

Substituting the values of 2×2 transfer matrices of $\tilde{G}$ and $\overline{C}$ from equation (4.41) and (4.35) to the characteristic equation of (4.42), we get [32],

$$\Delta = a^{+}a^{-}(P_0^{+}P_0^{-} - P_1^{+}P_1^{-}) + K[b^{+}a^{-}(Q_0^{+}P_0^{-} - Q_1^{-}P_1^{+}) + b^{-}a^{+}(Q_0^{-}P_0^{+} - Q_1^{+}P_1^{-})] + K^2 b^{+}b^{-}(Q_0^{+}Q_0^{-} - Q_1^{+}Q_1^{-}) = 0 \quad \ldots\ldots\ldots (4.48)$$

4.3.3 Loop Zero Placement

The loop-zeros (or zeros) of system may be defined as roots of the characteristic equation when the loop gain approaches to ∞.From the characteristic equation, the plant zeros are the coefficient of K^2 term. This term contains the factor $b^{+}b^{-}$, which represents the zeros of theplant. Due to the present of the term $b^{+}b^{-}$, loop-zeros cannot be placed arbitrarily. But in the other case, coefficient of K term does not contain any such term. As a result, the roots of this coefficient are fully assignable and can be assigned to the required places. So, if the coefficient of K^2 term can be made equal to zero, the locations of loop-zeros would be determined by the coefficient of K term, achieving the loop-zero placement. Thus, to make the coefficient of K^2 term equal to zero, any of the following four conditions are used [34].

i. $Q_0^{+} = Q_1^{-}$
ii. $Q_0^{+} = -Q_1^{-}$
iii. $Q_0^{+} = Q_1^{+}$
iv. $Q_0^{+} = -Q_1^{+}$

Now the characteristic equation becomes,

$$\Delta = a^{+}a^{-}(P_0^{+}P_0^{-} - P_1^{+}P_1^{-}) + K[b^{+}a^{-}(Q_0^{+}P_0^{-} - Q_1^{-}P_1^{+}) + b^{-}a^{+}(Q_0^{-}P_0^{+} - Q_1^{+}P_1^{-})] = 0 \quad \ldots\ldots\ldots (4.49)$$

This above equation can be rewritten as,

$$\hat{A}(z^2)\hat{P}(z^2) + k\tilde{Z}(z^2) = \hat{\Delta}(z^2) = \breve{\Delta}(z^2)\tilde{D}(z^2) = 0 \quad \ldots\ldots\ldots (4.50)$$

Where,

$\hat{A}(z^2) =$ Plant poles polynomial = a^+a^-

$$= a_0 + a_2z^2 + \cdots + (-1)^n z^{2n} \quad \ldots\ldots\ldots (4.51)$$

$\hat{P}(z^2) =$ Controller poles polynomial = $P_0^+P_0^- - P_1^+P_1^-$

$$= \hat{p}_0 + \hat{p}_2z^2 + \cdots + (-1)^m z^{2m} \quad \ldots\ldots\ldots (4.52)$$

$\tilde{Z}(z^2) =$ Zero polynomial of the overall system

$$= Kb^+a^-\left(Q_0^+P_0^{-Q_1^-P_1^+} + b^-a^+(Q_0^-P_0^+ - Q_1^+P_1^-)\right] \quad \ldots\ldots\ldots (4.53)$$

$$= r_0 + r_2z^2 + \cdots + r_{2\theta}z^{2\theta} \quad \ldots\ldots\ldots (4.54)$$

$\breve{\Delta}(z^2) =$ Desired closed loop poles polynomial.

$\tilde{D}(z^2) =$ Additional closed loop poles polynomial.

From the above equations it can be noted that the controller pole polynomial and the loop-zero polynomial both are assignable. So, by adjusting the parameters of zero polynomial, zero placement can be achieved.

4.3.4 Order of Controller

It can be observed from (4.50), the degree of polynomials $\hat{A}(z^2)$ and $\hat{P}(z^2)$ are $2n$ and $2m$ respectively. The degree of the polynomial $\hat{Z}(z^2)$ can be defined as [32],

$$\theta = m + \eta \ \ with\, \eta = n - I^+\left\{\frac{n-r}{2}\right\} \quad \ldots\ldots\ldots (4.55)$$

where,

I^+ is the ceiling operator,

θ is the total number of assignable loop-zeros,

η is the assignable plant zeros which depends upon the relative order of the plant.

From (4.15), (4.16) and (4.52), the total number of assignable coefficients is ($2m$+m) to place m controller poles and (m+ η) loop zeros. The order of the controller is defined by,

$$m \geq \eta = n - I^{+}\left\{\frac{n-r}{2}\right\} \quad \ldots\ldots\ldots (4.56)$$

Note that for plants of relative order either 1 or 2 one requires $m \geq n-1$

4.3.5 Evaluation of Controller Parameters

Controller parameters are evaluated by solving the characteristic equation. The controller is synthesized using approach of [33]. It is a two-stage method. In stage-I, an intermediate polynomial is obtained and in stage-II, controller parameters are calculated from the intermediate polynomial.

Stage-1: An Intermediate polynomial

For a given SISO, LDTI plant $G(z)$, the numerator and the denominator are given by eq (4.1), (4.2). The parameters required for calculation purpose are given as follows.

$$\begin{aligned}\hat{B}(z^2) &= a^{+}b^{-} \\ &= \left[\hat{b}_0 + \hat{b}_2 z^2 + \cdots + \hat{b}_0 z_{2\varphi_1}^{2\varphi_1}\right] + z[\hat{b}_1 + \hat{b}_3 z^2 + \cdots + \hat{b}_{2\varphi_2+1} z^{2\varphi_2} \\ &= \hat{B}_e(z^2) + z\hat{B}_d(z^2) \quad \ldots\ldots\ldots (4.57)\end{aligned}$$

Where, $\varphi_1 = I^{+}\left\{\frac{(n+r)}{2}\right\}$ and $\varphi_2 = I^{-}\left\{\frac{(n+r-1)}{2}\right\}$

$$\begin{aligned}\hat{L}(z^2) &= (Q_0^{+}P_0^{-} - Q_1^{-}P_1^{+}) \\ &= \left[\hat{l}_0 + \hat{l}_2 z^2 + \cdots + \hat{l}_{2m} z^{2m}\right] + z\left[\hat{l}_1 + \hat{l}_3 z^2 + \cdots + \hat{l}_{2m-1} z^{2(m-1)}\right] \\ &= \hat{L}_e(z^2) + z\hat{L}_d(z^2) \quad \ldots\ldots\ldots (4.58)\end{aligned}$$

Substituting equations (4.57) and (4.58) in (4.54) we get,

$$\begin{aligned}\hat{Z}(z^2) &= \hat{B}^{+}\hat{L}^{+} + \hat{B}^{-}\hat{L}^{-} \\ &= 2\hat{B}_e(z^2)\hat{L}_e(z^2) + 2z^2\hat{B}_d(z^2)\hat{L}_d(z^2) \\ &= r_0 + r_2 z^2 + \cdots + r_{2\theta} z^{2\theta} \quad \ldots\ldots\ldots (4.59)\end{aligned}$$

Now, to find the parameters of $\hat{L}(z^2)$,a Sylvester matrix like equation is obtained by,

$$\begin{bmatrix} r_0 \\ r_2 \\ r_4 \\ \vdots \\ r_{2\theta} \end{bmatrix} = \begin{bmatrix} \hat{b}_0 & \cdots & 0 & 0 & \cdots & 0 \\ \hat{b}_2 & \ldots & 0 & \hat{b}_1 & \ldots & 0 \\ \hat{b}_4 & \ldots & 0 & \hat{b}_3 & \ldots & 0 \\ \vdots & \ddots & \vdots & \vdots & \ddots & \vdots \\ 0 & \cdots & \hat{b}_{2\varphi_1} & 0 & \cdots & \hat{b}_{2\varphi_2+1} \end{bmatrix} \begin{bmatrix} \hat{l}_0 \\ \vdots \\ \hat{l}_{2m} \\ \hat{l}_1 \\ \vdots \\ \hat{l}_{2m-1} \end{bmatrix} \quad \ldots\ldots\ldots (4.60)$$

Now, from (4.59) we can say that (4.60) will be a consistent set of equations if the following conditions are satisfied [30]:

1. If the plant has a pole-zero cancelation at p then the effective loop transfer function would have the same at p^2, signifying that the loop-zero polynomial must have a root at p^2. (Clearly, for internal stability, the plant should not have any unstable pole-zero cancelation at p, when $|p|<1$)
2. If the plant denominator has an even factor (z^2+c), then also the loop transfer function would have a pole-zero cancelation at $-c$, and so the loop-zero polynomial must contain the same factor. (Again, for internal stability, $|c|<1$ must be satisfied.)
3. If the plant numerator has an even factor (z^2+c), then the loop-zero polynomial must also contain the same.

Equation (4.60) is solved using matrix inversion method and the $\hat{L}(z)$ polynomial is obtained. But the matrix $\bar{B}$ may become singular for the following cases:

i. If the plant has pole(s) or zero(s) at origin.
ii. If the plant has a pole-zero cancelation at origin.
iii. If the denominator and numerator contain only even factors.

All these cases will lead to some all-zero identities, which will make (4.39) an undeterminable but consistent set of linear equations.

Assume rank of $\bar{B}$= rank of $[\bar{B} \mid \bar{r}]$; then the equation (4.39) becomes consistent and the polynomial $\hat{L}(z)$ can be obtained.

Stage-2: Calculation of Controller Parameters

Polynomial $\hat{L}(z)$ which is obtained in stage-I, now, will be divided into two parts for all four conditions $Q_0^+ = \pm Q_1^{\pm}$ and will be suitably assigned to pole polynomials to calculate the controller parameters [32].

Condition-1: $Q_0^+ = Q_1^-$

From (4.58) we get,

$$\hat{L}(z) = Q_0^-(P_0^+ - P_1^-) \quad \ldots\ldots\ldots (4.61)$$

Then, to find Q_0^- and $(P_0^+ - P_1^-)$, polynomial $\hat{L}(z)$ is divided into two parts such that

a) Both the halves are real polynomials (i.e., a complex root and its conjugate should be present in the same half).
b) At least one of the halves has no even factor [32].

If the factor that satisfies the 2nd condition is, in addition, monic, then the same can be chosen as $(P_0^+ - P_1^-)$ and the rest would be Q_0^- . Values of $d_{i,0}$ and $d_{i,1}$ (for $i = 0,1,2, \ldots, m$) can be directly obtained from Q_0^- and Q_1^+ . Calculations for finding $c_{i,0}$ and $c_{i,1}$ (for $i = 0,1,2, \ldots, m$) are shown below.

Let,

$$(P_0^+ - P_1^-) = \Gamma(z) = \gamma_0 + \gamma_1 z + \cdots + \gamma_m z^m \quad \ldots\ldots\ldots (4.62)$$

From (4.16) and (4.62) it is obtained,

$$P_0^+\Gamma^- + P_0^-\Gamma^+ = \hat{P}(z^2) + \Gamma^+\Gamma^- \quad \ldots\ldots\ldots (4.63)$$

Now, comparing both sided of the equation (4.63), we get

$$\begin{bmatrix} \gamma_0 & 0 & 0 & 0 & \ldots & 0 & 0 \\ \gamma_2 & -\gamma_1 & \gamma_0 & 0 & \ldots & 0 & 0 \\ \gamma_4 & -\gamma_3 & \gamma_2 & -\gamma_1 & \ldots & 0 & 0 \\ \vdots & \vdots & \vdots & \vdots & \ddots & \vdots & \vdots \\ 0 & 0 & 0 & 0 & \ldots & (-1)^m\gamma_{m-1} & (-1)^m\gamma_{m-2} \\ 0 & 0 & 0 & 0 & \ldots & 0 & (-1)^m\gamma_m \end{bmatrix} \begin{bmatrix} c_{0,0} \\ c_{1,0} \\ c_{2,0} \\ \vdots \\ c_{(m-1),0} \\ 1 \end{bmatrix}$$

$$= \begin{bmatrix} \hat{p}_0 + \gamma_0^2 \\ \hat{p}_2 + 2\gamma_0\gamma_2 - \gamma_1^2 \\ \hat{p}_4 + \gamma_0\gamma_4 - 2\gamma_1\gamma_3 + \gamma_2^2 \\ \vdots \\ \hat{p}_{2(m-1)} + 2(-1)^m\gamma_m\gamma_{m-2} - (-1)^{(m-1)}\gamma_{m-1}^2 \\ (-1)^m + (-1)^m\gamma_m^2 \end{bmatrix} \quad \ldots\ldots\ldots (4.64)$$

The coefficients of P_0 i.e. $C_{0,0}$, $C_{1,0}$, $C_{2,0}$, …, $C_{(m-1),0}$ can be obtained by solving equation (4.64). Using these values, coefficients of P_1 i.e. $C_{0,1}$, $C_{1,1}$, $C_{2,1}$, …, $C_{(m-1),1}$ can be calculated from the following equation,

$$c_{i,1} = (-1)^i(c_{i,0} - \gamma_i) \quad \text{with} \quad i = 0,1, \ldots, (m-1) \ldots\ldots\ldots (4.65)$$

Condition-2: $Q_0^+ = -Q_1^-$

From (4.58) we get**,**

$$\hat{\mathrm{L}}(\mathrm{z}) = Q_0^-(P_0^+ + P_1^-) \quad \ldots\ldots\ldots (4.66)$$

Now, procedures shown for condition can be followed. But equation for obtaining coefficients of P_1 from coefficients of P_0 will change and become as follows,

$$c_{i,1} = (-1)^i(\gamma_i - c_{i,0}) \qquad \text{with } i = 0,1,\ldots,(m-1) \ldots\ldots\ldots (4.67)$$

4.3.6 Numerical Example of Second Order System

Let us consider a second order system consisting non-minimum phase,

$$G(z) = \frac{z - 1.3}{(z - 0.5)(z - 1.5)}$$

with sampling time, T_s=50 microsecond.

By choosing the desired closed loop poles, controller poles and the loop-zero positions carefully then following (4.50), the corresponding pole and zero polynomials become:

$\hat{A}(z^2) = (z^2 - 0.25)(z^2 - 2.25)$; $\hat{P}(z^2) = -z^2$; $\tilde{Z}(z^2) = -2.5z^2(z^2 - 0.225)$;

$\tilde{\Delta}(z^2) = (z^2)^2$; $\tilde{D}(z^2) = -z^2$

The corresponding Root Locus is shown in Fig. 4.2. The gain margin of the 2-periodic compensated system is 2.74.

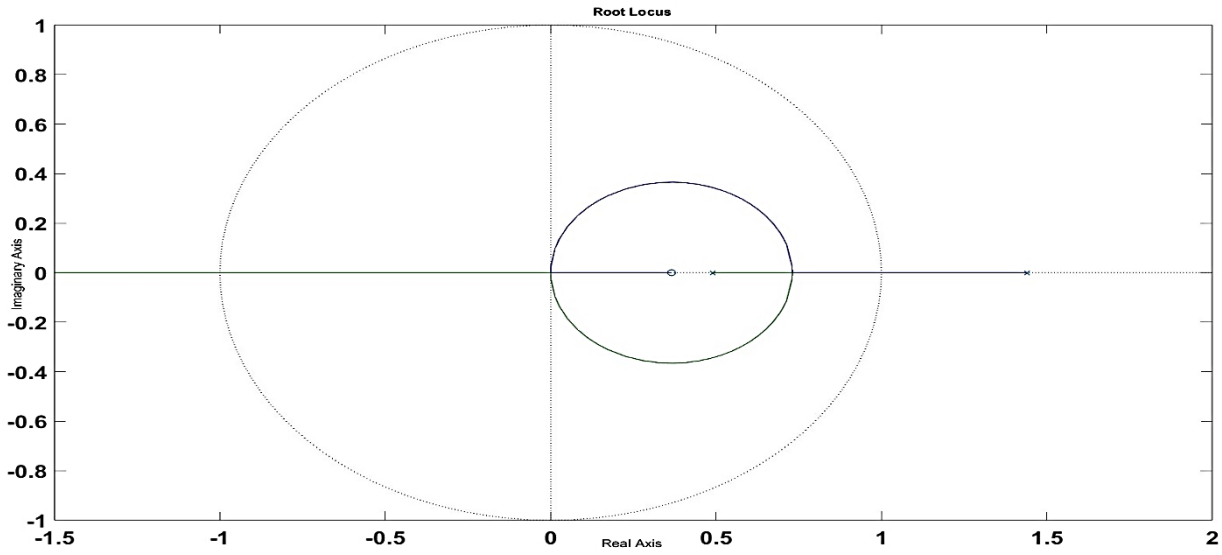

Fig.4.2: Root locus of given example compensated by 2-periodic controller

The controller parameters can be evaluated using technique discussed below.

Applying the condition $\boldsymbol{Q_0^+ = Q_1^-}$ and $\hat{\mathrm{L}}(\mathrm{z}) = Q_0^-(P_0^+ - P_1^-)$ we get the controller parameters as:

$$d_{0,0} = d_{0,1} = 0, \quad d_{1,0} = -d_{1,1} = 6.345, \qquad and \qquad c_{0,0} = -c_{0,1} = 0.25$$

By putting it in the below circuit shown, with initial condition given:

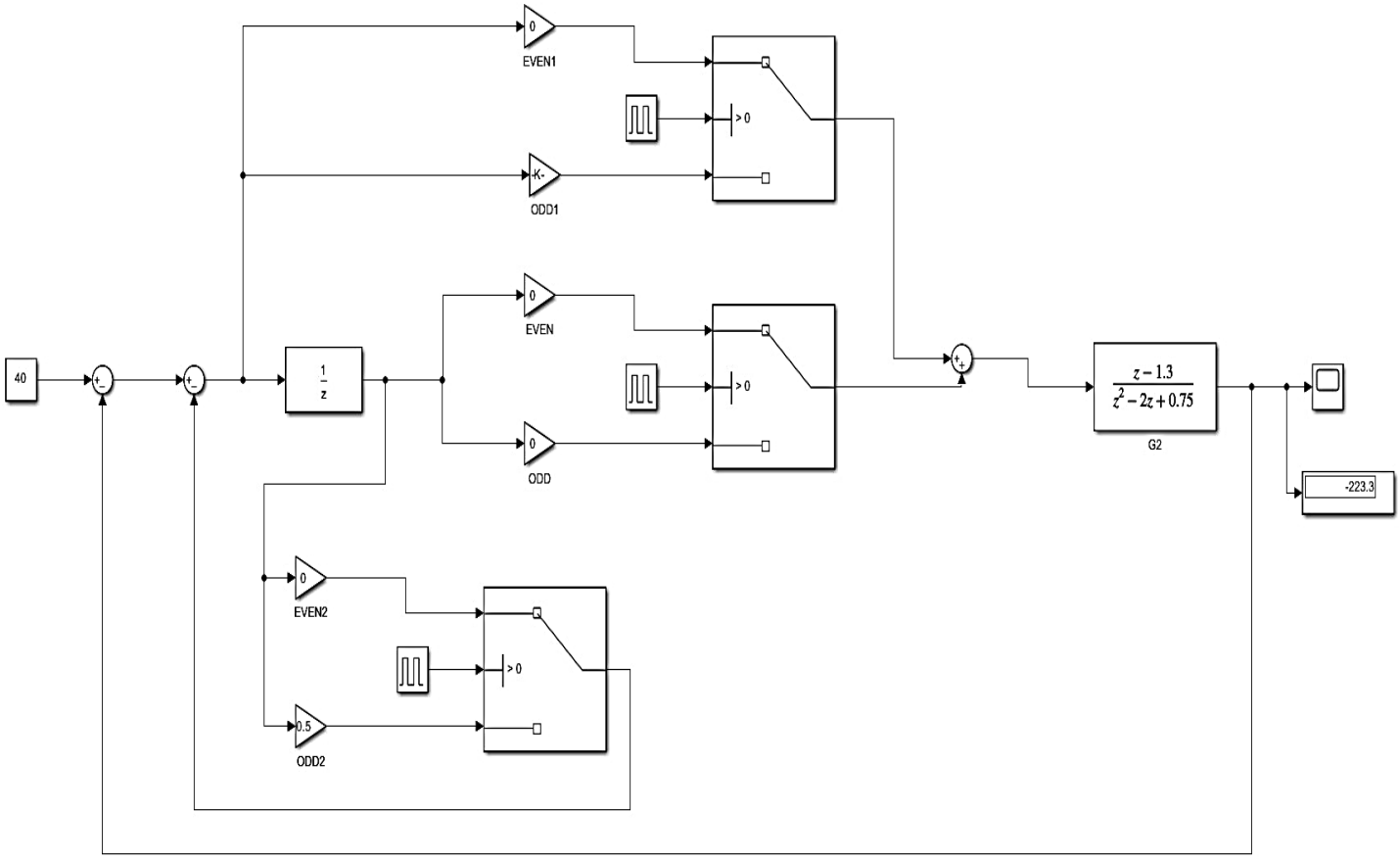

Fig.4.3: MATLAB Simulink implementation without augmentation

Now, in this example upon giving am input we are getting steady state response but ripples are observed at the steady state which later on can be made ripple-free using ripple-free theorems. Output of scope is given in Fig.4.4 in which ripples are observed.

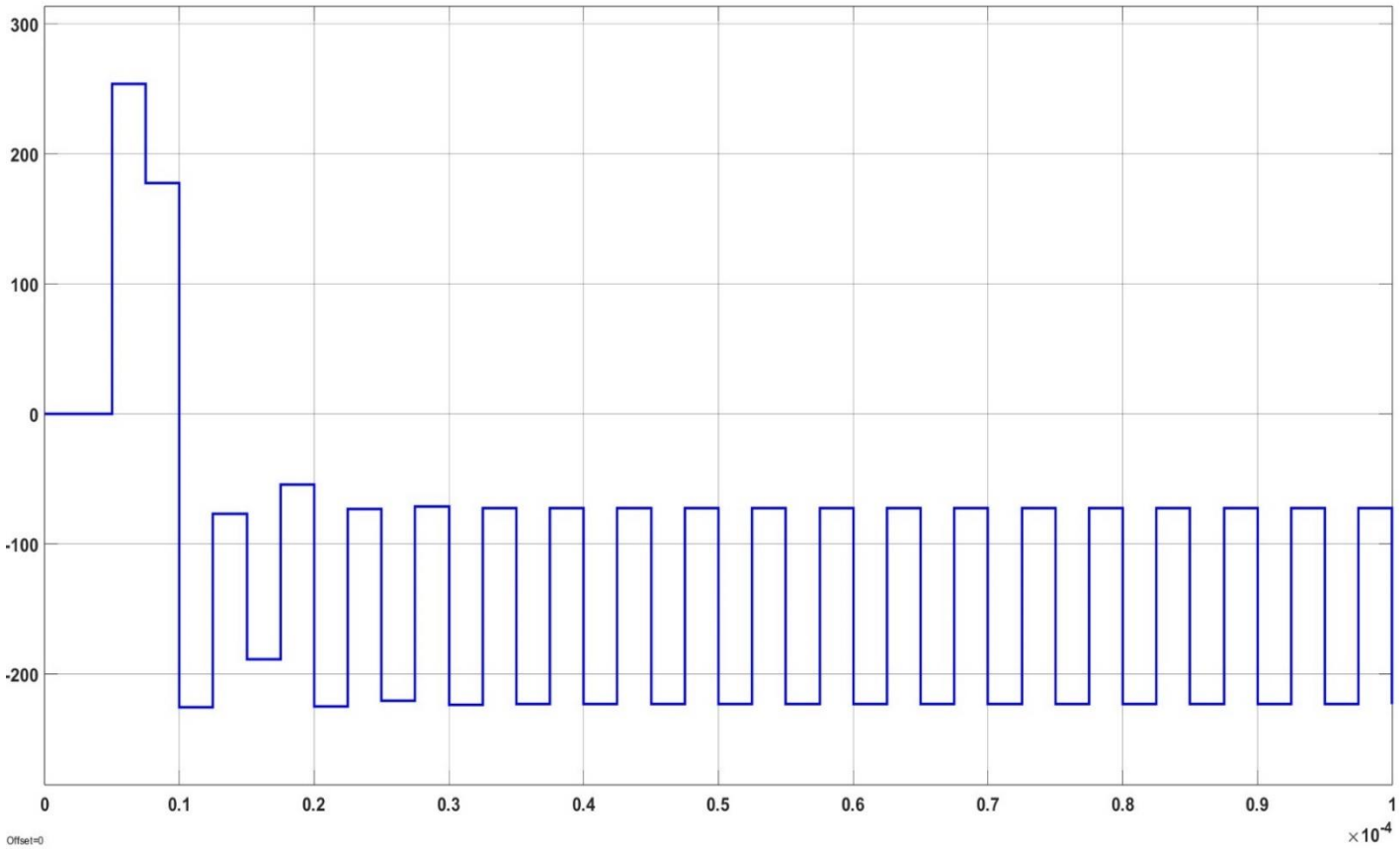

Fig.4.4: Output response for 2nd order plant without augmentation

In the next subchapter we have suggested a number of ways to remove the ripple from output during steady state.

4.4 Ripple-Free Response

In the example given previously, the 2-periodic controller design for a second order plant is shown and loop-zero placement capability of that controller is also demonstrated. It is observed from fig.(4.4) that a 2- periodic oscillation is present in the steady-state response, which makes the controller inconvenient. In this section, techniques of removing aforesaid 2-periodic ripple are discussed.

Theorem: The steady-state step-response of a 2-periodically compensated system would be ripple-free if the loop contains any of the following time-invariant components [30],[32],

i. Pole at -1
ii. Zero at 1
iii. Both Pole at -1 and zero at 1

I. Pole at -1

If the plant denominator contains a factor $(z-1)$ then the plant transfer function can be expressed as,

$$G(z) = K\left(\frac{b(z)}{a(z)}\right) = \frac{Kb(z)}{\check{a}(z)(z-1)} = \frac{Kb(z)(-1)^n\check{a}(-z)(z+1)}{\check{a}(z)(-1)^n\check{a}(-z)(z^2-1)}$$
$$= \frac{\check{n}(z)(z+1)}{\check{d}(z)(z^2-1)} \dots\dots\dots (4.68)$$

Where, $b(z)(-1)^n\check{a}(-z) = \check{n}(z)$ and $\check{a}(z)(-1)^n\check{a}(-z) = \check{d}(z)$

The lifted transfer function is represented as,

$$G(z^2) = \frac{[\check{n}_1(z^2) + z^{-1}\check{n}_2(z^2)](z+1)}{\check{d}(z)(z^2-1)} = \frac{[\check{n}_1(z^2) + \check{n}_2(z^2)] + z^{-1}[z^2\check{n}_1(z^2) + \check{n}_2(z^2)]}{\check{d}(z)(z^2-1)}$$
$$= \frac{[n_1(z^2) + z^{-1}n_2(z^2)]}{\check{d}(z)(z^2-1)} \dots\dots\dots (4.69)$$

With

$[\check{n}_1(z^2) + \check{n}_2(z^2)] = n_1(z^2) \dots\dots\dots (4.70)$ and $[z^2\check{n}_1(z^2) + \check{n}_2(z^2)] = n_2(z^2) \dots\dots\dots (4.71)$

From equation (4.70) and (4.71),

$n_1 - n_2 = -(z^2-1)\check{n}_1(z^2) \dots\dots\dots (4.72)$ and $n_1 - z^{-2}n_2 = z^{-2}(z^2-1)\check{n}_1(z^2) \dots (4.73)$

Now, steady-state error at even and odd instants of time are obtained as

$$\begin{bmatrix} E_{e,ss} \\ E_{o,ss} \end{bmatrix} = \lim_{z^2\to 1} \frac{z^2}{\Delta}\begin{bmatrix} \Delta_c d + z^{-1}(z^2-1)\check{n}_1(z^2)C_{12} + z^{-2}(z^2-1)\check{n}_1(z^2)C_{22} \\ \Delta_c d + (z^2-1)\check{n}_1(z^2)C_{12} + z^{-1}(z^2-1)\check{n}_1(z^2)C_{22} \end{bmatrix}$$
$$= \lim_{z^2\to 1} \frac{z^2}{\Delta}\begin{bmatrix} \Delta_c d \\ \Delta_c d \end{bmatrix} \dots\dots\dots (4.74)$$

It can be verified from (4.74) that the presence of a pole at 1 in plant transfer function make the response ripple free.

II. Zero at -1

If the plant numerator contains a factor $(z+1)$ then the plant transfer function can be expressed as,

$$G(z) = K\frac{b(z)}{a(z)} = K\frac{\check{b}(z)(z+1)}{a(z)} = K\frac{\check{b}(z)(-1)^n a(-z)(z+1)}{a(z)(-1)^n\check{a}(-z)} = \frac{\check{n}(z)(z+1)}{\check{d}(z)} \dots\dots\dots (4.75)$$

Where, $b(z)(-1)^n \breve{a}(-z) = \breve{n}(z)$ and $\breve{a}(z)(-1)^n \breve{a}(-z) = \breve{d}(z)$

The lifted transfer function is represented as,

$$G(z^2) = \frac{[\breve{n}_1(z^2) + z^{-1}\breve{n}_2(z^2)](z+1)}{\breve{d}(z)} = \frac{[\breve{n}_1(z^2) + \breve{n}_2(z^2)] + z^{-1}[z^2\breve{n}_1(z^2) + \breve{n}_2(z^2)]}{\breve{d}(z)}$$

$$= \frac{[n_1(z^2) + z^{-1}n_2(z^2)]}{\breve{d}(z)} \quad \dots\dots\dots (4.76)$$

With

$[\breve{n}_1(z^2) + \breve{n}_2(z^2)] = n_1(z^2) \dots\dots\dots (4.77)$ and $[z^2\breve{n}_1(z^2) + \breve{n}_2(z^2)] = n_2(z^2) \dots\dots\dots (4.78)$

From equation (4.70) and (4.71),

$n_1 - n_2 = -(z^2-1)\breve{n}_1(z^2) \dots\dots\dots (4.79)$ and $n_1 - z^{-2}n_2 = z^{-2}(z^2-1)\breve{n}_1(z^2) \dots (4.80)$

Now, steady-state error at even and odd instants of time are obtained as

$$\begin{bmatrix} E_{e,ss} \\ E_{o,ss} \end{bmatrix} = \lim_{z^2 \to 1} \frac{z^2}{\Delta} \begin{bmatrix} \Delta_c d + z^{-1}(z^2-1)\breve{n}_1(z^2)C_{12} + z^{-2}(z^2-1)\breve{n}_1(z^2)C_{22} \\ \Delta_c d + (z^2-1)\breve{n}_1(z^2)C_{12} + z^{-1}(z^2-1)\breve{n}_1(z^2)C_{22} \end{bmatrix}$$

$$= \lim_{z^2 \to 1} \frac{z^2}{\Delta} \begin{bmatrix} \Delta_c d \\ \Delta_c d \end{bmatrix} \quad \dots\dots\dots (4.81)$$

It can be concluded from (4.81) that the presence of a zero at -1 in plant transfer function make the response ripple free.

III. A Pole at 1 and a zero at -1:

This is also a theorem to remove ripple but in our study we haven't included and used this theorem so we will continue with the first two theorems.

4.5 Numerical example

The first two theorems which we studied will be now augmented to the plant given in previous example to obtain a ripple-free steady-state step response besides robustness.

A. With Augmentation $\frac{z}{z-1}$

The augmented transfer function is,

$$G(z) = \frac{(z)(z-1.3)}{(z-1)(z-0.5)(z-1.5)}$$

The order of the 2-periodic controller is, m = 2 and number of controller zeros is, r = 4.

$\hat{A}(z^2) = -(z^2 - 0.25)(z^2 - 2.25)(z^2 - 1)$; $\hat{P}(z^2) = z^4$;

$\tilde{Z}(z^2) = -2.05z^4(z^2 - 0.25)(z^2 - 0.922)$; $\tilde{\Delta}(z^2) = -(z^2)^2(z^2 - 0.25)$; $\tilde{D}(z^2) = (z^2 - 0.6)^2$

The corresponding Root Locus is shown in Fig. 4.5. with a gain margin of 2.54

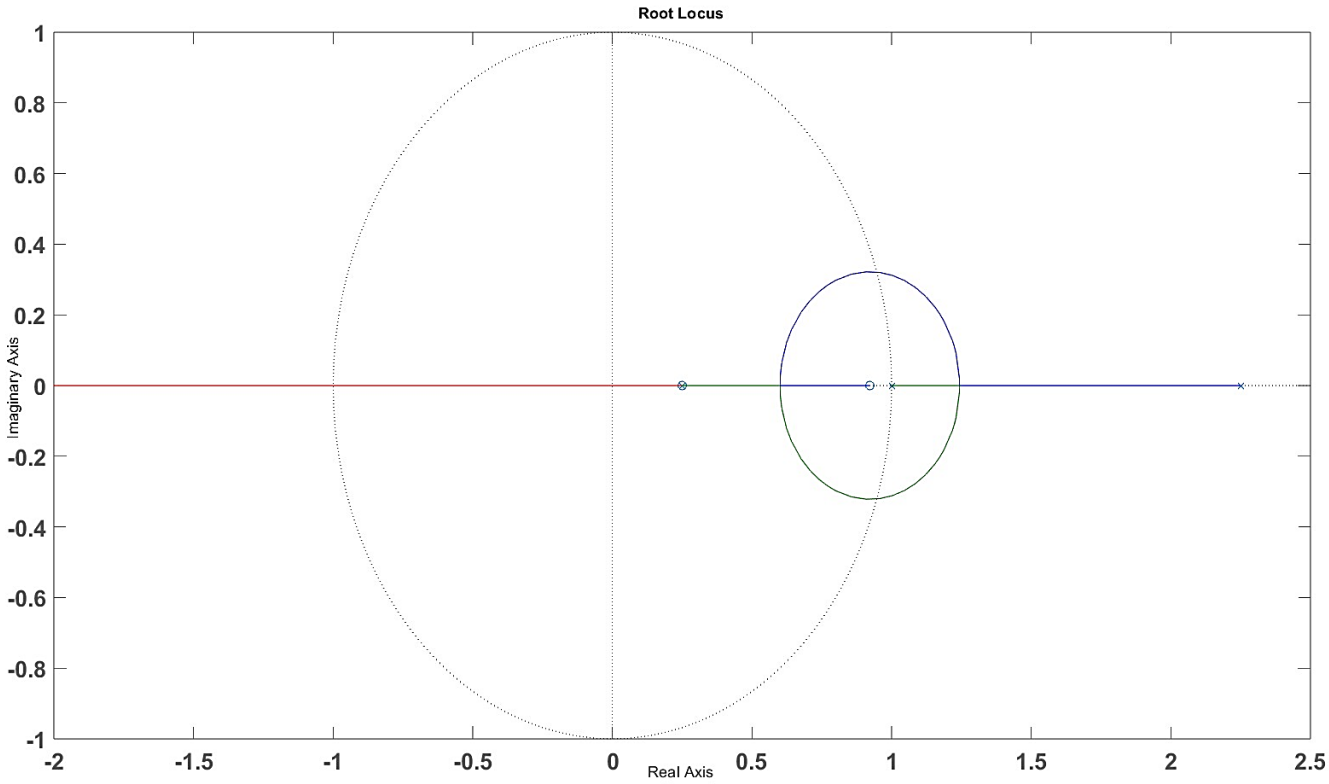

Fig.4.5: Root locus of given example compensated by 2-periodic controller after $\frac{z}{z-1}$ augmentation

Then applying the condition $Q_0^+ = -Q_1^-$ and $\hat{L}(z) = Q_0^-(P_0^+ + P_1^-)$ we get the controller parameters as:

$$d_{0,0} = d_{0,1} = 0, \quad d_{1,0} = d_{1,1} = -2.8292, \quad d_{2,0} = -d_{2,1} = 5.6583,$$

$$c_{0,0} = -c_{0,1} = -0.2547, and\ c_{1,0} = 0.2595, c_{1,1} = -0.7594$$

By putting it in the below circuit shown, with initial condition given in Fig.4.6:

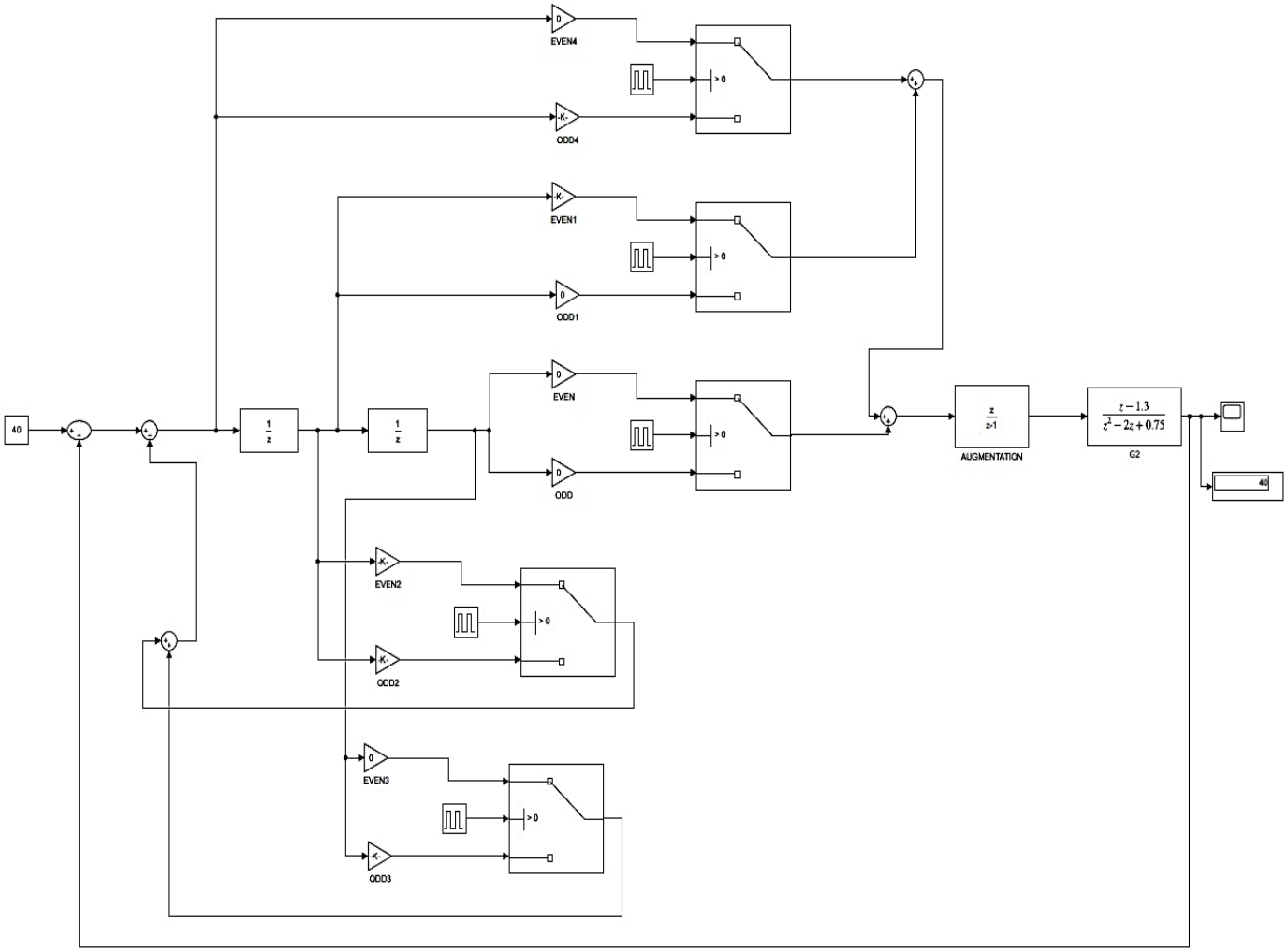

Fig.4.6: MATLAB Simulink implementation with $\frac{z}{z-1}$ augmentation

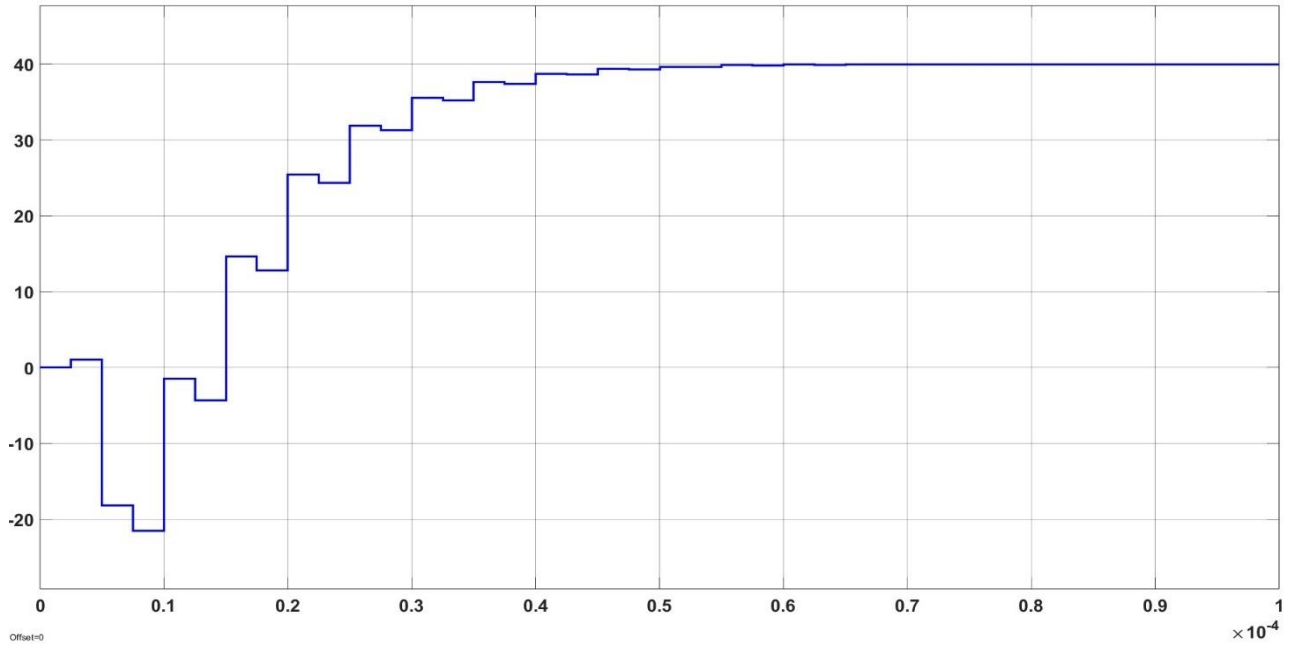

Fig.4.7: MATLAB Simulink implementation with $\frac{z}{z-1}$ augmentation

In the Fig.4.7 it can be seen that due to $\frac{z}{z-1}$ augmentation the ripples that can be observed in Fig.4.4 has now settled around the specific input reference in steady-state.

B. With Augmentation $\frac{z+1}{z}$

Let us consider a second order system consisting non-minimum phase

$$G(z) = \frac{(z-1.3)(z+1)}{z(z-0.5)(z-1.5)}$$

By choosing the desired closed loop poles, controller poles and the loop-zero positions carefully then following ( ), the corresponding pole and zero polynomials become:

$$\hat{A}(z^2) = -z^2(z^2-0.25)(z^2-2.25), \hat{P}(z^2) = z^2(z^2-0.322),$$

$$\tilde{Z}(z^2) = -0.872(z^2)^3(z^2-0.25), \tilde{\Delta} = -(z^2)^2(z^2-0.25), and\ \tilde{D}(z^2) = (z^2-0.85)^2$$

The corresponding Root Locus is shown in Fig. 4.8. with a gain margin of 5.07

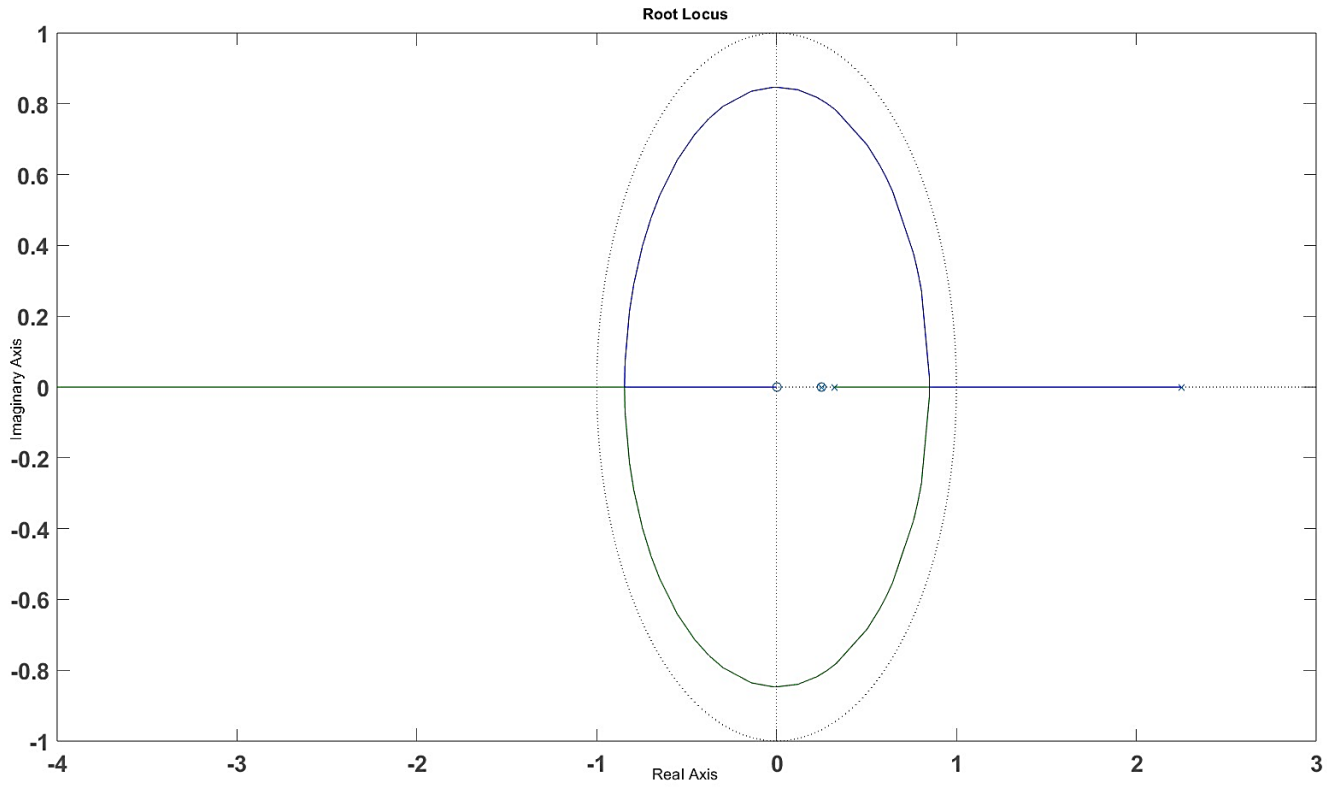

Fig.4.8: Root locus of plant with $\frac{z}{z-1}$ augmentation

Then applying the condition $Q_0^+ = -Q_1^-$ and $\hat{L}(z) = Q_0^-(P_0^+ + P_1^-)$ we get the controller parameters as:

$$d_{0,0} = d_{0,1} = 0, \quad d_{1,0} = d_{1,1} = -2.8292, \quad d_{2,0} = -d_{2,1} = 5.08,$$

$$c_{0,0} = c_{0,1} = 0.2785, and\ c_{1,0} = 1.0794, c_{1,1} = -0.5348$$

By putting it in the below circuit shown, with initial condition given:

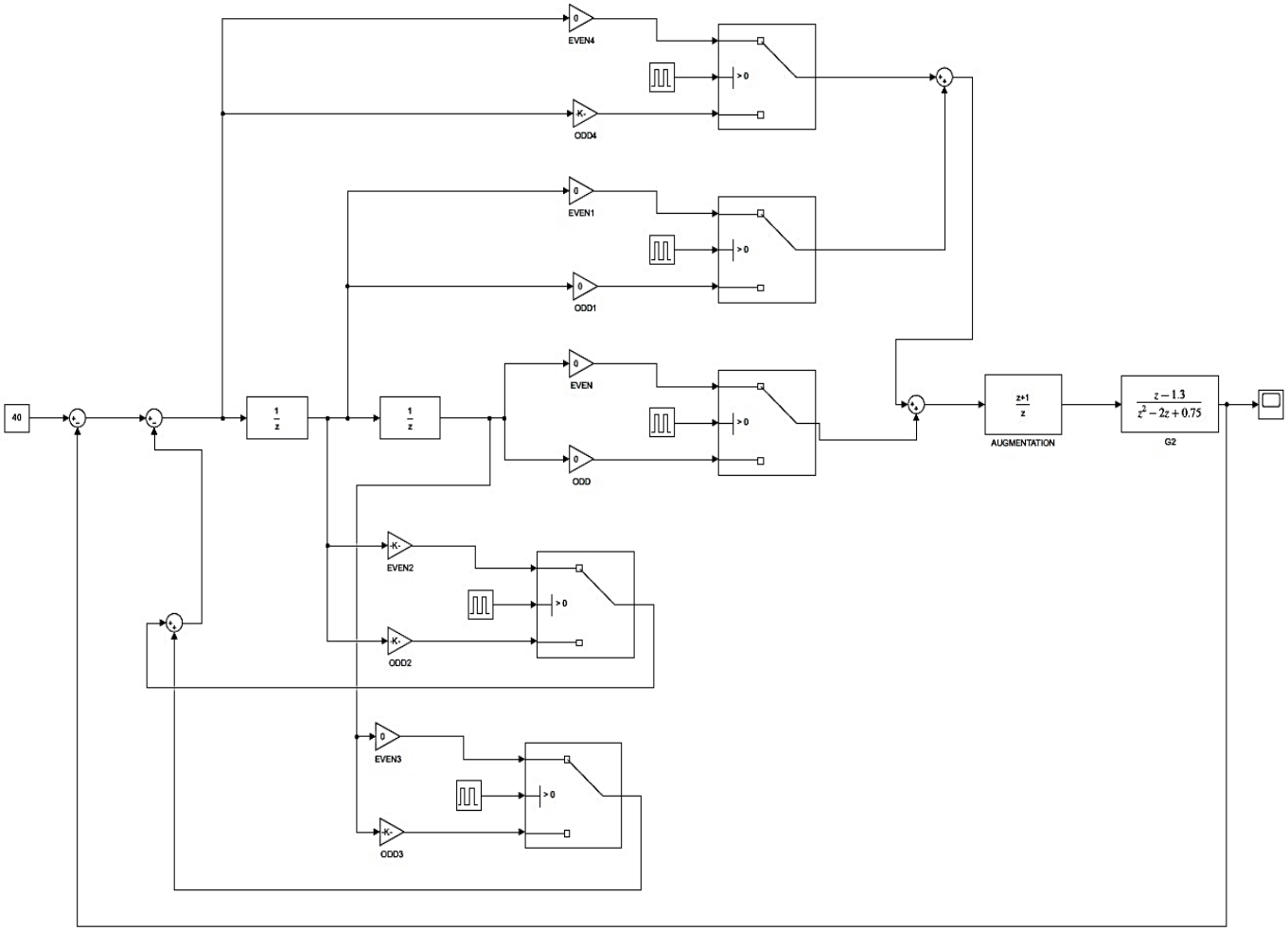

Fig.4.9: MATLAB Simulink implementation with $\frac{z}{z+1}$ augmentation

The output of this implementation is shown in Fig.4.10 and we can see that after $\frac{z}{z+1}$ augmentation there are no ripples that exists around steady-state.

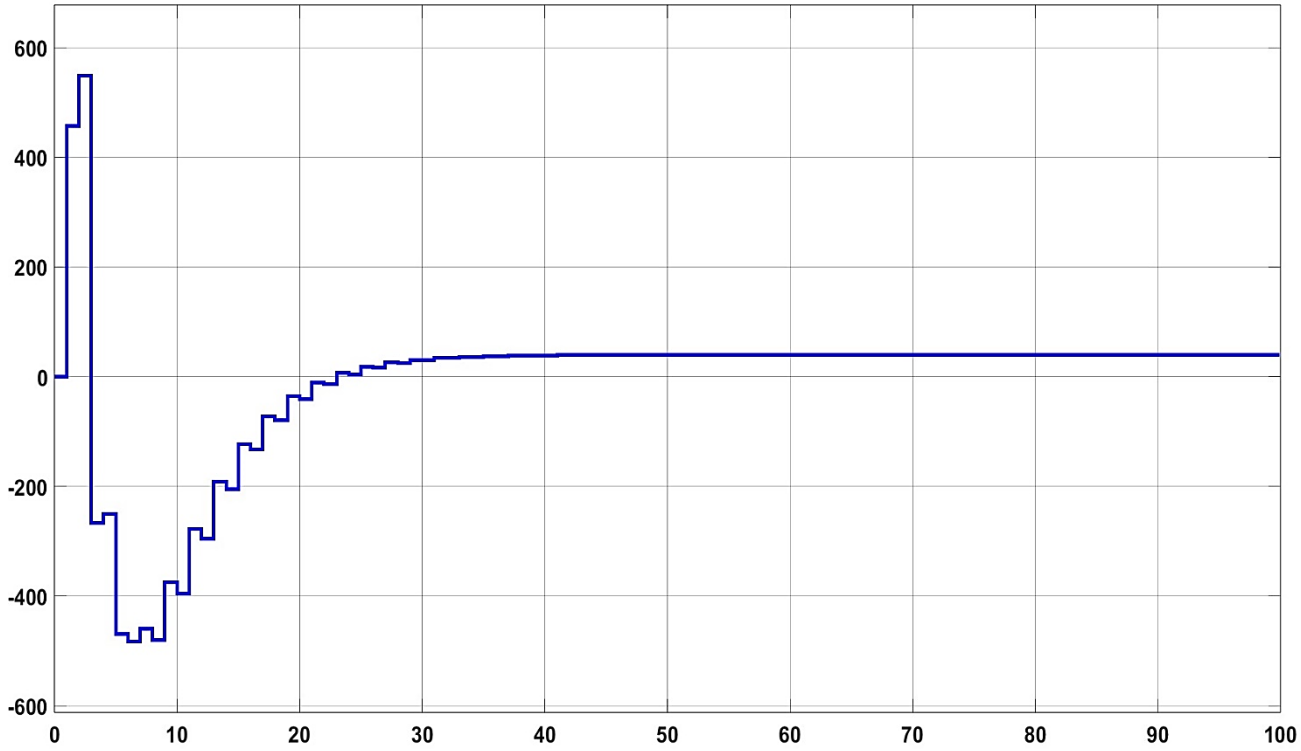

Fig.4.10: MATLAB Simulink implementation with $\frac{z+1}{z}$ augmentation

This, concludes this section in which we tried to augment plant to get ripple-free response around steady state. The third ripple-free theorem is not explained and hence not implemented with the help of an example.

Chapter 5

Implementation of 2-Periodic Control for Boost Converter

5.1 Boost converter as an LTI plant

In Chapter 3 it is discussed how a boost converter is modelled in a double-loop PI configuration where the entire transfer function of boost converter is separated for implementing double-loop PI control. In the current(inner-loop) expressed by the transfer function "$G_1(z)$", controller parameters for the PI controller "C_1" are calculated in order to meet the desired the transient characteristics and to reduce steady state error. Thus inner-loop transfer function is defined by $G_{in}(z)$ which can be written as:

$$G_{in}(z) = \frac{C_1(z)G_1(z)}{1 + C_1(z)G_1(z)} = \frac{2.2942(z - 0.4258)}{(z + 0.1681)(z + 0.1281)} \quad \ldots\ldots\ldots (5.1)$$

Now, we are replacing the outer-loop PI controller "C_2" with a periodic-controller due to the limitations of PI controller discussed in chapter 3, for that specific purpose, the voltage(outer-loop) transfer function "$G_2(z)$" is needed to be multiplied with "$G_{in}(z)$" shown in eqn. (5.1) to get the overall transfer function "$G(z)$" which can be written as:

$$G(z) = G_{in}(z) * G_2(z) = \frac{-23.582(z-0.4258)(z-1.015)}{(z+0.1681)(z+0.1281)(z-0.9968)} \quad \ldots\ldots\ldots (5.2)$$

From the above eqn. (5.2) "$G(z)$" is obtained which will be used as an LTI plant that can be compensated by using periodic-controller in the outer-loop.

5.2 Overall Transfer-function for Ripple-free steady-state response of boost converter

To ensure, ripple-free response we need to augment the LTI plant as discussed in Chapter 4.

Thus, overall transfer function can be written for two different augmentations:

1. **With augmentation $\left(\frac{z+1}{z}\right)$:**

The overall transfer function "$G(z)$" as discussed in eqn. (5.2) is augmented with $\left(\frac{z+1}{z}\right)$ augmentation thus, the overall transfer function "$G'(z)$" can be written as:

$$G'(z) = \frac{-23.582(z-0.4258)(z-1.015)(z+1)}{z(z+0.1681)(z+0.1281)(z-0.9968)} \quad \ldots\ldots\ldots (5.3)$$

shown in Fig.5.1

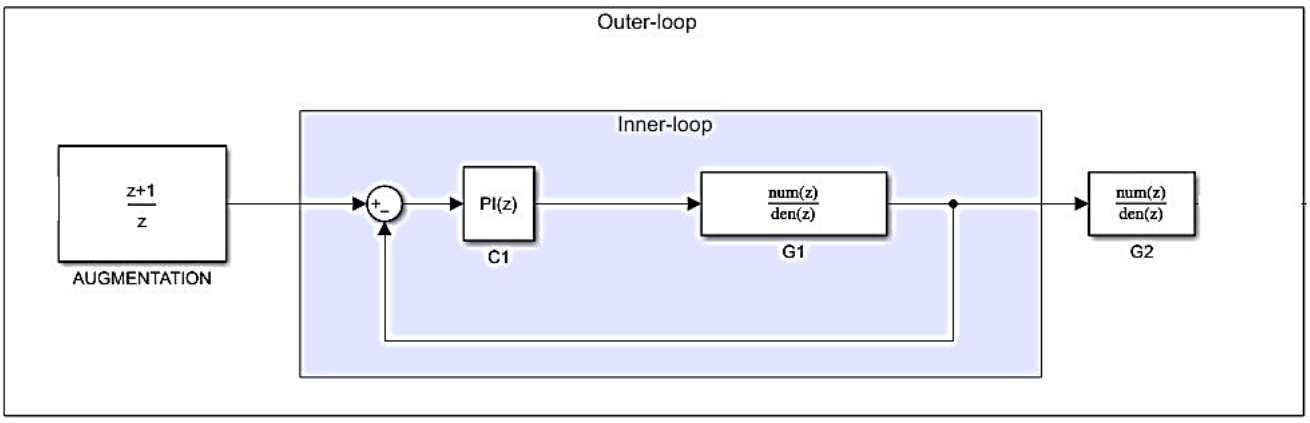

Fig.5.1 : Block diagram for overall Transfer-function $G'(z)$

2. **With augmentation $\left(\frac{z}{z-1}\right)$:**

The overall transfer function "$G(z)$" as discussed in eqn. (5.2) is augmented with $\left(\frac{z}{z-1}\right)$ augmentation thus, the overall transfer function "$G''(z)$" can be written as:

$$G''(z) = \frac{-23.582(z-0.4258)(z-1.015)(z)}{(z-1)(z+0.1681)(z+0.1281)(z-0.9968)} \quad \ldots\ldots\ldots (5.4)$$

shown in fig.5.2

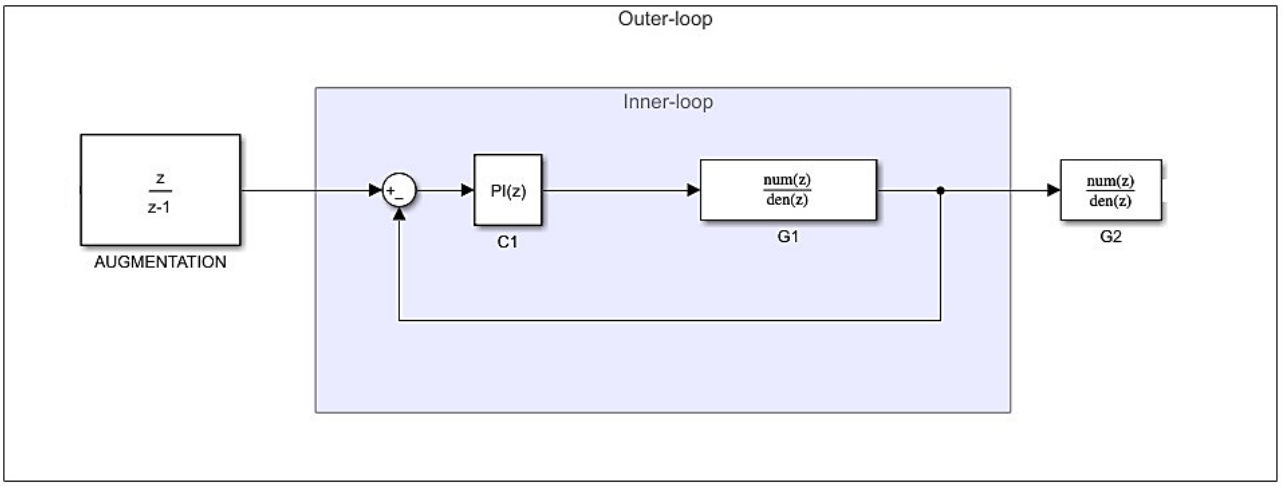

Fig.5.2 : Block diagram for overall Transfer-function $G''(z)$

5.3 Controller synthesis and output response

In this section we shall discuss the steps involved in obtaining the controller gains as well as we will implement them for different augmentation and finally, we will observe the output after implementing controller gains.

5.2.1 With augmentation $\left(\frac{z+1}{z}\right)$:

A. Lifting the plant:

$$\hat{A}(z^2) = a^+a^- = z^2(z^2 - 0.9936)(z^2 - 0.0164)(z^2 - 0.02825) \quad \ldots\ldots\ldots (5.5)$$

B. Order of the controller(m):

$n =$ order of denominator of plant = 4; $r =$ order of numerator of plant = 3;

$$m = 4 - I^+\left(\frac{4-3}{2}\right) = 3 \quad \ldots\ldots\ldots (5.6)$$

C. Choosing controller poles:

We are choosing the controller poles at different locations to ensure that we can relocate loop zeros to improve loop robustness.

$$\hat{P}(z^2) = -[(z^2 - 0.5)(z^2 - 0.6)(z^2 - 0.7)] \quad \ldots\ldots\ldots (5.7)$$

D. Desired closed loop poles:

The order of the plant is 4; hence there must be 4 desired closed-loop pole locations which are chosen according to root-locus diagram.

$$\breve{\Delta}(z^2) = [z^2(z^2 - 0.0164)(z^2 - 0.02825)(z^2 - 0.5)] \quad \ldots\ldots\ldots (5.8)$$

E. Additional closed-loop poles introduced by the controller:

Additional closed-loop controller poles are chosen similar to controller poles to cancel out controller poles with loop-zero polynomial.

$$\widetilde{D}(z^2) = -[(z^2 - 0.5)(z^2 - 0.6)(z^2 - 0.7)] \quad \ldots\ldots\ldots (5.9)$$

F. Loop zero polynomial:

From characteristic equation in eqn,(4.50), we can say:

$$k\tilde{Z}(z^2) = \breve{\Delta}(z^2)\widetilde{D}(z^2) - \hat{A}(z^2)\hat{P}(z^2) \quad \ldots\ldots\ldots (5.10)$$

Applying this here we get:

$$\tilde{Z}(z^2) = -0.4936\, z^2\, (z^2 - 0.7)(z^2 - 0.6)(z^2 - 0.5)(z^2 - 0.02825)(z^2 - 0.0164) \ldots\ldots\ldots (5.11)$$

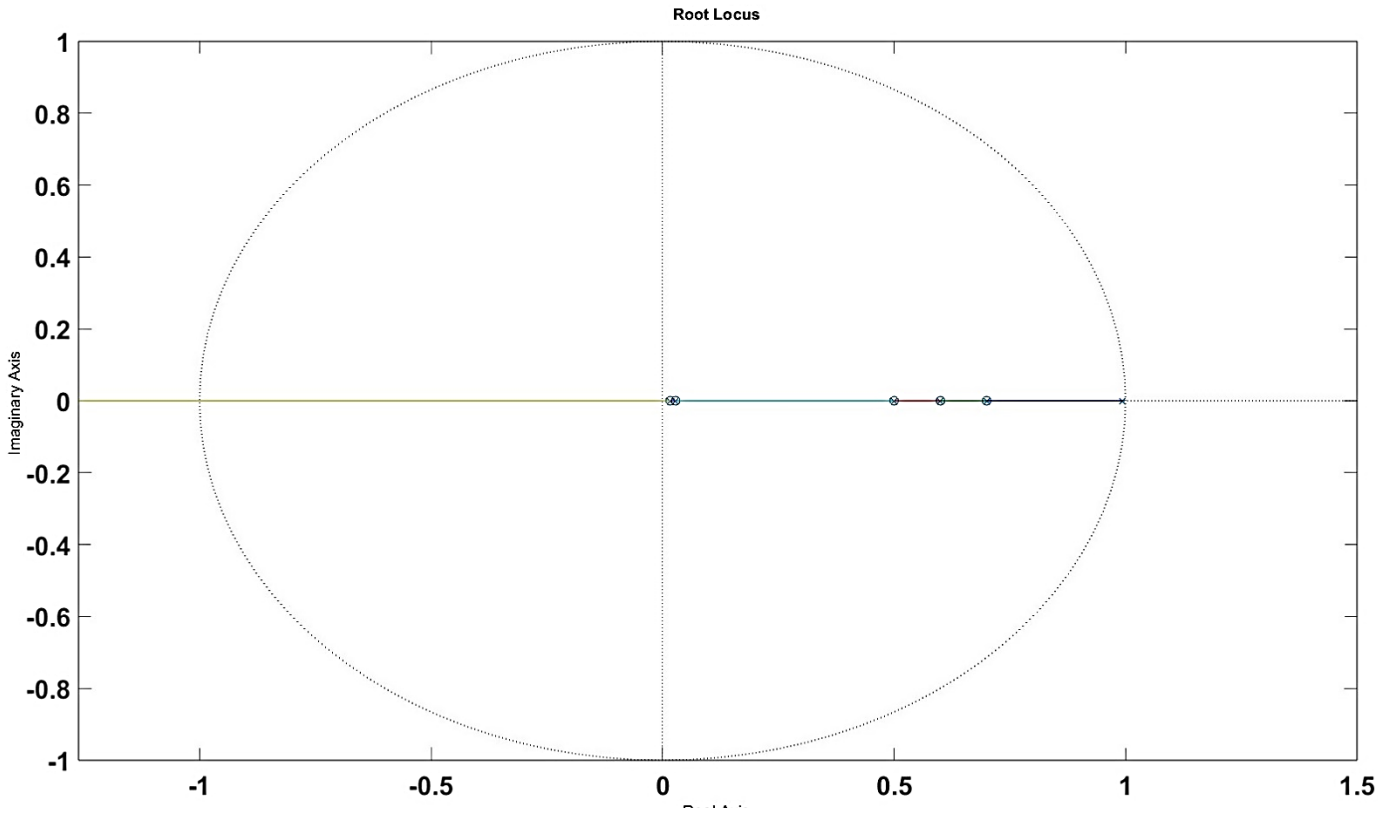

Fig.5.3: Root locus for 2-rate compensation using $\left(\frac{z+1}{z}\right)$ augmentation

The root locus corresponding to the equivalent time-lifted loop transfer function is shown in Fig.5.3. As can be obtained from the root locus the GM for the 2-rate compensated system will be 9.1863, which can be shown to be significantly larger than the GM obtained by employing PI controller in the outer loop.

G. Degree of the loop-zero polynomial (θ):

From eqn. (4.55) : $\theta = m + \eta \; with \; \eta = n - I^{+}\left\{\frac{n-r}{2}\right\}$

$n = 4$ and from eqn.( ), $m = 3$; thus, $\eta = 3$; which makes $\theta = 3 + 3 = 6$ ... ... (5.12)

H. Controller Synthesis:

a) as $\theta = 6$;

$$\tilde{Z}(z^2) = r_0 + r_2 z^2 + r_4 z^4 + r_6 z^6 + r_8 z^8 + r_{10} z^{10} + r_{12} z^{12} \; \ldots\ldots\ldots (5.13)$$

b) Expanding eqn. (5.11) we get:

$$\tilde{Z}(z^2) = -0.4936\, z^{12} + 0.9105\, z^{10} - 0.5681\, z^8 + 0.1276\, z^6 - 0.004873\, z^4 + 4.802e-05\, z^2 \; \ldots\ldots (5.14)$$

Comparing eqn.(5.13) and eqn.(5.14) we can say that:

$$r_0 = 0; r_2 = 4.802e-05\,; r_4 = -0.004873;$$
$$r_6 = 0.1276; r_8 = -0.5681; r_{10} = 0.9105; r_{12} = -0.4936$$

c) $\varphi_1 = I^{-}\left\{\frac{n+r}{2}\right\} = I^{-}\left(\frac{7}{2}\right) = 3 \quad and \;\; \varphi_2 = I^{-}\left\{\frac{n+r-1}{2}\right\} = 3$

d) Now, $a^{+}b^{-} = \hat{B}(z) = \hat{B}_e(z^2) + z\hat{B}_d(z^2)$

$$= \hat{b}_0 + \hat{b}_2 z^2 + \hat{b}_4 z^4 + \hat{b}_6 z^6 + z[\hat{b}_1 + \hat{b}_3 z^2 + \hat{b}_5 z^4 + \hat{b}_7 z^6]$$

$$= 0 + 0.2188z + 3.3z^2 + 13.43z^3 + 3.121z^4 - 37.52z^5 - 6.127z^6 + 23.58z^7$$

Thus, upon comparing we get:

$$\hat{b}_0 = 0; \hat{b}_1 = 0.2188; \hat{b}_2 = 3.3; \hat{b}_3 = 13.43;$$
$$\hat{b}_4 = 3.121;\; \hat{b}_5 = -37.52; \hat{b}_6 = -6.127;\; \hat{b}_7 = 23.58$$

e) Now we know that;

$$\hat{L}(z) = \hat{L}_e(z^2) + z\hat{L}_d(z^2) = \hat{l_0} + \hat{l}_2 z^2 + \hat{l}_4 z^4 + \hat{l}_6 z^6 + z\left[\hat{l}_1 + \hat{l}_3 z^2 + \hat{l}_5 z^4\right] \ldots\ldots\ldots (5.15)$$

f) $\tilde{Z}(z^2) = 2\hat{B}_e(z^2)\hat{L}_e(z^2) + 2z^2\hat{B}_d(z^2)\hat{L}_d(z^2)$

$$= r_0 + r_2 z^2 + r_4 z^4 + r_6 z^6 + r_8 z^8 + r_{10} z^{10} + r_{12} z^{12}$$

Thus by (4.60) we get the Sylvester matrix as;

$$\begin{bmatrix} r_0 \\ r_2 \\ r_4 \\ r_6 \\ r_8 \\ r_{10} \\ r_{12} \end{bmatrix} = 2 * \begin{bmatrix} \hat{b}_0 & 0 & 0 & 0 & 0 & 0 & 0 \\ \hat{b}_2 & \hat{b}_0 & 0 & 0 & \hat{b}_1 & 0 & 0 \\ \hat{b}_4 & \hat{b}_2 & \hat{b}_0 & 0 & \hat{b}_3 & \hat{b}_1 & 0 \\ \hat{b}_6 & \hat{b}_4 & \hat{b}_2 & \hat{b}_0 & \hat{b}_5 & \hat{b}_3 & \hat{b}_1 \\ 0 & \hat{b}_6 & \hat{b}_4 & \hat{b}_2 & \hat{b}_7 & \hat{b}_5 & \hat{b}_3 \\ 0 & 0 & \hat{b}_6 & \hat{b}_4 & 0 & \hat{b}_7 & \hat{b}_5 \\ 0 & 0 & 0 & \hat{b}_6 & 0 & 0 & \hat{b}_7 \end{bmatrix} \begin{bmatrix} \hat{l}_0 \\ \hat{l}_2 \\ \hat{l}_4 \\ \hat{l}_6 \\ \hat{l}_1 \\ \hat{l}_3 \\ \hat{l}_5 \end{bmatrix} \quad \dots\dots\dots (5.16)$$

$$\begin{bmatrix} 0 \\ 4.802e-05 \\ -0.004873 \\ 0.1276 \\ -0.5681 \\ 0.9105 \\ -0.4936 \end{bmatrix} = 2 * \begin{bmatrix} 0 & 0 & 0 & 0 & 0 & 0 & 0 \\ 3.3 & 0 & 0 & 0 & 0.2188 & 0 & 0 \\ 3.121 & 3.3 & 0 & 0 & 13.43 & 0.2188 & 0 \\ -6.127 & 3.121 & 3.3 & 0 & -37.52 & 13.43 & 0.2188 \\ 0 & -6.127 & 3.121 & 3.3 & 23.58 & -37.52 & 13.43 \\ 0 & 0 & -6.127 & 3.121 & 0 & 23.58 & -37.52 \\ 0 & 0 & 0 & -6.127 & 0 & 0 & 23.58 \end{bmatrix} \begin{bmatrix} \hat{l}_0 \\ \hat{l}_2 \\ \hat{l}_4 \\ \hat{l}_6 \\ \hat{l}_1 \\ \hat{l}_3 \\ \hat{l}_5 \end{bmatrix} \dots\dots (5.17)$$

Now, since one row of the matrix is zero, so are reducing the rank of the matrix by eliminating the 1st row of $\bar{B}$-matrix and 1st element of $\hat{r}$-matrix and hence $\hat{l}_0$ also =0. Thus the matrix becomes:

$$\begin{bmatrix} 4.802e-05 \\ -0.004873 \\ 0.1276 \\ -0.5681 \\ 0.9105 \\ -0.4936 \end{bmatrix} = 2 * \begin{bmatrix} 3.3 & 0 & 0 & 0 & 0.2188 & 0 & 0 \\ 3.121 & 3.3 & 0 & 0 & 13.43 & 0.2188 & 0 \\ -6.127 & 3.121 & 3.3 & 0 & -37.52 & 13.43 & 0.2188 \\ 0 & -6.127 & 3.121 & 3.3 & 23.58 & -37.52 & 13.43 \\ 0 & 0 & -6.127 & 3.121 & 0 & 23.58 & -37.52 \\ 0 & 0 & 0 & -6.127 & 0 & 0 & 23.58 \end{bmatrix} \begin{bmatrix} \hat{l}_2 \\ \hat{l}_4 \\ \hat{l}_6 \\ \hat{l}_1 \\ \hat{l}_3 \\ \hat{l}_5 \end{bmatrix} \dots\dots (5.18)$$

Solving the above matrix equation we get:

$$\hat{l}_1 = 0; \hat{l}_3 = -0.1992\ ; \hat{l}_5 = -0.4004; \hat{l}_2 = 0.012\ ; \hat{l}_4 = 0.8466; \hat{l}_6 = -1.501$$

I. Controller Parameters:

To find the controller parameters we choose the condition: $Q_0^+ = Q_1^-$

According, to the condition mentioned above one can say, $\hat{L}(z) = Q_0^-(P_0^+ - P_1^-)$

$$\hat{L}(z) = -1.501\, z^6 - 0.4004\, z^5 + 0.8466\, z^4 - 0.1992\, z^3 + 0.012\, z^2 \quad \dots\dots\dots (5.19)$$

$$= (-1.501\, z^3 - 0.835\, z^2 + 0.6332\, z)(z^3 - 0.2896\, z^2 + 0.01895\, z) \quad \dots\dots\dots (5.20)$$

Q_0^- $\qquad$ $P_0^+ - P_1^-$

Assigning the non-monic part as Q_0^- and the monic part as $(P_0^+ - P_1^-)$

$$\therefore Q_0^- = -1.501\,z^3 - 0.835\,z^2 + 0.6332\,z \quad \ldots\ldots\ldots (5.21)$$

$$and\ (P_0^+ - P_1^-) = z^3 - 0.2896\,z^2 + 0.01895\,z \quad \ldots\ldots\ldots (5.22)$$

a) Calculation of D_0, D_1, D_2, D_3:

From (4.15) for m=3

$Q_0^+ = Q_0(z) = [d_{3,0}z^3 + d_{2,0}z^2 + d_{1,0}z + d_{0,0}]$

$\therefore Q_0^- = \left[-d_{3,0}z^3 + d_{2,0}z^2 - d_{1,0}z + d_{0,0}\right] = (-1.501\,z^3 - 0.835\,z^2 + 0.6332\,z) \ldots (5.23)$

Thus by comparing:

$$d_{3,0} = 1.501; d_{2,0} = -0.835; d_{1,0} = -0.6332;\ d_{0,0} = 0$$

Now, according to condition: $Q_0^+ = Q_1^-$

$$=>\ \left[d_{3,0}z^3 + d_{2,0}z^2 + d_{1,0}z + d_{0,0}\right] = \left[-d_{3,1}z^3 + d_{2,1}z^2 - d_{1,1}z + d_{0,1}\right] \ldots\ldots\ldots (5.24)$$

Thus, by comparing:

$$d_{3,1} = -d_{3,0} = -1.501;\ d_{2,1} = d_{2,0} = -0.835;\ d_{1,1} = -d_{1,0} = 0.6332;\ d_{0,1} = d_{0,0} = 0$$

According to eqn. (4.11) :

- $D_0 = d_{0,0} + d_{0,1} = 0\ (Even)\quad and\ \ d_{0,0} - d_{0,1} = 0\ (Odd)$
- $D_1 = d_{1,0} + d_{1,1} = 0\ (Even)\quad and\ \ d_{1,0} - d_{1,1} = -1.2644\ (odd)$
- $D_2 = d_{2,0} + d_{2,1} = -1.6700\ (Even)\quad and\quad d_{2,0} - d_{2,1} = 0\ (Odd)$
- $D_3 = d_{3,0} + d_{3,1} = 0\ (Even)\quad and\ \ d_{3,0} - d_{3,1} = 3.0020\ (Odd)$

b) Calculation of C_0, C_1, C_2:

From eqn. (4.62) for m=3 : $(P_0^+ - P_1^-) = \Gamma(z) = \gamma_0 + \gamma_1 z + \gamma_2 z^2 + \gamma_3 z^3 \ldots\ldots\ldots (5.25)$

$$= z^3 - 0.2896\,z^2 + 0.01895\,z \ldots\ldots\ldots (5.26)$$

Comparing eqn.(5.25) and eqn.(5.26) we get:

$$\gamma_0 = 0; \gamma_1 = 0.01895\ ; \gamma_2 = -0.2896; \gamma_3 = 1$$

Now, we know for m=3, $\hat{P}(z^2) = \hat{p}_0 + \hat{p}_2 z^2 + \hat{p}_4 z^4 - z^6 \quad \ldots\ldots\ldots (5.27)$

Upon, expanding eqn.(5.7) we get: $\hat{P}(z^2) = -z^6 + 1.8\,z^4 - 1.07\,z^2 + 0.21 \ldots\ldots\ldots (5.28)$

Comparing, eqn.(5.27) and eqn.(5.28) we get:

$$\hat{p}_0 = 0.21;\ \hat{p}_2 = -1.07; \hat{p}_4 = 1.8$$

From ( ) we got : $P_0^+\Gamma^- + P_0^-\Gamma^+ = \hat{P}(z^2) + \Gamma^+\Gamma^-$ ... ... (5.29)

Expressing the above equation in matrix form for m=3 we get:

$$2 * \begin{bmatrix} \gamma_0 & 0 & 0 & 0 \\ \gamma_2 & -\gamma_1 & \gamma_0 & 0 \\ 0 & -\gamma_3 & \gamma_2 & -\gamma_1 \\ 0 & 0 & 0 & -\gamma_3 \end{bmatrix} \begin{bmatrix} c_{0,0} \\ c_{1,0} \\ c_{2,0} \\ 1 \end{bmatrix} = \begin{bmatrix} \hat{p}_0 + \gamma_0^2 \\ \hat{p}_2 + 2\gamma_0\gamma_2 - \gamma_1^2 \\ \hat{p}_4 - 2\gamma_1\gamma_3 + \gamma_2^2 \\ -1 - \gamma_3^2 \end{bmatrix} \quad \text{... ... ... (5.30)}$$

Putting the values in the above matrix equation we get:

$$2 * \begin{bmatrix} 0 & 0 & 0 & 0 \\ -0.2896 & -0.01895 & 0 & 0 \\ 0 & -1 & -0.2896 & -0.01895 \\ 0 & 0 & 0 & -1 \end{bmatrix} \begin{bmatrix} c_{0,0} \\ c_{1,0} \\ c_{2,0} \\ 1 \end{bmatrix} = \begin{bmatrix} -2 \\ 1.8460 \\ -1.0704 \\ -0.2100 \end{bmatrix} \text{... ... ... (5.31)}$$

Solving, eqn.(5.31) we get:

$$c_{0,0} = 1.9042; c_{1,0} = -0.8594; c_{2,0} = -0.2850$$

Thus from eqn. (4.65):

$$c_{0,1} = c_{0,0} - \gamma_0 = c_{0,0} - 0 = 1.9042 \quad \text{... ... ... (5.32)}$$

$$c_{1,1} = -\left(c_{1,0} - \gamma_1\right) = -(-0.8594 - 0.01895) = 0.8784 \quad \text{... ... ... (5.33)}$$

$$c_{2,1} = c_{2,0} - \gamma_2 = -0.2850 - (-0.2896) = 0.0046 \quad \text{... ... ... (5.34)}$$

Eventually, we get:

$$c_{0,1} = 1.9042; c_{1,1} = 0.8784; c_{2,1} = 0.0046$$

According to eqn. (4.12) :

- $C_0 = c_{0,0} + c_{0,1} = 3.8084\ (Even) \quad and \quad c_{0,0} - c_{0,1} = 0\ (Odd)$
- $C_1 = c_{1,0} + c_{1,1} = 0.0190\ (Even) \quad and \quad c_{1,0} - c_{1,1} = -1.7378\ (odd)$
- $C_2 = c_{2,0} + c_{2,1} = -0.2804\ (Even) \quad and \quad c_{2,0} - c_{2,1} = -0.2896\ (Odd)$

Implementing all the calculated controller feedback and feedforward gains in a 3rd order 2-periodic controller for 4th order plant is shown in fig.(5.4):

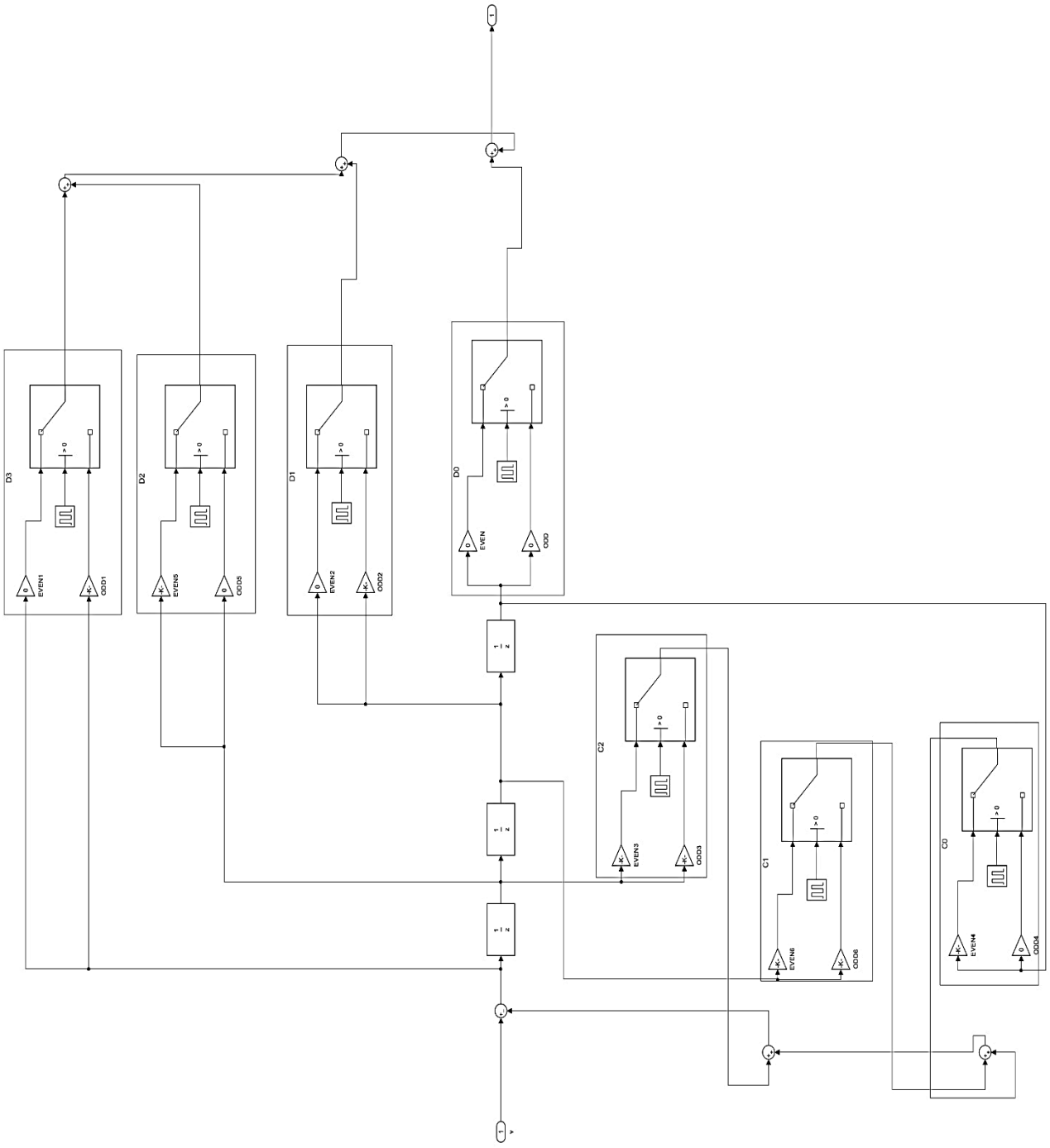

Fig.5.4: 3rd order 2-periodic controller for 4th order LTI plant

The 3rd order 2-periodic controller system is now converted into a subsystem having solar PV array output as a reference input to the system in a 2-loop architecture as shown in fig,(5.5)

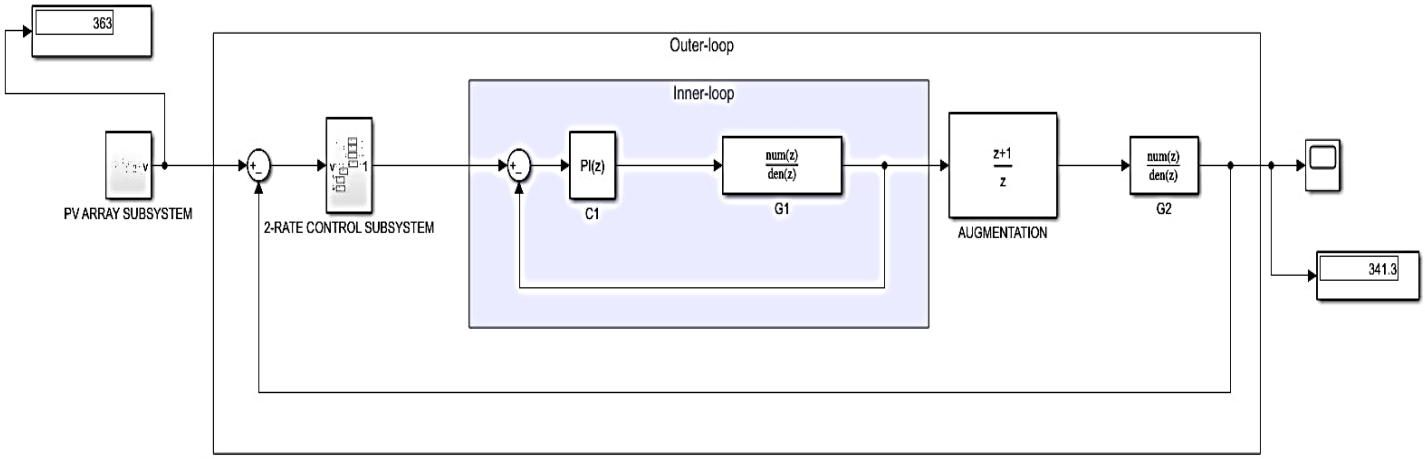

Fig.5.5: 2-periodic controller system for boost converter with $\left(\frac{z+1}{z}\right)$ augmentation taking solar PV array as a reference input

The components inside the PV array subsystem is similar to Fig. 2.10.

Thus, the output response for this 2-periodic compensation of boost converter with $\left(\frac{z+1}{z}\right)$ augmentation taking PV array as a reference input is shown below in Fig. 5.6.

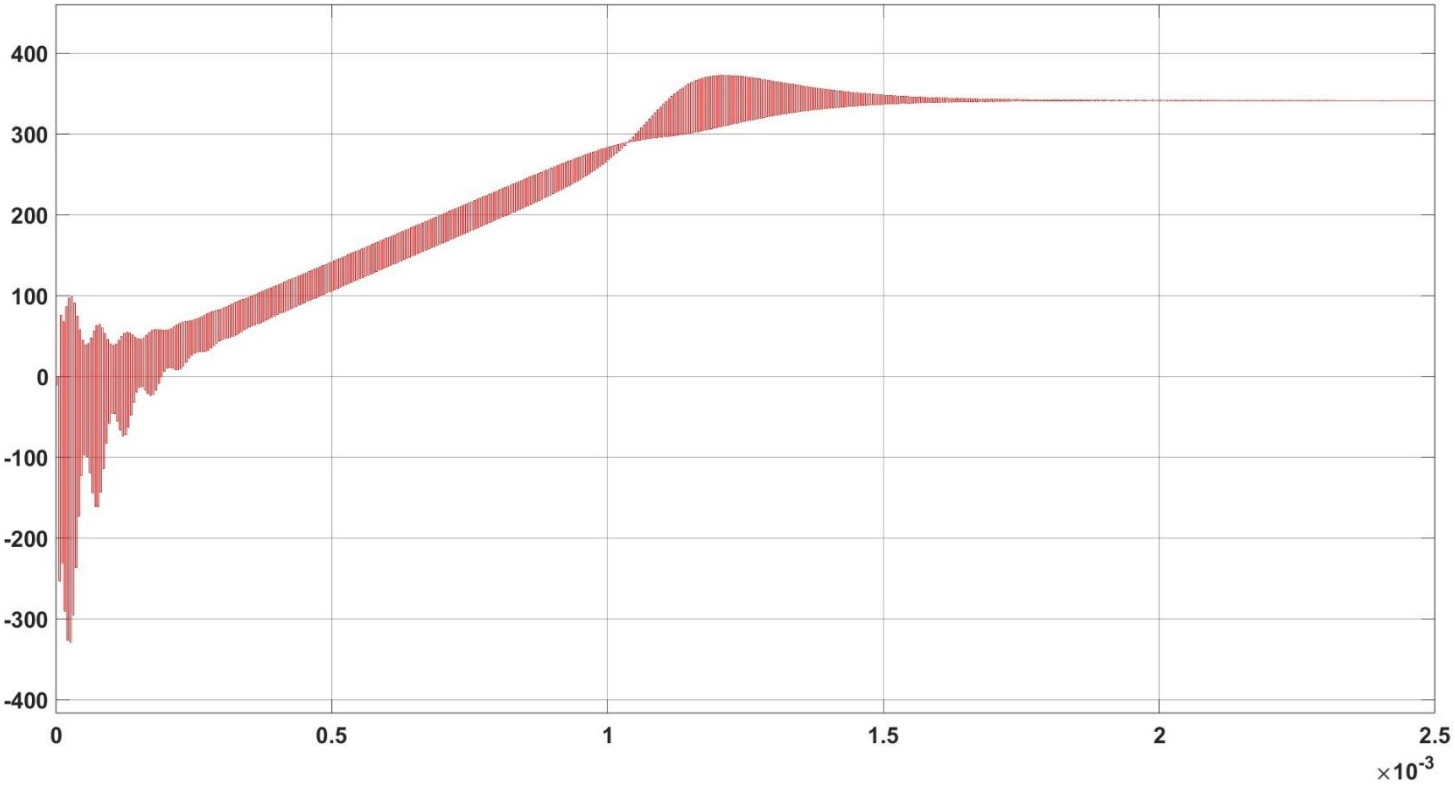

Fig. 5.6: Output response curve for double-loop compensation of boost converter with $\left(\frac{z+1}{z}\right)$

Hence, for a reference of 363V we are getting an output value of 341.3V, in-spite of using 2-periodic controller in the outer-loop which is giving us a better Gain Margin compared to double-loop PI compensation but as there is an offset so we are opting to see the results after using $\left(\frac{z}{z-1}\right)$ augmentation.

5.3.2 With augmentation $\left(\frac{z}{z-1}\right)$:

A. Lifting the plant:

$$\hat{A}(z^2) = a^+a^- = (z^2-1)(z^2-0.9936)(z^2-0.0164)(z^2-0.02825) \dots\dots\dots (5.35)$$

B. Order of the controller(m):

$n =$ order of denominator of plant = 4; $r =$ order of numerator of plant = 3; so m = 3;

C. Choosing controller poles:

We are choosing the controller poles at different locations to ensure that we can relocate loop zeros to improve loop robustness.

$$\hat{P}(z^2) = -[(z^2-0.3)(z^2-0.4)(z^2-0.5)] \dots\dots\dots (5.36)$$

D. Desired closed loop poles:

The order of the plant is 4; hence there must be 4 desired closed-loop pole locations which are chosen according to root-locus diagram.

$$\breve{\Delta}(z^2) = (z^2-0.0164)(z^2-0.02825)(z^2-0.28)(z^2-0.35) \dots\dots\dots (5.37)$$

E. Additional closed-loop poles introduced by the controller:

Additional closed-loop controller poles are chosen similar to controller poles to cancel out controller poles with loop-zero polynomial.

$$\widetilde{D}(z^2) = -[(z^2-0.3)(z^2-0.4)(z^2-0.5)] \dots\dots\dots (5.38)$$

F. Loop zero polynomial:

From eqn.(5.10); we can say that,

$$\tilde{Z}(z^2) = -1.3636(z^2-0.6567)(z^2-0.5)(z^2-0.4)(z^2-0.3)(z^2-0.02825)(z^2-0.0164) \dots\dots\dots (5.39)$$

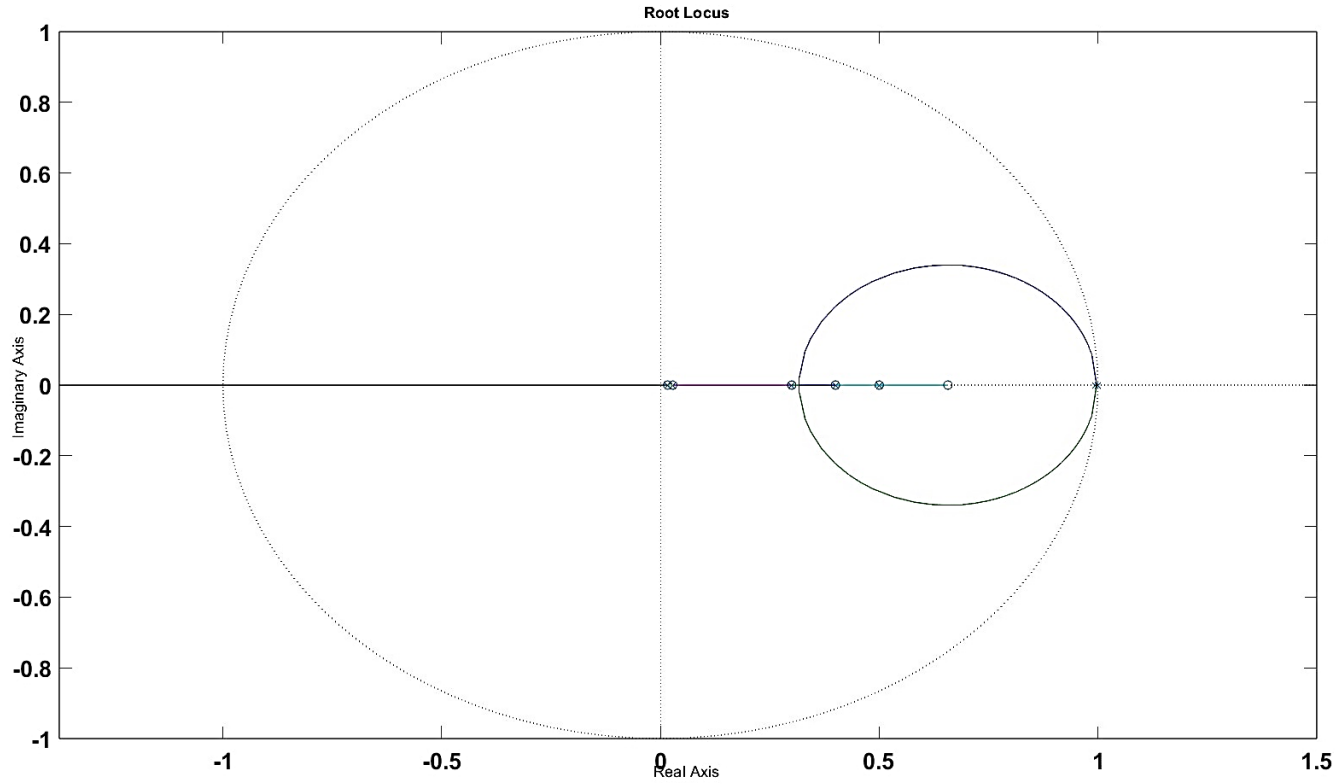

Fig.5.7: Root locus for 2-rate compensation using $\left(\frac{z}{z-1}\right)$ augmentation

The root locus corresponding to the equivalent time-lifted loop transfer function is shown in Fig.5.7. As can be obtained from the root locus the GM for the 2-rate compensated system will be 1.298, which can be shown to be smaller than the GM obtained by employing PI controller in the outer loop.

G. Degree of the loop-zero polynomial (θ):

$n = 4$ and from eqn.(4.56), $m = 3$; thus, $\eta = 3$; which makes $\theta = 3 + 3 = 6$

H. Controller Synthesis:

a) Expanding eqn. (5.39) we get

$$\tilde{Z}(z^2) = -1..364z^{12} + 2.593z^{10} - 1.829z^8 + 0.5805z^6 - 0.07698z^4 + 0.002632z^2 - 2.49e - 5 \ldots (5.40)$$

Comparing eqn.(5.40) with eqn.(5.13) we get:

$$r_0 = -2.49e - 5; r_2 = 0.002632\ ; r_4 = -0.07698;$$
$$r_6 = 0.5805; r_8 = -1.829; r_{10} = 2.593; r_{12} = -1.364$$

b) $\varphi_1 = I^-\left\{\frac{n+r}{2}\right\} = I^-\left(\frac{7}{2}\right) = 3 \quad and \;\; \varphi_2 = I^-\left\{\frac{n+r-1}{2}\right\} = 3$

c) Now, $a^+b^- = \hat{B}(z) = \hat{B}_e(z^2) + z\hat{B}_d(z^2)$

$$= \hat{b}_0 + \hat{b}_2 z^2 + \hat{b}_4 z^4 + \hat{b}_6 z^6 + z[\hat{b}_1 + \hat{b}_3 z^2 + \hat{b}_5 z^4 + \hat{b}_7 z^6]$$

$$= 0 + 0.2188z + 3.3z^2 + 13.43z^3 + 3.121z^4 - 37.52z^5 - 6.127z^6 + 23.58z^7$$

Thus, upon comparing we get:

$$\hat{b}_0 = 0; \hat{b}_1 = 0.2188; \hat{b}_2 = 3.3; \hat{b}_3 = 13.43;$$
$$\hat{b}_4 = 3.121;\ \hat{b}_5 = -37.52; \hat{b}_6 = -6.127;\ \hat{b}_7 = 23.58$$

d) Now we know that;

$$\hat{L}(z) = \hat{L}_e(z^2) + z\hat{L}_d(z^2) = \hat{l_0} + \hat{l}_2 z^2 + \hat{l}_4 z^4 + \hat{l}_6 z^6 + z\left[\hat{l}_1 + \hat{l}_3 z^2 + \hat{l}_5 z^4\right]$$

Thus, comparing with eqn.(5.16) we get:

$$\begin{bmatrix} -2.49e-5 \\ 0.002632 \\ -0.07698 \\ 0.5805 \\ -1.829 \\ 2.593 \\ -1.364 \end{bmatrix} = 2 * \begin{bmatrix} 0 & 0 & 0 & 0 & 0 & 0 & 0 \\ 3.3 & 0 & 0 & 0 & 0.2188 & 0 & 0 \\ 3.121 & 3.3 & 0 & 0 & 13.43 & 0.2188 & 0 \\ -6.127 & 3.121 & 3.3 & 0 & -37.52 & 13.43 & 0.2188 \\ 0 & -6.127 & 3.121 & 3.3 & 23.58 & -37.52 & 13.43 \\ 0 & 0 & -6.127 & 3.121 & 0 & 23.58 & -37.52 \\ 0 & 0 & 0 & -6.127 & 0 & 0 & 23.58 \end{bmatrix} \begin{bmatrix} \hat{l_0} \\ \hat{l_2} \\ \hat{l_4} \\ \hat{l_6} \\ \hat{l_1} \\ \hat{l_3} \\ \hat{l_5} \end{bmatrix} \ldots\ldots (5.41)$$

Now, since one row of the matrix is zero, so are reducing the rank of the matrix by eliminating the 1st row of $\bar{B}$-matrix and 1st element of $\hat{r}$-matrix and hence $\hat{l}_0$ also =0. Thus the matrix becomes:

$$\begin{bmatrix} 0.002632 \\ -0.07698 \\ 0.5805 \\ -1.829 \\ 2.593 \\ -1.364 \end{bmatrix} = 2 * \begin{bmatrix} 3.3 & 0 & 0 & 0 & 0.2188 & 0 & 0 \\ 3.121 & 3.3 & 0 & 0 & 13.43 & 0.2188 & 0 \\ -6.127 & 3.121 & 3.3 & 0 & -37.52 & 13.43 & 0.2188 \\ 0 & -6.127 & 3.121 & 3.3 & 23.58 & -37.52 & 13.43 \\ 0 & 0 & -6.127 & 3.121 & 0 & 23.58 & -37.52 \\ 0 & 0 & 0 & -6.127 & 0 & 0 & 23.58 \end{bmatrix} \begin{bmatrix} \hat{l_2} \\ \hat{l_4} \\ \hat{l_6} \\ \hat{l_1} \\ \hat{l_3} \\ \hat{l_5} \end{bmatrix} \ldots\ldots (5.42)$$

Solving eqn.(5.42) we get:

$$\hat{l_1} = 0; \hat{l_3} = -0.6364\ ; \hat{l_5} = -1.304; \hat{l_2} = 0.0061\ ; \hat{l_4} = 2.827; \hat{l_6} = -4.909$$

I. Controller Parameters:

To find the controller parameters we choose the condition: $Q_0^+ = -Q_1^-$

Then from (4.66) one gets, $\hat{L}(z) = Q_0^-(P_0^+ + P_1^-)$

Now according to the condition discussed before in chapter 4 we divide the $\hat{L}(z)$ polynomial into two parts:

$$\hat{L}(z) = -4.909\,z^6 - 1.304\,z^5 + 2.827\,z^4 - 0.6364\,z^3 + 0.0061\,z^2 \ldots\ldots\ldots (5.43)$$

$$= (-4.909\,z^3 - 3.061\,z^2 + 1.749\,z)(z^3 - 0.3577\,z^2 + 0.003487\,z) \ldots\ldots\ldots (5.44)$$

Q_0^- $\qquad$ $P_0^+ + P_1^-$

Assigning the non-monic part as Q_0^- and the monic part as $(P_0^+ + P_1^-)$

$$Q_0^- = -4.909z^3 - 3.061z^2 + 1.749z \ldots\ldots\ldots (5.45)$$

$$P_0 + P_1^- = z^3 - 0.3577z^2 + 0.003487z \ldots\ldots\ldots (5.46)$$

a) Calculation of D_0, D_1, D_2, D_3:

$$Q_0^- = \left[-d_{3,0}z^3 + d_{2,0}z^2 - d_{1,0}z + d_{0,0}\right] = -4.909z^3 - 3.061z^2 + 1.749z \ldots\ldots\ldots (5.47)$$

Thus, by comparing:

$$d_{3,0} = 4.909; d_{2,0} = -3.061; d_{1,0} = -1.749;\ d_{0,0} = 0$$

Now, according to condition: $Q_0^+ = -Q_1^-$

$$\Rightarrow \left[d_{3,0}z^3 + d_{2,0}z^2 + d_{1,0}z + d_{0,0}\right] = -\left[-d_{3,1}z^3 + d_{2,1}z^2 - d_{1,1}z + d_{0,1}\right] \ldots\ldots\ldots (5.48)$$

Comparing both sides we get;

$$d_{3,1} = d_{3,0} = 4.909;\ d_{2,1} = -\,d_{2,0} = 3.061;\ d_{1,1} = d_{1,0} = -1.749;\ d_{0,1} = -d_{0,0} = 0$$

According to eqn. (4.11)

- $D_0 = d_{0,0} + d_{0,1} = 0\ (even) \quad and \quad d_{0,0} - d_{0,1} = 0\ (odd)$
- $D_1 = d_{1,0} + d_{1,1} = -3.498\ (even) \quad and \quad d_{1,0} - d_{1,1} = 0\ (odd)$
- $D_2 = d_{2,0} + d_{2,1} = 0\ (even) \quad and \quad d_{2,0} - d_{2,1} = -6.122\ (odd)$
- $D_3 = d_{3,0} + d_{3,1} = 9.818\ (even) \quad and \quad d_{3,0} - d_{3,1} = 0\ (odd)$

b) Calculation of C_0, C_1, C_2:

For m=3 : $(P_0^+ + P_1^-) = \Gamma(z) = \gamma_0 + \gamma_1 z + \gamma_2 z^2 + \gamma_3 z^3 \qquad \ldots\ldots\ldots (5.49)$

Comparing eqn.(5.49) with eqn.(5.46) we get:

$$(P_0^+ + P_1^-) = \Gamma(z) = \gamma_0 + \gamma_1 z + \gamma_2 z^2 + \gamma_3 z^3 = z^3 - 0.3577z^2 + 0.003487z \ldots\ldots\ldots (5.50)$$

Thus, $\gamma_0 = 0; \gamma_1 = 0.003487\ ; \gamma_2 = -0.3577; \gamma_3 = 1$

Now, $\hat{P}(z^2) = \hat{p}_0 + \hat{p}_2 z^2 + \hat{p}_4 z^4 - z^6 = -z^6 + 1.2\, z^4 - 0.47\, z^2 + 0.06 \ldots\ldots\ldots (5.51)$

Upon comparing, we get: $\hat{p}_0 = 0.06;\ \hat{p}_2 = -0.47;\ \hat{p}_4 = 1.2$

From (4.62) we got : $P_0^+\Gamma^- + P_0^-\Gamma^+ = \hat{P}(z^2) + \Gamma^+\Gamma^-$

Expressing the above equation in matrix form for m=3 we get:

$$2\begin{bmatrix} \gamma_0 & 0 & 0 & 0 \\ \gamma_2 & -\gamma_1 & \gamma_0 & 0 \\ 0 & -\gamma_3 & \gamma_2 & -\gamma_1 \\ 0 & 0 & 0 & -\gamma_3 \end{bmatrix}\begin{bmatrix} c_{0,0} \\ c_{1,0} \\ c_{2,0} \\ 1 \end{bmatrix} = \begin{bmatrix} \hat{p}_0 + \gamma_0^2 \\ \hat{p}_2 + 2\gamma_0\gamma_2 - \gamma_1^2 \\ \hat{p}_4 - 2\gamma_1\gamma_3 + \gamma_2^2 \\ -1 - \gamma_3^2 \end{bmatrix}$$

Putting the values in the above matrix equation we get:

$$2\begin{bmatrix} 0 & 0 & 0 & 0 \\ -0.3577 & -0.003487 & 0 & 0 \\ 0 & -1 & -0.3577 & -0.003487 \\ 0 & 0 & 0 & -1 \end{bmatrix}\begin{bmatrix} c_{0,0} \\ c_{1,0} \\ c_{2,0} \\ 1 \end{bmatrix} = \begin{bmatrix} 0.06 \\ -0.470012 \\ 1.3209 \\ -2 \end{bmatrix} \ldots\ldots (5.52)$$

Solving the above matrix equation we get: $c_{0,0} = 0.6627; c_{1,0} = -0.5879; c_{2,0} = -0.2126$

Thus from eqn. (4.67):

$$c_{0,1} = \gamma_0 - c_{0,0} = 0 - c_{0,0} = -0.6627 \qquad \ldots\ldots\ldots (5.53)$$

$$c_{1,1} = -(\gamma_1 - c_{1,0}) = -(0.003487 + 0.5879) = -0.591387 \ldots\ldots\ldots (5.54)$$

$$c_{2,1} = \gamma_2 - c_{2,0} = -0.3577 - (-0.2126) = -0.1451 \quad \ldots\ldots\ldots (5.55)$$

According to eqn. (4.12)

- $C_0 = c_{0,0} + c_{0,1} = 0\ (Even) \quad and \quad c_{0,0} - c_{0,1} = 1.3254\ (Odd)$
- $C_1 = c_{1,0} + c_{1,1} = -1.17928\ (Even) \quad and \quad c_{1,0} - c_{1,1} = 0.00348\ (odd)$
- $C_2 = c_{2,0} + c_{2,1} = -0.3577\ (Even) \quad and \quad c_{2,0} - c_{2,1} = -0.0675\ (Odd)$

Implementing all the calculated controller feedback and feedforward gains in a 3rd order 2-periodic controller for 4th order plant is shown in fig.(5.8):

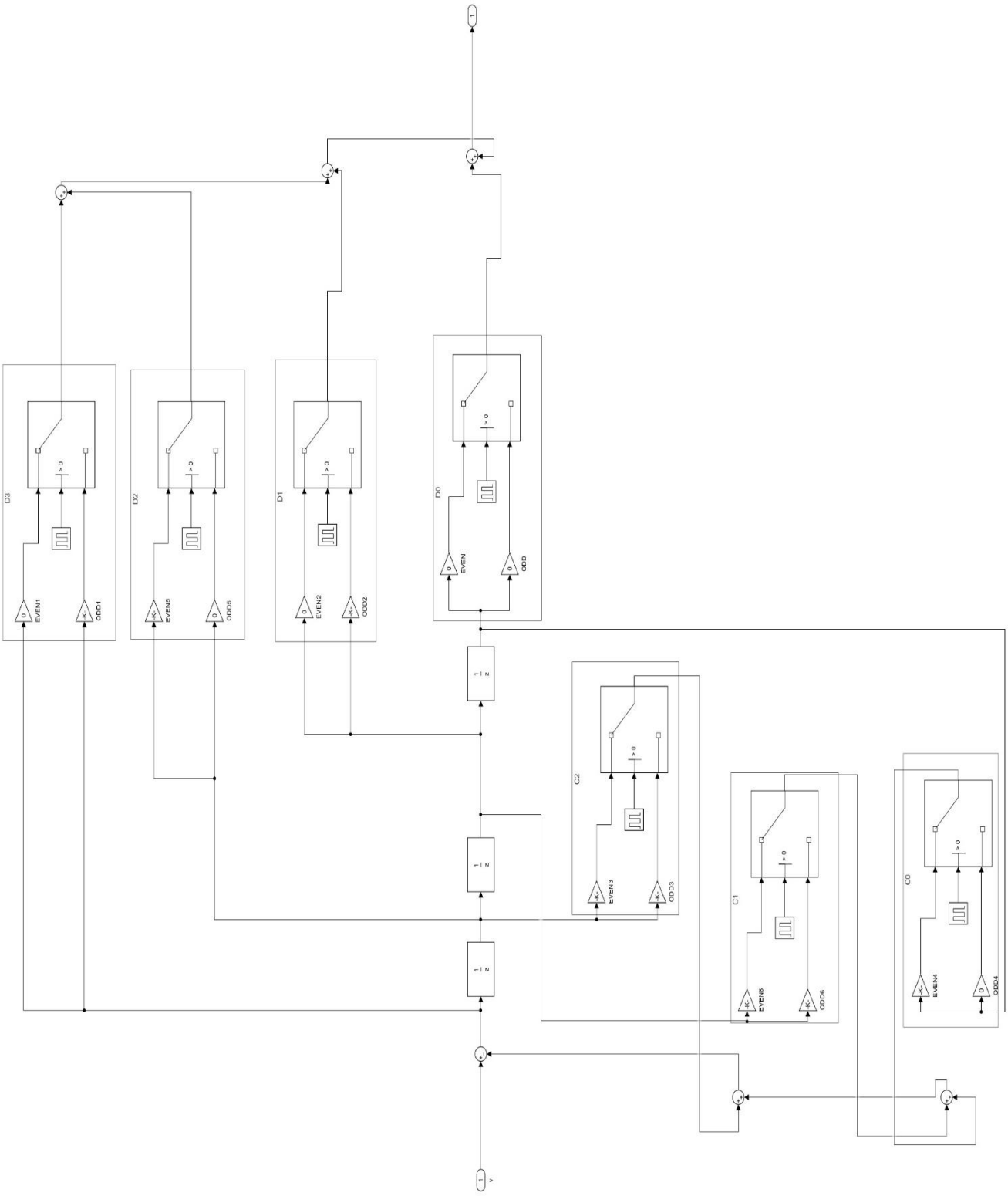

Fig.5.8: 3rd order 2-periodic controller for 4th order LTI plant

The 3rd order 2-periodic controller system is now converted into a subsystem having a solar PV array output as a reference input to the system in a 2-loop architecture as shown in fig,(5.9)

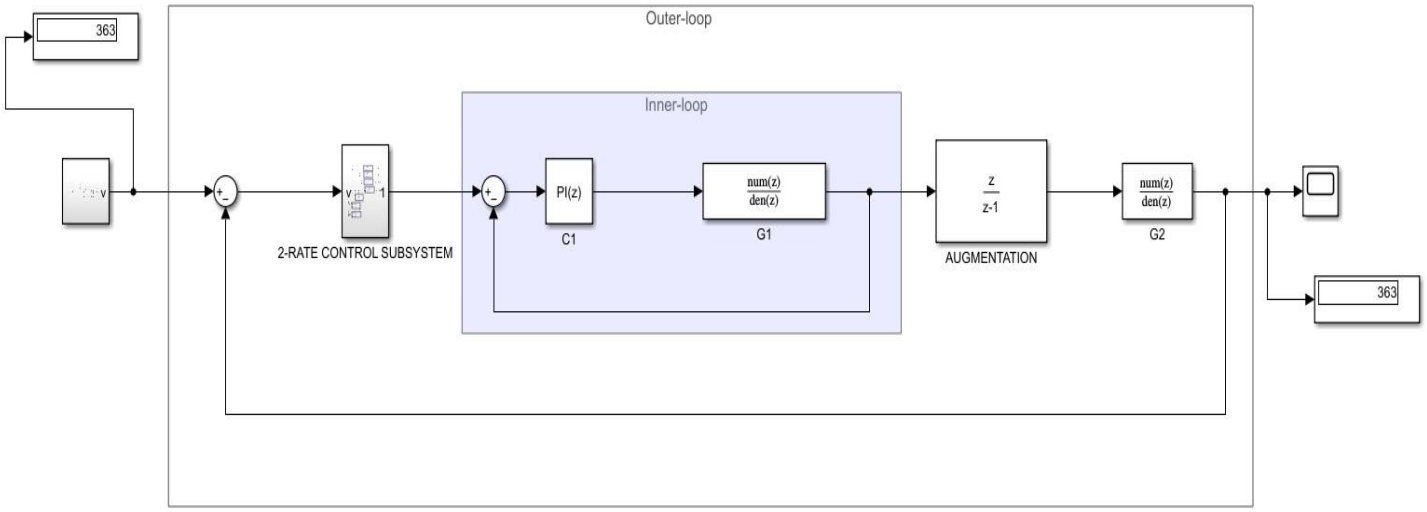

Fig.5.9: 2-periodic controller system for boost converter with $\left(\frac{z}{z-1}\right)$ augmentation taking solar PV array as a reference input

Thus, the output response for this 2-periodic compensation of boost converter with $\left(\frac{z}{z-1}\right)$ augmentation taking PV array as a reference input is shown below in fig.(5.10)

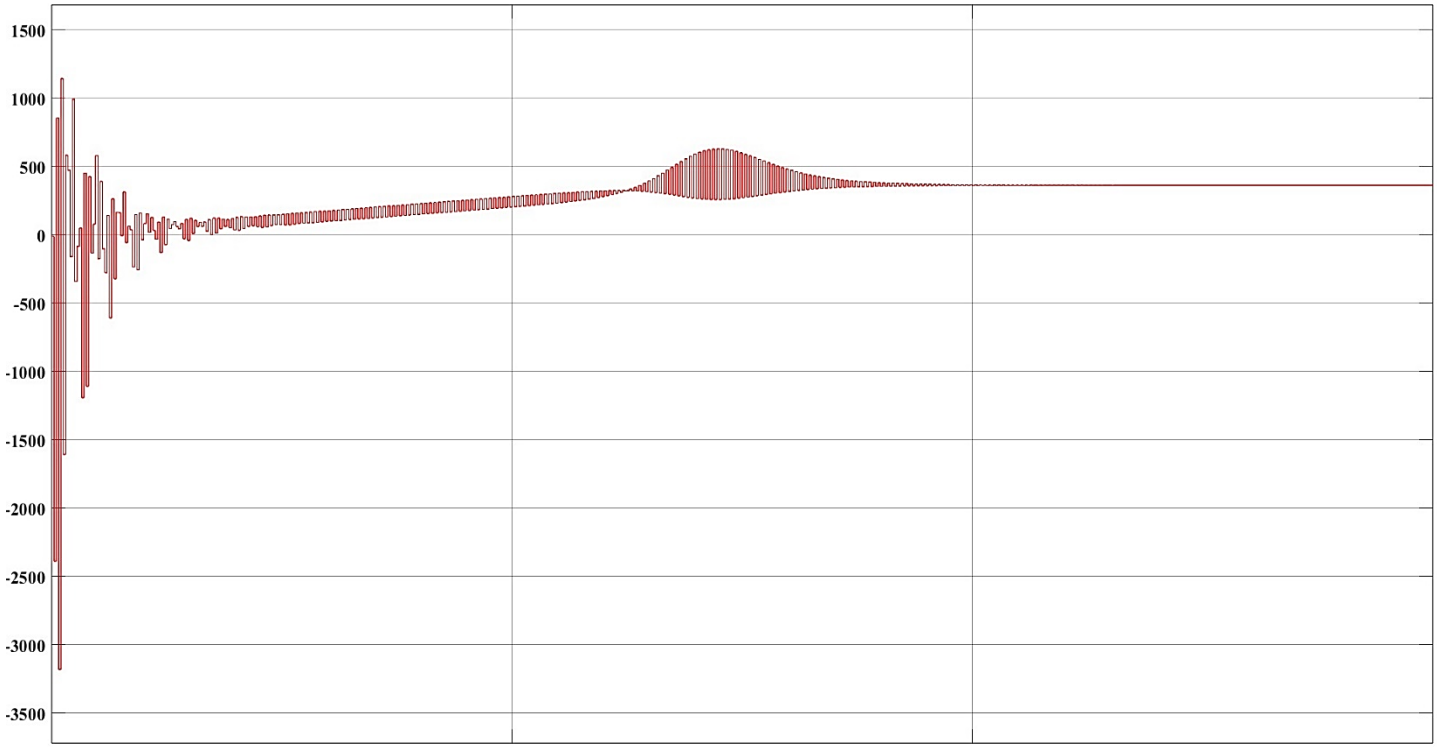

Fig.5.10: Output response curve for double-loop compensation of boost converter with $\left(\frac{z}{z-1}\right)$ augmentation

As, we can see here that the output for $\left(\frac{z}{z-1}\right)$ augmentation is following the input reference voltage of 363V and the output is also 363V which was difficult to achieve in $\left(\frac{z+1}{z}\right)$ augmentation, but here we can see an overshoot which was not present in the previous augmentation.

5.4 Conclusions:

This chapter discusses the implementation of 2-Periodic controller for Boost Converters. In order to ensure ripple free steady state step response two types of LDTI augmentations to the plant are considered along with the 2-periodic controller. Simulation results indicate that although the augmentation given by $\boldsymbol{\frac{(z+1)}{z}}$ yields better transient response it fails to achieve the desired steady state level leading to steady state offset. On the other hand, the augmentation $\boldsymbol{\frac{z}{(z-1)}}$ yields zero steady state error, owing to the fact that the presence of the pole at $z = 1$ increases the system type by 1. However, due to presence of the pole at $z = 1$ the transient behaviour exhibits considerable overshoot and undershoot. A more detailed study in respect of the choice of controller poles and loop zeros may be carried out to improve the transient behaviour.

Chapter 6

Conclusion and Future Scope

6.1 Conclusion

In this work the design and implementation of a 2-periodic compensation strategy for DC-DC boost converters, particularly in photovoltaic (PV) applications is investigated. The study addresses the challenges posed by the non-minimum phase zeros in boost converters, which complicates control system stability and performance. By replacing the conventional outer-loop PI controller with a 2-periodic controller, the system achieves enhanced gain margin. A systematic simplified design methodology for the same is presented here. Simulation studies using MATLAB/Simulink validate the improved dynamic response and stability of the proposed control scheme. The findings demonstrate its applicability in renewable energy systems, paving the way for more efficient integration of PV cells in sustainable energy solutions.

6.2 Future Scope

The proposed 2-periodic compensation method for DC-DC boost converters offers significant improvements in stability and efficiency, but there is scope for further research and development:

1. **Real-Time Implementation**: The next step would involve real-world testing and implementation to validate the proposed system's performance under actual operating conditions.
2. **Integration with Advanced Energy Systems**: Exploring integration with advanced energy systems like hybrid renewable systems, including wind and energy storage devices, could extend its applicability.
3. **Optimization Algorithms**: Incorporating advanced optimization algorithms, such as machine learning or adaptive control techniques, could further enhance performance and robustness.
4. **Wide Applications**: Investigating the use of this control strategy in other DC-DC converters or renewable energy systems could broaden its industrial and practical usage.
5. **Hardware Simplification**: Future work could focus on reducing hardware complexity and cost while maintaining or improving performance.

These directions aim to bridge the gap between theoretical advancements and practical applications, making the system more efficient, scalable, and versatile.

REFERENCES

[1] M. A. Green, "Solar cells: operating principles, technology, and system applications," *Prentice-Hall*, 1982.

[2] B. Bose, "Power electronics and motor drives recent progress and perspective," *IEEE Transactions on Industrial Electronics*, vol. 56, no. 2, pp. 581–588, Feb. 2009.

[3] J. S. Salmi, M. Bouzguenda, A. Gastli, and A. Masmoudi, "MATLAB/Simulink based modeling of solar photovoltaic cell," *International Journal of Renewable Energy Research (IJRER)*, vol. 2, no. 2, pp. 213–218, 2012.

[4] S. Khalid and S. V. Kulkarni, "Comparison of MPPT algorithms for DC-DC converters based photovoltaic systems," *IEEE Conference on Emerging Devices and Smart Systems (ICEDSS)*, Mar. 2016, pp. 26–30.

[5] T. Esram and P. L. Chapman, "Comparison of photovoltaic array maximum power point tracking techniques," *IEEE Transactions on Energy Conversion*, vol. 22, no. 2, pp. 439–449, Jun. 2007.

[6] S. Jain and V. Agarwal, "A single-stage grid connected inverter topology for solar PV systems with maximum power point tracking," *IEEE Transactions on Power Electronics*, vol. 22, no. 5, pp. 1928–1940, Sep. 2007.

[7] J. M. Enrique, E. Durán, M. Sidrach-de-Cardona, and J. M. Andújar, "Theoretical assessment of the maximum power point tracking efficiency of photovoltaic facilities with different converter topologies," *IEEE Transactions on Industrial Electronics*, vol. 55, no. 7, pp. 2674–2683, Jul. 2008.

[8] A. Luque and S. Hegedus, *Handbook of Photovoltaic Science and Engineering*, 2nd ed. Wiley, 2011, pp. 39-62.

[9] T. Markvart and L. Castaner, *Practical Handbook of Photovoltaics: Fundamentals and Applications*, 2nd ed. Academic Press, 2012, pp. 705-724.

[10] J. A. Duffie and W. A. Beckman, *Solar Engineering of Thermal Processes*, 4th ed. Wiley, 2013, pp. 891-900.

[11] S. R. Wenham, M. A. Green, M. E. Watt, and R. Corkish, *Applied Photovoltaics*, 2nd ed. Routledge, 2007, pp. 345-360.

[12] F. Blaabjerg and K. Ma, "Future on Power Electronics for Wind Turbine Systems," *IEEE Journal of Emerging and Selected Topics in Power Electronics*, Vol. 1, no. 3, pp. 139-152, Sept. 2013.

[13] Electrical4U, "Boost Converter (Step-Up Chopper)," *Electrical4U*. [Online]. Available: https://www.electrical4u.com/boost-converter-step-up-chopper/. [Accessed: Aug. 25, 2024].

[14] M. Rashid, *Power Electronics: Circuits, Devices, and Applications*, 4th ed. Pearson, 2013.

[15] A. R. Ali and M. I. L. Saleh, *Renewable Energy Systems and Technologies*, 1st ed., Berlin, Germany: Springer, 2015.

[16] S. K. Jain and V. K. Gupta, "Performance Analysis of Boost Converter," *International Journal of Electronics and Electrical Engineering*, vol. 3, no. 2, pp. 143-150, Jun. 2011.

[17] S. H. Lee, "Advanced Control Techniques for Boost Converters," *IEEE Transactions on Power Electronics*, vol. 25, no. 6, pp. 1520-1530, Jun. 2010.

[18] M. W. O'Neill, *Practical Power Electronics*, 2nd ed., New York, NY, USA: Wiley, 2018.

[19] J. B. Miller, "Design Considerations for High Efficiency Boost Converters," *IEEE Power Electronics Conference*, pp. 152-159, Aug. 2014.

[20] A. K. Jain and A. K. Agarwal, "A Comparative Study of Different Control Strategies for DC-DC Converters," in *Proceedings of the 2012 IEEE International Conference on Power Electronics, Drives and Energy Systems (PEDES),* Bengaluru, India, Dec. 2012.

[21] A. G. Yepes, F. D. Freijedo, Ó. López, and J. Doval-Gandoy, "High-Performance Digital Control for Single-Phase Active Power Filters Based on FPGA Implementation," *IEEE Transactions on Industrial Electronics*, Vol. 55, no. 8, pp. 2761-2770, Aug. 2008.

[22] IEEE Standard 1562-2007, *Guide for Array and Battery Sizing in Stand-Alone Photovoltaic (PV) Systems*. [2.1]

[23] IEEE Std 1013-2007, *IEEE Recommended Practice for Sizing Lead-Acid Batteries for Stand-Alone Photovoltaic (PV) Systems[2.1.1],[temp]*

[24] IEEE Std 1526-2019, *IEEE Recommended Practice for Testing the Performance of Stand-Alone Photovoltaic Systems*.[2.1.1]

[25] IEEE Std 1562-2007, *Guide for Array and Battery Sizing in Stand-Alone Photovoltaic (PV) Systems*.[2.1.1]

[26] IEEE Std 937-2019, *IEEE Recommended Practice for Installation and Maintenance of Lead-Acid Batteries for Photovoltaic (PV) Systems*.[irradiance]

[27] A. Luque and S. Hegedus, *Handbook of Photovoltaic Science and Engineering*, 2nd ed. Hoboken, NJ, USA: Wiley, 2011.

[28] National Programme on Technology Enhanced Learning (NPTEL). 'Control and Tuning Methods in Switched Mode Power Converters' NPTEL. Available: https://archive.nptel.ac.in/courses/108/105/108105180/. [Accessed: 29-Aug-2024]

[29] A. Ozdemir and Z. Erdem, "Double-loop PI controller design of the DC-DC boost converter with a proposed approach for calculation of the controller parameters," in *Proceedings of the Institution of Mechanical Engineers part I journal of Systems and Control Engineering*, 2017

[30] Kalyan Das, "Application of 2-periodic controller in boost converter for solar module", M. E. dissertation, Jadavpur University, India, 2019.

[31] Nirmal Murmu, "2-Periodic compensation of SISO discrete-time LTI plants", M. E. dissertation, Jadavpur University, India, 2017.

[32] S. Chakraborty, "2-periodic/2-rate compensation of discrete-time plants", Ph.D. dissertation, Indian Institute of Technology, Kharagpur, India, 2015.

[33] S. K. Das and P. K. Rajagopalan, "Techniques of analysis and robust control via zero placement of periodically compensated discrete-time plant" in *Control and Dynamics Systems, Advances in Theory and Applications*: Academic, Vol.74,1996.

[34] Spandita Das, "2-Periodic Compensation of Discrete Time Plants: A 2-Degrees-of-Freedom Approach", M. E. dissertation, Jadavpur University, India, 2018.